Water Disinfection Using Metal Doped Titania Nanoparticles

By

HASSAN YOUNAS
(2009-NUST-MSPhD-Env Sci-03)

A thesis submitted in partial fulfillment of requirements for the degree of Master of Science in Environmental Science

Institute of Environmental Sciences and Engineering (IESE)
School of Civil and Environmental Engineering (SCEE)
National University of Sciences and Technology (NUST)
Islamabad, Pakistan
(2011)

It is certified that the contents and forms of the thesis entitled

Water Disinfection Using Metal Doped Titania Nanoparticles

Submitted by

HASSAN YOUNAS

Has been found satisfactory for the requirements of the degree of

Master of Science in Environmental Science

Supervisor: _____
Dr. Ishtiaq A. Qazi
Associate Dean & Professor
IESE, SCEE, NUST

Member: _____
Dr. Imran Hashmi
Assistant Professor
IESE, SCEE, NUST

Member: _____
Dr. Muhammad Ali Awan
Assistant Professor
IESE, SCEE, NUST

External Examiner:_____
Dr. Muhammad Mujahid
Principle Material Engineering and Professor
SCME, NUST

Dedicated to.....

My Loving Parents,

Brothers and Sisters

ACKNOWLEDGEMENTS

Nothing is completed without the assistance of others and a few people must be mentioned for their help throughout this work.

First and foremost, my supervisor, ***Prof. Dr. Ishtiaq A. Qazi*** *for his guidance and patience throughout the MS journey, who, as Associate Dean of Institute of Environmental Sciences and Engineering provided me a conducive environment for the completion of the research work. Many thanks also go to* ***Dr. Imran Hashmi*** *for his never-ending help.*

I am also very thankful to the other members of my Guidance and Examination Committee namely ***Dr. M. Ali Awan*** *and* ***Prof. Dr. Mohammad Mujahid*** *(SCME) for their help in the resolution of many problems.*

The support staff never receives enough thanks, but without them most laboratories would fell apart. I would also like to pay special thanks to all of my friends who gave me support by all means in all my hardships. Finally, to my Father: without your support and understanding this would have taken a much longer time to finish.

HASSAN YOUNAS

TABLE OF CONTENTS

List of abbreviation

Ag- TiO_2	Silver doped Titanium Dioxide
CFU/ml	Colony Forming Unit per milli-liter
e^-	Electeron
eV	Electron Volt
Fe- TiO_2	Iron doped Titanium Dioxide
GPR	General purpose reagent
h^+	Hole
ICPS	International Programme on Chemical Safety
K	Inactivation rate constant
LI	Liquid Impregnation method
O.D	Optical Density
$^*O^-_2$	Oxygen Radical
$^*OH$	Hydroxyl Radical
OH^-	Hydroxyl Ion
T	Temperature
THMs	Tri-halomethanes
TiO_2	Titanium Dioxide
UN	United Nations
UNFAO	Food and Agriculture organization United Nations
UNICEF	United Nations International Children's Emergency Fund
US EPA	United States Environmental Protection Agency
WHO	World Health Organization
λ	Wavelength

List of Figures

Chapter 2

Chapter 3

Chapter 4

List of Tables

Chapter 2

Chapter 3

Chapter 4

ABSTRACT

The thesis presents the results of a study that examined the effectiveness of silver-doped titanium dioxide (TiO_2) or titania nanoparticles. The nanoparticles synthesized by liquid impregnation method and were characterized using X-Ray Difrraction (XRD), Scanning Electron Microscopy (SEM) and Energy Disperssive Spectroscopy (EDS). The size of the nanoparticles were found to be ranged from 11 to 42 nm well below the cut-off range (100 nm) that defines such particles. 1% Ag-TiO_2 was found to be very effective photocatalytic agent against gram –ve (*E. coli*) and gram +ve (*S. aureus*) bacterial groups. As expected, the death rate and extent, of these organisms, by photocatalysis under UV-A light was the maximum; more interestingly, however, was the observation that the silver-doped titania is also very effective in killing both type of bacteria under light in the visible spectrum from an ordinary fluroscent tube. Results with nanoparticles immobilized on a glass surface indicate that the development of self-sterilizing surface for commercial use is a distinct possibility.

Chapter 1

INTRODUCTION

1.1 BACKGROUND

The world health organization estimates that 1.1 billion people lack access to satisfactory drinking water supplies. Many are forced to rely on contaminated water for potable use, therefore increasing their risk of contracting waterborne diseases like Typhoid, hepatitis A and hepatitis E, polio and cholera. In developing countries around half of the population is exposed to polluted water sources which, along with inadequate supplies of water for personal hygiene and poor sanitation, contribute to an estimated 4 billion cases of diarrheal disease each year. This has been estimated to result in 2.2 million deaths, most of which are children under the age of five (UN, 2003).

1.2 WATER CONTAMINATION

The problem upon which this study focuses is water contamination by microbes. As water-borne-diseases are increasing day by day and deaths due to water contamination are being enhanced, and it is being recorded that the developing countries are the major victims. So it is necessary to find out ways by which inhabitants of developing countries could utilize safe drinking water at an affordable cost.

1.3 DISINFECTION

The common techniques used for disinfection of drinking water are effective for remaining most of the infectious agents and include chlorination (chlorine and its derivatives), UV-C, and ozonation (O_3). Chlorination is the most widely used technique at commercial scale. Now days, UV disinfection has gained great importance for water disinfection at household level. Traditional disinfection methods are effective against most pathogens but may be too costly to implement in developing regions.

1.4 PROPOSED SOLUTION

Advanced oxidation technologies (AOT), including semiconductor photocatalysis, may present alternatives for the disinfection of contaminated water in situations where energy efficiency and cost are of paramount importance. Heterogeneous photocatalysis utilizes light along with a semiconductor, to produce reactive oxygen species (ROS) which can inactivate bacteria and degrade a wide range of chemical contaminants in water (Alrousan *et al.*, 2009).

The photocatalytic activity of Titania is reported by many researchers. The first test of biocidal effect of Titania (TiO_2) was carried out on bacteria in 1985 by Matsunaga and coworkers (Matsunaga *et al.*, 1988) and then it was applied on various organisms e.g. fungi, algae and cancer cells (Huang *et al.*, 1999a; Maneerat & Hayata, 2006).

Heterogeneous photocatalysis is a rapidly expanding technology for air and water treatment. This interest received a boost after the discovery of photochemical cleavage of water by Fujishima and Honda in 1972 using TiO_2 (Al-Rasheed,

2005). Since the discovery of photo-induced water cleavage, TiO_2 has received ever more attention from scientists for its application towards air and water purification (Maneerat & Hayata, 2006). Titania heterogeneous photo-catalysis has proved to be one of the powerful techniques for complete degradation of environmental pollutants. The technique has the potential of commercialization due to several advantages regarding advanced oxidation process and extended applicability to the natural contaminated systems (Sakkas *et al.*, 2004). The US food and drug administration (FDA) has approved it for use to approach hygienic conditions in different perspectives including foods, drugs and cosmetics. In sunlight exposure TiO_2 exhibits antibacterial activity due to its strong catalytic activity (Maneerat & Hayata, 2006).

Thus, antibacterial tests under sunlight performed against *E. coli* in water using TiO_2 and TiO_2/Ag have been performed with the composite system of TiO_2/Ag being more effective (Kumar & Raza, 2009).

The minimum inhibitory concentration (MIC) of doping TiO_2 powder prepared at various temperatures and the best results were obtained at 400^{o} C. The MIC is the minimum concentration of sample at which more than 90% of bacteria could not grow. The best minimum inhibitory concentration of Titania is in composite form with metal and proved to be 2ppm in sample, which indicates that the composite powder has stronger antibacterial activity against *E. coli*. The MIC of doping TiO_2 powder increases with increasing the pyrolysis temperature (Shun-wen *et al.*, 2008).

The exogenous and endogenous microbial contamination is a great problem especially in plant tissue culture. To eliminate bacterial contamination for

successful *in vitro* experimentation several antibiotics are being used but those antibiotics have several adverse affects on plant i.e. growth inhibition, genetic mutation, hormonal imbalances etc. and disturb the successful completion of the experiments. It has been proved that silver nanoparticles, either pure or in composite (doped), similarly control the bacterial contamination in tissue culture conditions (Abdi *et al.*, 2008).

1.5 THE PRESENT STUDY

Photocatalytic disinfection is known to be very effective in order to killing microbes in water. A well-known photo catalyst, TiO_2, in its anatase form can be used for the purpose of disinfecting water. Several studies have proved its biocidal activity in different ways.

- In this study silver doped titania nanoparticles were developed with the aim of examining their toxic properties towards microbes.

Chapter 2

LITERATURE REVIEW

2.1 WATER: THE NECESSITY OF LIFE

2.1.1 Need of Drinking Water Disinfection

Lack of access to safe drinking water is indeed a major health issue for a large number of people on the globe. WHO and UNICEF reported 4500-5000 children's death every day due to inappropriate sanitation and polluted drinking water. 1.1 billion people still lack access to safe drinking water (WHO, 2007).

The sources of microbial contamination include a variety of anthropogenic and non-anthropogenic origin. If untreated fecal wastewater, from human settlements, is discharged into river then it has the potential to contaminate the downstream water. Domestic animal waste, including that from cattle also introduces microbial contamination in such waters. Contaminated water used for drinking, bathing or irrigation then contributes to water borne diseases (WHO, 2006). A major portion of the population in developing countries is exposed to polluted drinking water which results in an approximately 4 billion diarrheal cases annually (UN, 2003).

2.1.2 Need of Irrigation Water Disinfection

The second most important issue is the disinfection of water for agriculture. The Food and Agriculture Organization of the United Nations (UNFAO) has reported that agriculture consumes almost 70 percent of fresh water worldwide, and upto 95 percent in developing countries. Almost 1000-3000 m^3 of water is

required to yield one ton of cereals. Thus, 2000-5000 L of water takes to produce a person's daily food requirement comparing that only 2-4 L of water is consumed daily in drinking by an individual (FAO, 2008).

More than 60 percent of world's food is produced by rain fed areas which contribute to over 80 percent of cultivated land worldwide. Accumulation of phytopathogens, fungi and bacteria, is the common problem in stored rain water and surface water. *Fusarium solani* the plant and human pathogen is reported almost everywhere, even in water distribution system of hospitals (Migheli *et al.*, 2010).

2.2 DRINKING WATER STANDARDS: WORLD HEALTH ORGANIZATION (WHO)

2.2.1 Microbial Water Quality

Microbiological testing is carried out to check the microbial water quality. Fecal indicator microorganisms are considered in most cases, but, in some circumstances assessment of specific pathogen densities are verified too. Verification is usually done by testing the source water, water immediately after treatment, water in distribution systems or stored household water. *E. coli* is selected as an indicator of fecal pollution that should not be present in water to claim its fitness for drinking use. In many circumstances, thermo-tolerant coliform bacteria are also monitored other than *E. coli.* Many organisms, like enteric viruses and protozoa are more resistant to disinfection than bacteria so absence of bacteria does not assure the absence of these organisms. So depending upon the surveys, types of organisms are being selected for analysis of microbial assessment.

Water quality can vary rapidly, and all systems are subject to occasional failure. For example, rainfall can greatly increase the levels of microbial contamination in source waters, and waterborne outbreaks often occur following rainfall. Results of analytical testing must be interpreted taking this into account (WHO, 2006).

2.3 POSSIBLE BACTERIOLOGICAL CONTAMINATION IN DRINKING WATER

The bacteria present in drinking water cause numerous diseases and have different level of resistivity to the disinfectants. For example, gram positive bacteria have greater susceptibility than the gram negative bacteria and the spores of bacteria more resistant in both cases. The most common bacteria in drinking water system is *E. coli*, although it may not have pathogenic affect, but is taken as an indication of presence of other pathogenic bacteria. Some of the *Escherichia* species have pathogenic characteristics. The presence of *E. coli* ensures fecal contamination in drinking water system as it is present in the intestines of man and animals. Total coliform and fecal coliform is the test usually performed to detect the presence of disease causing bacteria and other microbes like fungi, protozoa etc. The list of possible bacterial contamination in drinking water is given in table 2.1.

Table 2. 1: Possible bacterial species in water and their health impacts

Bacteria	Possible Health Impacts	References
Acinetobacter baumannii	Pneumonia and infections of the urinary tract, bloodstream and other parts of the body	Gerischer (2008)
Aeromonas hydrophila	Produces Aerolysin Cytotoxic Enterotoxin (ACT), a toxin that can cause tissue damage	Chopra et al. (2000)
Citrobacter freundii	An opportunistic pathogen and causes a variety of nosocomial infections of the urinary tract, respiratory tract, blood and several other normally sterile sites in patients	Badger et al. (1999), Drelichman and Band(1985)
Campylobacter species	Diarrhoea (gastroenteritis) and food poisoning	Humphrey et al. (2007)
E. coli	Mostly harmless but some strains cause serious food poisoning and virulent strains may cause gastroenteritis, urinary tract infections, and neonatal meningitis	Todar (2008)
Edwardsiella tarda	Opportunistic pathogen in humans causing gastroenteritis and diarrhea	Verjan et al. (2005)
Enterobacter species	Several strains are opportunistic pathogens and cause infections in immunocompromised host, urinary and respiratory tracts being the most common infection sites	Feigin (2004)
Klebsiella species	Variety of diseases like pneumonia, septicemia, spondylitis and ankylosing.	Podschun and Ullmann (1998)
Proteus species	Opportunistic human pathogens and may cause many infections in human urinary tract.	Guentzel (1991)
Pseudomonas aeruginosa	Opportunistic pathogen of immunocompromised individuals and typically infects the urinary tract, pulmonary tract, wounds and burns	Nicolle (1995)
Salmonella typhi	Typhoid	Farooqui et al. (2009)
Shigella dysenteriae	Shigellosis (also known as bacillary dysentery)	Herold et al. (2004)
Shigella sonnei	Shigellosis	Keusch and Jacewicz (1977)
Staphylococcus aureus	Skin infections like pimples, carbuncles, scalded skin syndrome, impetigo and cellulitis folliculitis, and life-threatening diseases like meningitis, osteomyelitis, endocarditis, toxic shock syndrome (TSS), pneumonia, chest pain, bacteremia, and sepsis.	Jarraud et al. (2002)
Stenotrophomonas species	Latent pulmonary infections	McGowan (2006)
Streptococcus species	Although many of the streptococcal species are nonpathogenic, certain species are responsible for streptococcal pharyngitis, many cases of meningitis, bacterial pneumonia, endocarditis, erysipelas and necrotizing fasciitis	Carapetis et al. (2005), Musser and Krause (1998)
Vibrio parahaemolyticus	Gastroenteritis and wound infection	Baffone et al. (2005)
Vibrio cholarae	Cholera	Faruque and Nair (2008)
Vibrio mimicus	Produces toxins which cause diarrheal diseases	Chowdhury et al. (1987)

2.3.1 Bacteriological Water Condition in Pakistan

Pakistan is one of the developing countries and depends upon agriculture, so indirectly depends upon water. Water in many areas of Pakistan is contaminated biologically and affects the crop yield and human health greatly. The water condition in some major cities of Pakistan is given in the figures 2.2 & 2.3.

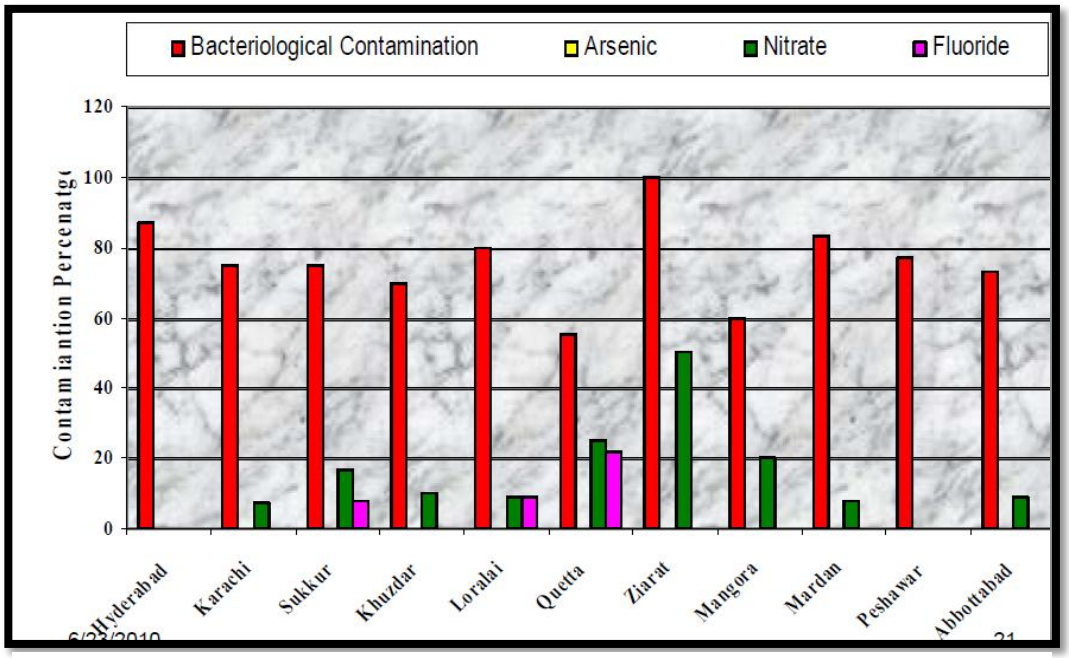

Figure 2. 1: Bacteriological contamination in different cities of Pakistan (1)

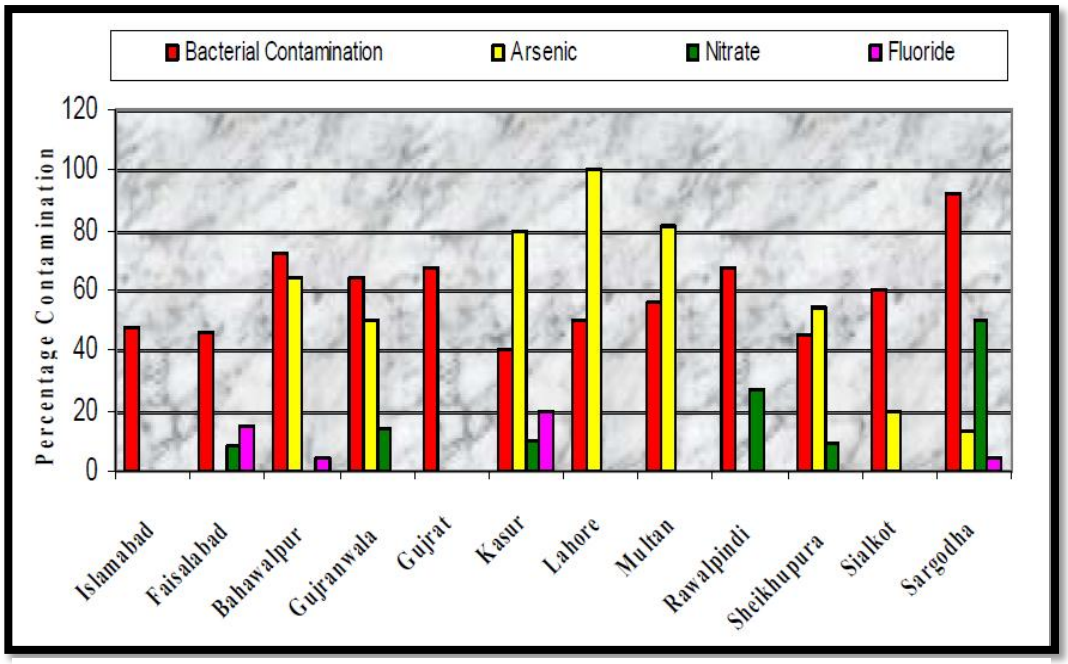

Figure 2. 2: Bacteriological contamination in different cities of Pakistan (2)

Table 2. 2: Bacteriological contamination of drinking water in various parts of Pakistan

Sampling location	No. of samples			% of samples		References
	Total	Contaminated with total coliform	Contaminated with fecal coliform	Contaminated with total coliform	Contaminated with fecal coliform	
Rural areas of Punjab	–	–	–	91.30–95.83	–	Anwar et al. (1999)
Tap water Lahore city	–	–	–	42.85	–	Anwar et al. (1999)
Four villages in Peshawar	39	38	–	97.4	–	Zahoorullah et al. (2003)
In and around Peshawar	224	134	52	100		Sarwar et al. (2004)
Nine different localities in Lahore	2160	446	–	20.64	–	Anwar et al. (2004)
Filtration plants, Islamabad	5	3	–	60	–	PAK-EPA (2005a)
Filtration plants, Rawalpindi	26	14	–	53.8	–	PAK-EPA (2005a)
Groundwater samples from various	344	223	122	65	35	PCRWR (2005)
sources in Pakistan						
Groundwater, Karachi	115			66.63	60.89	Mah-Urooj et al. (2007)
Tap water (treated) Karachi city	329	–	94	–	28.5	Shaikh et al. (2008)
Khairpur city, Sindh	90	90	90	100	100	Shar et al. (2008a)
Ratta Amral water distribution network, Rawalpindi	8	6	6	75	75	Hashmi et al. (2009b)
Input water sources of Rawal Lake, Islamabad	4	4	4	100	100	Mashiatullah et al. (2010)

(Azizullah *et al.*, 2011).

2.4 GRAM POSITIVE AND GRAM NEGATIVE BACTERIA

Bacteria are divided into two major groups, called gram-positive and gram-negative. These can be distinguished by the Gram-staining procedure but differences in cell wall structure are the most important in the reaction. The gram-negative cell wall is a complex, multilayered structure, while the gram-positive bacteria have much thicker single layer. The gram-positive cell wall consists of 90% peptidoglycan layer with 20 – 80 nm average thickness. The reminder 10% consists of teichoic acids, proteins and lipopolysaccharides.

The gram-negative cell wall is much more complex with 2 – 6 nm thick layer of peptidoglycan, comprising of 10% of cell wall. The cell wall also consists of an outer membrane, consisting of 50% lipopolysaccharides, 35% phospholipids and 15% proteins.

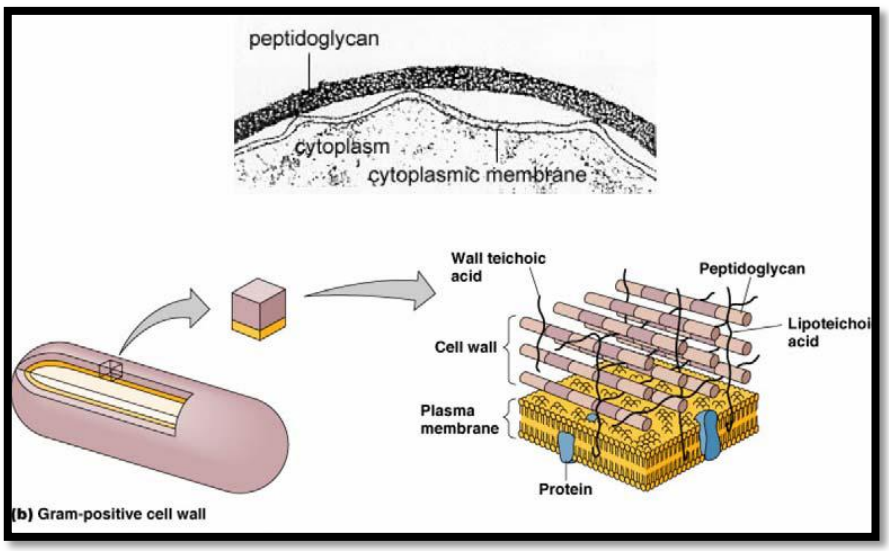

Figure 2. 3: Cell wall structure of gram-positive bacteria

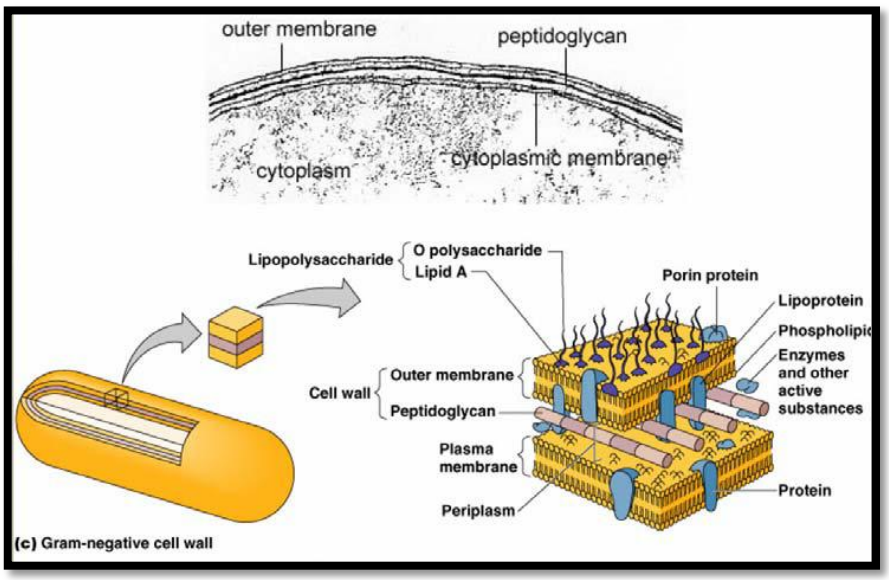

Figure 2. 4: Cell wall structure of gram-negative bacteria

2.4.1 Bacteriological Growth Curve

The growth of bacteria is divided into four phases under ideal conditions. The curve formed showing the bacterial growth which forms the shape of an English letter "S". The phases of the curve are named:

1) Lag phase

2) Log/exponential phase

3) Stationary phase

4) Death/decline phase.

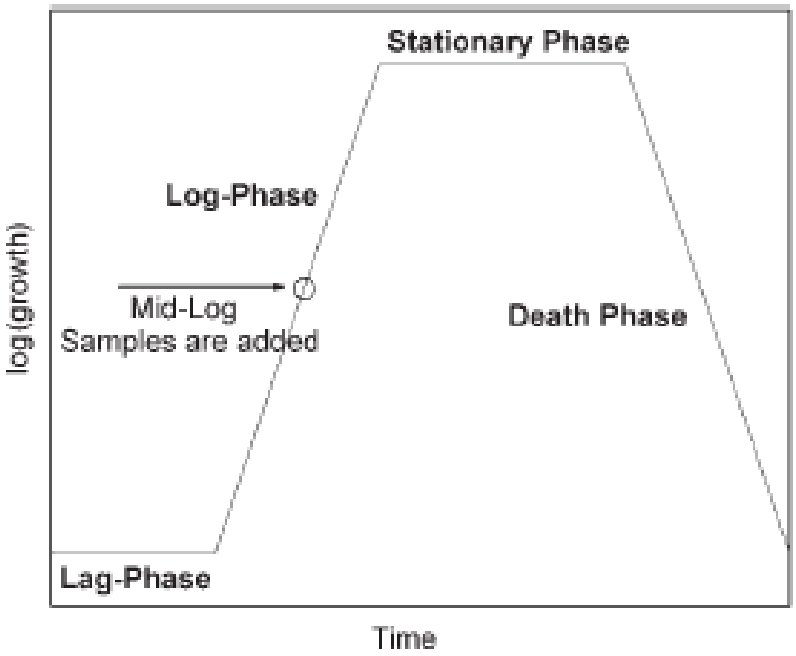

Figure 2. 5: Phases include in bacterial growth
(Thiel *et al.*, 2007)

When bacteria are added into a growth medium first they try to acclimatize themselves into the new environment and are not able to use the nutrients efficiently for their growth rather used limited amount for their survival, and hence the phase is called lag phase. After acclimatization the typical division (binary fission) under optimum conditions is initiated and one cell is divided into two after 20 min. This is the log phase. The process continues until the nutrients are present, but when the nutrients are depleted the growth is inhibited and no further increase in cell number is observed, so the stationary phase starts. After that phase the natural death phenomenon occurs and the number of viable cells decreases with effect of time. This interprets an ideal growth curve of bacteria.

In order to determine the curve *in situ* optical density (O.D) of inoculated broth is determined at different time intervals which leads to the formation of the curve as shown in the Figure 2.5.

2.5 WATER DISINFECTION

The disinfection of drinking water is defined by the microbe's inactivation causing epidemic diseases, like cholera, typhoid etc. The phenomenon includes organism's protein structure destruction and inhibition of enzyme activities. The resistance of organisms is determined by the permeability of cell wall although their complexity and size also influence the resistivity. Among the infectious agents the least vulnerable are Prions, increasing in order with coccidian (*Cryptosporidium*), bacterial spores (*Bacillus*), mycobacteria (M. *tuberculosis*), viruses (poliovirus), fungi (*Aspergillus*), followed by Gram-negative (*Pseudomonas*) and finally Gram-positive bacteria (*Enterococcus*).

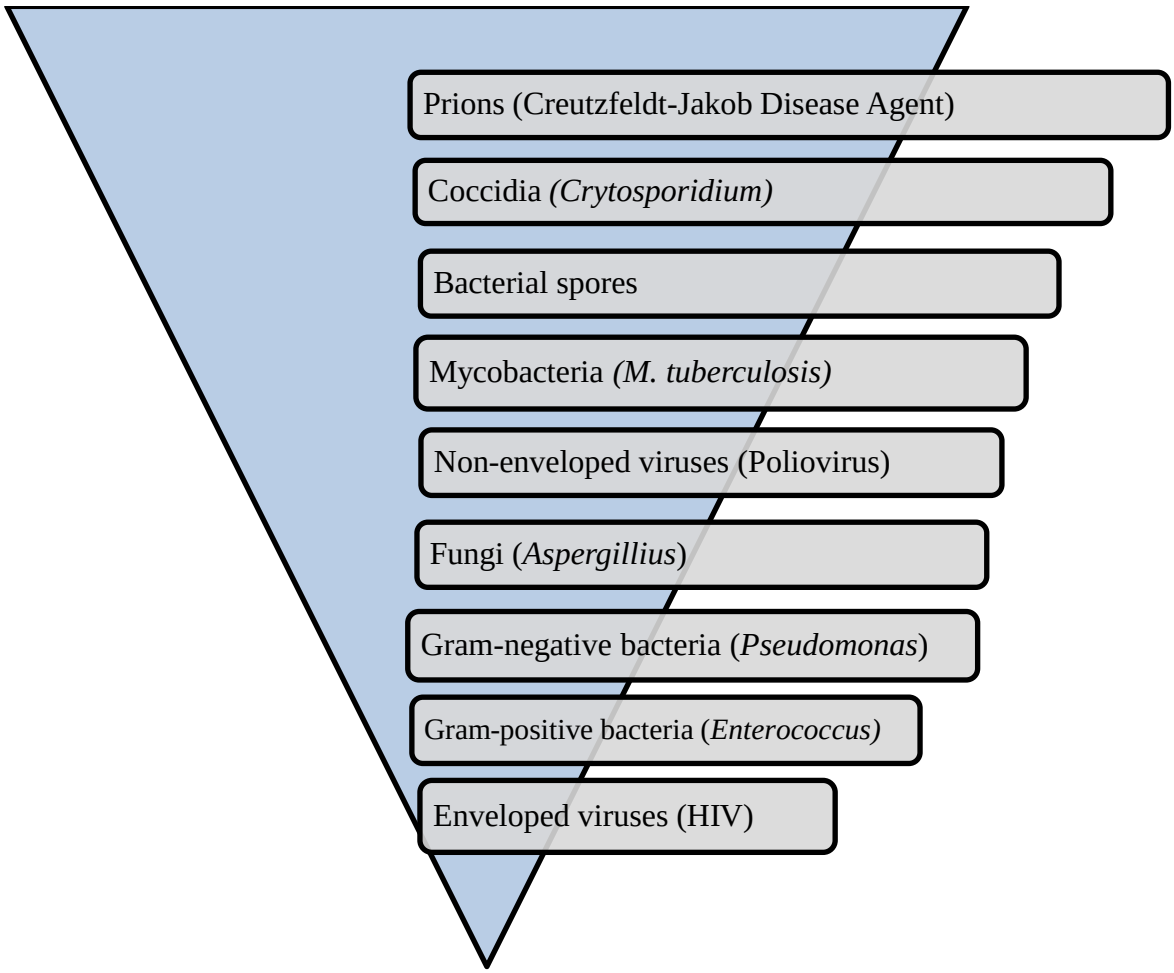

Figure 2. 6: Organisms resistance to disinfection in decreasing order

2.5.1 Conventional Water Disinfection Methods

The common techniques used for disinfection of drinking water are effective for most of the infectious agents and include chlorination (chlorine and derivatives), UV-C (λ 100-400 nm) and ozonation (O_3). Both, UV-C and ozonation techniques are very effective in killing bacteria that also inactivate the viruses and many protozoa, but involve considerable expenses to install, run and maintain. In addition to their high cost, the conventional water disinfection processes include the formation of different harmful disinfection by-products (DBPs). The most dangerous is trihalomethanes (THMs), which are highly carcinogenic (Benabbou *et al.*, 2007).

2.5.1.1 Ozone disinfection

The process of ozone production involves the dissociation of oxygen molecules in oxygen atoms and subsequent collision of these atoms with the oxygen molecules to form an unstable gas O_3, used for water disinfection. Ozone is generated in plants by using high voltage (6 to 20 kilovolts) on oxygen bearing gas source. Usually ozone is produced on spot because of its instability and quick decomposition into elemental oxygen after generation. The result of decomposition comes in the form of hydrogen peroxy (HO_2) and hydroxyl (OH) radicals, being very strong oxidants. Disinfection is caused by protoplasmic oxidation due to which cells become unstable. Low dosage of ozone is required to remove up to 99% of bacteria, i.e., 0.02 mg per min per liter with temperature and pH being at 5 ^{o}C and 6-7 respectively. For Cryptosporidium, a dose as high as 40 mg per min per liter at 1 ^{o}C may be needed (ICPS, 2004). The mechanisms of disinfection using ozone include:

- direct oxidation of the cell wall and cell constituent leakage out of cell
- reactions among cell constituent and radical by-products result by ozone decomposition,
- damage to the nitrogen bases of DNA/RNA (purines and pyrimidines),
- breakage of carbon-nitrogen bonds leading to depolymerization.

2.5.1.2 UV disinfection

UV light is a strong disinfectant and widely used in water purification applications. The wavelength (λ) of UV ranges from 10 nm to 400 nm. Depending upon wavelength UV is devided into four catagories

- Far UV, ranges 10-200 nm
- UV-C, ranges 200-280 nm
- UV-B, ranges 280-320 nm
- UV-A, ranges 320-400 nm

UV-A oxidizes protein structures and damages the membrane causing the cell death. Oxidation occurs by reactive oxygen species (ROS). UV-B modifies the nucleic bases by single stranded breaks which is mutagenic and lethal to organisms. UV-C effects the pyrimidine and purine bases and produce their dimmers. As a result DNA of the cell is damaged and replication is inhibited.

The most energetic part of UV spectrum is UV-C and is usually used as an antibacterial agent in air and water disinfection. For clear water, 7 mJ/cm^2 dose of UV-C is used which inactivates up to 99 percent of bacteria and 5 mJ/cm^2 is enough for Cryptosporidium (Ibáñez *et al.*, 2003; Masschelein, 2002).

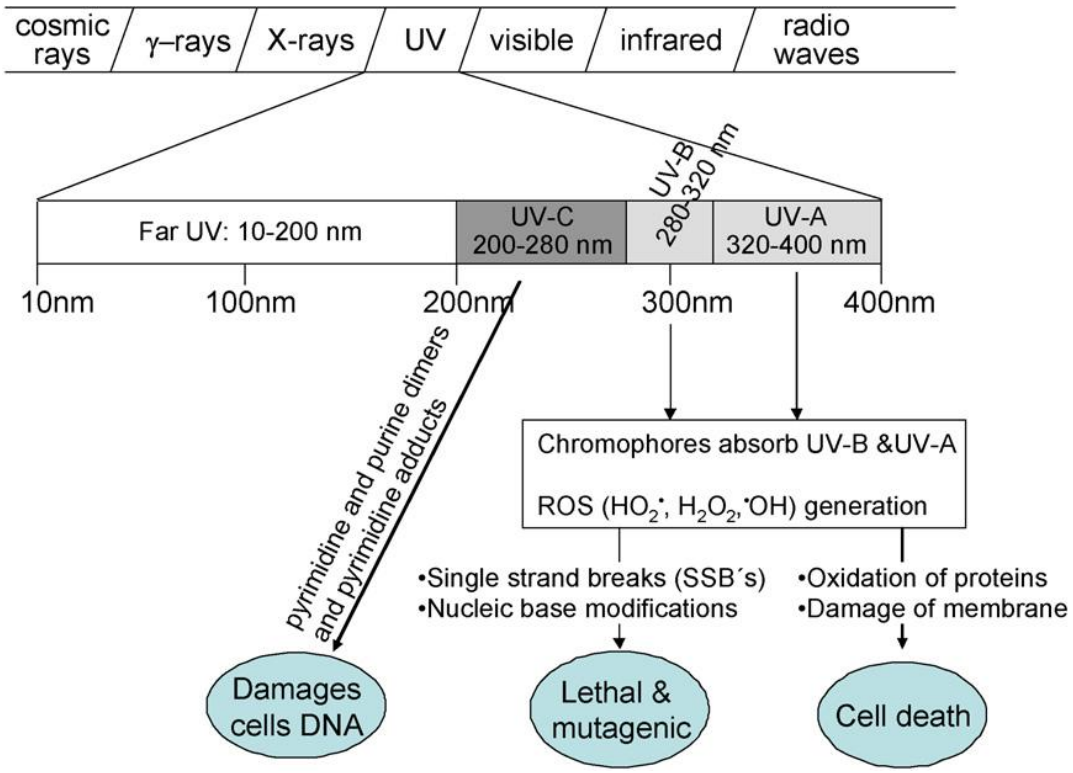

Figure 2. 7: Distribution of UV-light spectrum and its impact on life

2.5.1.3 Chlorine disinfection

Chlorine is considered to be a strong disinfectant for most microorganisms. A dose of 0.08 mg per min per liter at neutral pH and 1-2 ^{o}C can kill 99 percent of bacteria. To attain the maximum killing capacity against viruses 12 mg per min per liter is optimum at 0-5 ^{o}C and neutral pH, but the concentration reaches to 230 mg per min per liter at 0.5 ^{o}C and neutral pH for inactivation of 99 percent of *Giardia sp.* (WHO, 2006). A major drawback for use of chlorine, in drinking water disinfection and even for irrigation water disinfection, is the production of disinfection by-products which include organohalides and trihalomethanes (THMs), first observed in 1970s.

Research seeking alternative methods of drinking water disinfection is, therefore, necessary to solve above mentioned limitations and issues. Any such solution will have to take into account many factors: (i) low cost, (ii) low power consumption, (iii) sustainability, and (iv) absence of negative effects on health, and taste.

2.6 PHOTOCATALYSIS

A photo degradation process is actually an oxidation reaction in the presence of light and oxygen, and, the photo catalyst is only the agent, capable of combining light and oxygen (reactants) efficiently in order to enhance the degradation process. So, in spite of terminology, light is a reactant in photo catalytic process. Thus, photo catalysis can be defined as (Braslavsky, 2007):

"A change in the rate of chemical reaction, or its initiation, under the action of ultraviolet, visible or infrared radiation in the presence of a substance, the photo catalyst, that absorbs light and is involved in the chemical transformation of the reaction partners."

The overall process takes place in five independent steps (Herrmann, 2005):

i. Reactant diffusion from bulk phase to catalyst surface
ii. Adsorption of at least one of the reactants on the catalyst surface
iii. Reaction in adsorption phase
iv. Desorption of the product
v. Removal of the product from the interface region

Scientists have divided the photo catalysis process into two broad categories based on initial excitation process (Linsebigler *et al.*, 1995):

- Catalyzed photoreaction
- Sensitized photoreaction

Catalyzed photoreaction

In this process the initial photo excitation occurs on the adsorbate molecule, which then interacts with the ground state catalyst substrate.

Sensitized photoreaction

When the initial photo excitation occurs on the catalyst substrate and then it interacts with the ground state molecule to transfer energy or electron, the process is referred to as sensitized photoreaction.

2.6.1 Factors Affecting the Photo Catalysis

The photo catalytic processes are extremely complex reactions which involve water, oxygen, catalyst, light and the substrate to be degraded. These are the components which are necessary for a photo catalytic process to take place, so the reaction rate is being affected by several operational conditions related to these e.g., pressure of oxygen, catalyst loading, light intensity, extent of continuous irradiation, concentration of substrate, pH of medium and temperature etc. (Rincón & Pulgarin, 2003).

The acquired physical and chemical properties of the photo catalyst also affect the process or catalyst efficiency. These properties include crystal structure, surface area, and presence of surface hydroxyl group (Herrmann, 2005).

2.6.2 An Ideal Photo Catalyst

There are certain properties which are considered while selecting a photo catalyst and presence of all of these in a single photo catalyst make it ideal (Bhatkhande *et al.*, 2002).

- ❖ Photoactive
- ❖ Excitable with visible and/or near UV light
- ❖ Biologically and chemically inert
- ❖ Photo stable
- ❖ Inexpensive
- ❖ Non-toxic

Furthermore, a photo catalyst is generally a semiconductor, and it will be chemically active as a sensitizer if the redox potential of hydroxyl radical will lie within the band gap of photo catalyst.

2.6.3 Catalysts for Photo Catalytic Reactions

Heterogeneous photo catalysts are usually solids which are not consumed in the overall reaction and enhance the process efficiency. The photo catalysts are invariably semiconductor materials, which include several metal oxide like CeO_2, Fe_2O_3, TiO_2, WO_3, ZnO, ZrO_2 etc. and some sulfides e.g., CdS, MoS_2 and ZnS (Benabbou *et al.*, 2007; Herrmann, 2005).

2.7 TITANIA AS A PHOTO CATALYST

2.7.1 Introduction

TiO_2 was discovered by William Gregor, in 1790s, on the beaches of Cornwall, England in the form of black sand. He found that the black grains can be separated from ordinary silica by magnet. He then treated those black grains with HCl and dissolved out the iron oxide leaving behind a white residue. Then the white residue was dissolved into sulphuric acid and after treatment of this solution with soda, followed by calcination, white powdered "TiO_2" was obtained.

The process established by William Gregor in 1790, was used until 1960 to produce TiO_2 for all commercial needs. Now a days, the process has been modified and TiO_2 is being produced by either sulfate method or chlorine method.

Sulfate Method

Ilmenite ($FeTiO_3$) is the root material for this process, obtained from metamorphic rocks. It is transformed into iron and titanium sulfate by reacting with sulfuric acid. Titanium hydroxide is precipated by hydrolysis, filtered and calcined at high temperature.

Chlorine Method

In chlorine method, the seed crystals generated by alkaline hydrolysis, are allowed to react with chlorine to produce titanium tetrachloride which is purified and reoxidized yielding very pure TiO_2.

TiO_2 has received a lot of attention due to the following reasons (Benabbou *et al.*, 2007; Kumar & Raza, 2009);

- Good photoactivity
- Non toxicity
- High stability
- Low cost

TiO_2 is widely used as a white pigment in paints (51% of total production), plastic (19%) and paper (17%) (Carp *et al.*, 2004). It also has every day uses which include whitener in tooth pastes and UV absorber in sunscreens (Zallen & Moret, 2005).

2.7.2 TiO_2 Polymorphs

Three polymorphs of TiO_2 exist namely Anatase (tetragonal), Rutile (tetragonal) and Brookite (orthorhombic).

The difference lies in their crystal structure which is formed by distortion of each TiO_2 octahedral and assemblage pattern of these chains. In Anatase, octahedral are attached to each other with their vertices while in rutile the octahedral linkages is in between their edges and in brookite both, the vertices and edges are joined together (Carp *et al.*, 2004).

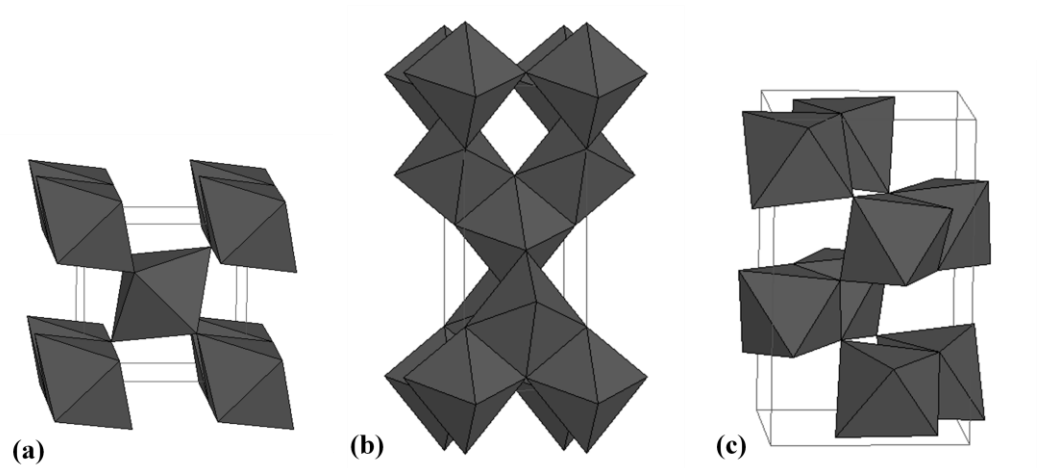

Figure 2. 8: Crystal structure of polymorphs of Titanium dioxide, (a) Rutile, (b) Anatase, (c) Brookite

Only anatase and rutile are used for photo catalytic processes and thought to be strong photo catalyst. Although in most literature, anatase is considered a strong photo catalyst than rutile (Beydoun *et al.*, 1999; Carp *et al.*, 2004), but there is a great conflict into their activities and according to some is the vice versa case of above mentioned (Neppolian *et al.*, 2002). It is also claimed that a mixture of anatase (70%-75%) and rutile (30%-25%) is more effective than anatase or rutile alone (Giolli *et al.*, 2007; Sun *et al.*, 2008).

Table 2. 3: Required wavelength for activation of polymorphs of TiO_2

Polymorph	Band Gap value	λ for photo excitation (nm)
Anatase	3.2 eV	Upto 385
Rutile	3.02 eV	Upto 385
Brookite	2.96 eV	Upto 375

2.7.3 Photo Catalytic Activity of TiO_2

Although TiO_2 is considered as an excellent photo catalyst but there are some considerations which restricts its wider use (Linsebigler *et al.*, 1995).

- Low photonic yield of the degradation process
- Band gap energy of 3.2 eV (correspond to 388 nm λ) thus in order to photo excite and process activation UV light is prerequisite which is only 5% of the solar spectrum.
- In liquid phase treatment, the use of suspension requires a final step to separate the photo catalyst from treated water.

The extent of photoactivity depends on various properties e.g., crystallinity, morphology and surface area (Sheel *et al.*, 2008). In recent years, efforts have been made to improve TiO_2 photo catalytic efficiency by focusing on following (Gaya & Abdullah, 2008):

- Incorporation of energy levels within the band gap of TiO_2.
- Changing life-time of charge carriers.
- Substitution of Ti^{4+} with the cation of the same size.

- ❖ Shifting the conduction band and/or valance band to enable photo excitation at low energy levels.

2.7.4 Modifications in TiO_2

A number of elements from the periodic table have been used as dopant to modify TiO_2 and consequently have changed its rate of activity. Different metals such as Ag, Fe, Cr, Pd, Cu, Pt etc (Araña *et al.*, 2004; Wu *et al.*, 2004) and numerous non-metal elements like B, C, N, V, S have been successfully doped into TiO_2 (Bettinelli *et al.*, 2007; Hamal & Klabunde, 2007). The very essential consideration while doping is dopant optimized ratio because,

I. A reduction in the number of photo generated e^-/h^+ pairs occurs as a result of limitation of light access to TiO_2 surface due to excessive coverage by dopant, so photo activity of TiO_2 is reduced (Carp *et al.*, 2004).

II. A probability to arrest the active sites on TiO_2 surface by metal deposits leads to lose its activity (Coleman *et al.*, 2005).

III. Metal deposits may become the recombination centers, if dopant metals begin to attract holes and recombine these with electrons (Carp *et al.*, 2004).

2.7.5 Photo catalytic mechanism in TiO_2

$$TiO_2 + h\upsilon \longrightarrow TiO_2 (e^- + h^+)$$

Reactions involving conduction band

$$TiO_2 (e^-) + O_2 \longrightarrow TiO_2 + {}^*O^-_2$$

$$TiO_2 (e^-) + {}^*O^-_2 + 2H^+ \longrightarrow TiO_2 + H_2O_2$$

$$TiO_2 (e^-) + H_2O_2 \longrightarrow TiO_2 + {}^*OH + OH^-$$

$${}^*O^-_2 + H_2O_2 \longrightarrow {}^*OH + OH^- + O_2$$

$${}^*O^-_2 + H^+ \longrightarrow {}^*HO_2$$

$$TiO_2 (e^-) + {}^*HO_2 \longrightarrow TiO_2 + HO^-_2$$

$$HO^-_2 + H^+ \longrightarrow H_2O_2$$

$$2\ {}^*HO_2 \longrightarrow O_2 + H_2O_2$$

Reactions involving valance band h^+

$$TiO_2 (h^+) + H_2O_{ads} \longrightarrow TiO_2 + {}^*OH_{ads} + H^+$$

$$TiO_2 (h^+) + 2H_2O_{ads} \longrightarrow TiO_2 + 2H^+ + H_2O_2$$

$$TiO_2 (h^+) + OH^-_{ads} \longrightarrow TiO_2 + {}^*OH_{ads}$$

2.8 CELL DEATH MECHANISM OF PHOTO CATALYTIC DISINFECTION

In bactericidal mechanism of TiO_2 photo catalysis the first attack is considered to be on cell wall by one of the ROS species, the hydroxyl radical, proceeds into leakage of potassium ions rapidly from cell and hence cell viability decreases (WHO, 2006). It is also reported that essential cell functions are also inhibited due to peroxidation of polyunsaturated lipid contents of cell membrane and consequently the cell dies (Huang *et al.*, 1999b).

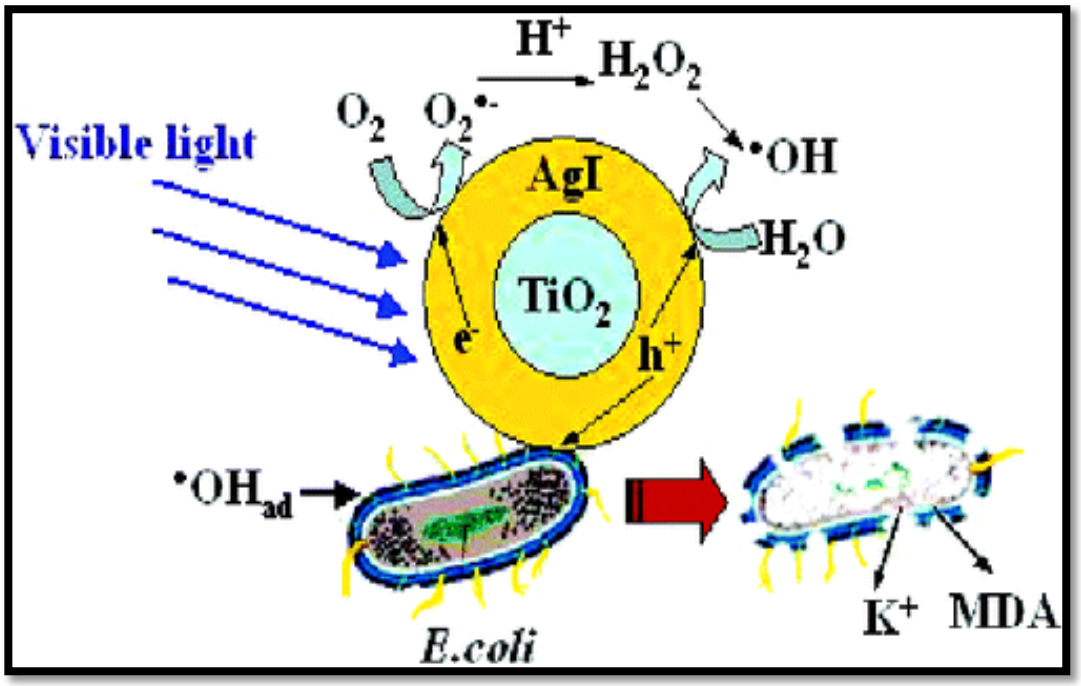

Figure 2. 9: Mechanism of Photo catalytic Disinfection

The consensus is there regarding bacterial destruction mechanism. The oxidative radical first contacts and destroys the external membrane of cell wall. Initially the lipopolysachharides layer and peptidoglycan layer of external cell wall is targeted. Then the lipid membrane peroxidation (the radical oxidizes to fatty acids), protein membrane oxidation (amino acids) and finally the oxidation of polysachharide occurs (Ireland *et al.*, 1993). Some researchers argue that, there is a direct photochemical oxidation, which oxidizes the intracellular coenzyme A to its dimeric forms which reduces the respiratory capability of the cell and eventually the cell dies (Benabbou *et al.*, 2007).

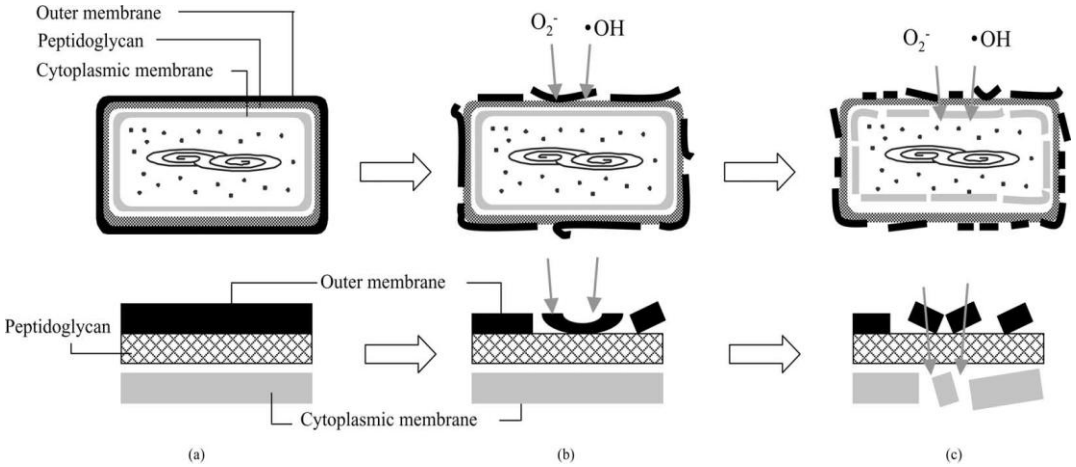

Figure 2. 10: Disruption of cell wall of bacteria

2.9 DISINFECTION KINETICS

The photo catalytic inactivation rate follows the first order kinetics as a function of initial bacterial concentration. The validity of first order kinetics for microorganism's concentration is strongly dependant on microorganism itself. The rate of deactivation is independent of initial concentration if it is between 10 and

1010 CFU/ml (Sunada *et al.*, 2003). Different bacterial disinfection kinetics model have been proposed and all of those depict first order kinetics or pseudo-first order kinetics (Marugán *et al.*, 2008).

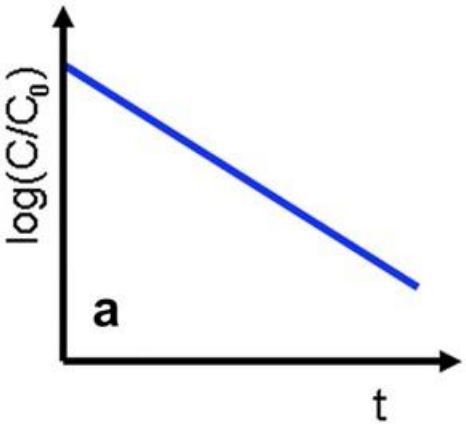

Figure 2. 11: : Chick-Watson model

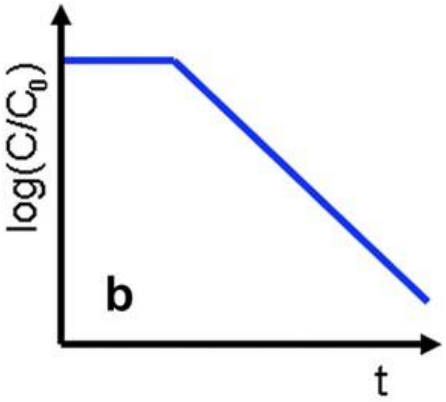

Figure 2. 12: Delayed Chick-Watson model

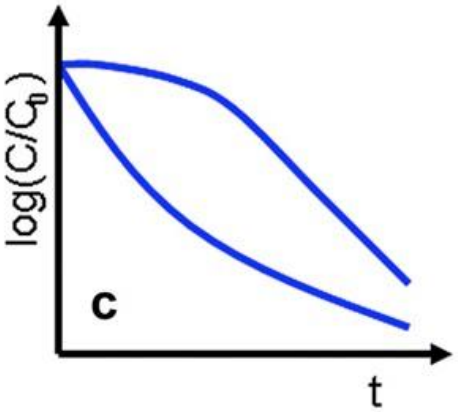

Figure 2. 13: Modified Chick-Watson model

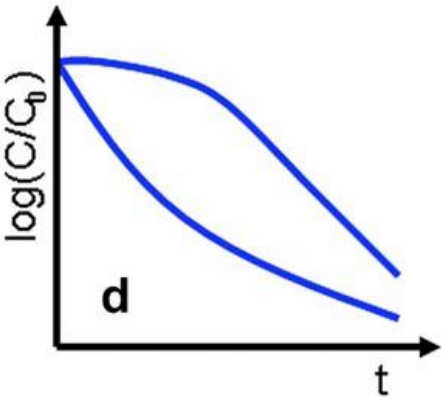

Figure 2. 14: Hom model

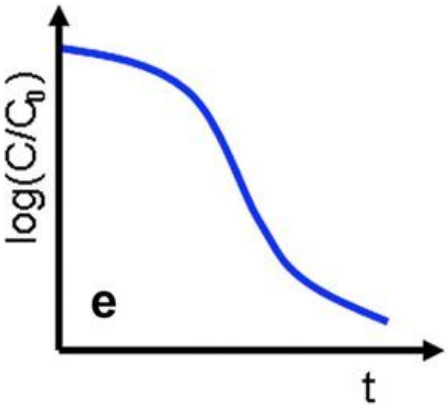

Figure 2. 15: Modified Hom model

Due to the complex mechanism of the disinfection processes, the kinetic analysis of the photo catalytic bacterial inactivation has been usually carried out using empirical equations. That is the case of the disinfection model reported in the literature by Chick and Watson:

$$Log\left(\frac{N}{No}\right) = -kct$$

Where N_0 is the initial microorganism population (CFU per milliliter), N is the remaining population at time t, k is the disinfection kinetic constant, c is the concentration of the disinfecting agent at time t. In photo catalytic processes, the concentration of the disinfecting agent could be considered to be constant with time, the general expression of the Chick–Watson equation is reduced to (Marugán *et al.*, 2008):

$$Log\left(\frac{N}{No}\right) = -kt$$

2.10 EFFECT OF SURFACE INTERACTIONS

The relative size of microorganisms and photo catalyst present a concept of how the process occurs. The key parameters will be the relative location of particles and microorganisms, their surface electric charges as well as their mean particle size, the subsequent adsorption and eventual incursion of oxide particles into cellular wall and the photo catalytic process.

Gumy et al. explain the inactivation efficiency behavior of *E. coli* as a function of isoelectric points of different types of TiO_2 powders. The specific

surface area of isoelectric points of the photocatalysts were 335 m^2/g and 3-7 respectively. They also showed that the initial pH concentration of suspension did not affect the *E. coli* inactivation kinetics when TiO_2 consisted on a mixture of anatase nad rutile phases. The correlation between IEP and photo catalytic efficieny was developed and explains the inverse relationship i.e., lower the IEP of TiO_2 the lower the bacterial inactivation activity. Evidence also exists for partial contact between *E. coli* and clusters of TiO_2.

Chapter 3

MATERIALS AND METHODS

3.1 METHODOLOGY

Amorphous Titania (GPR, BDH Chemicals Ltd. Poole England) was selected for the preparation of Titania nanoparticles, and Silver Nitrate (GR, Merk, Germany) as precursor of silver for doped Titania nanoparticles. Nutrient Agar (Merck, VM 100650 943) was used as a solidified growth medium for bacteria and bacterial cultures were prepared using Nutrient Broth (Merck, VM 747243 703). Saline blanks were prepared by; Sodium chloride (NaCl, Riedel-deHaën®, max. 0.00002% Al). Pure *E. coli* culture (dh5a strain) was obtained from Centre of Excellence in Molecular Biology (CEMB), University of the Punjab, Lahore.

3.2 SYNTHESIS OF NANOPARTICLES

3.2.1 Synthesis of Pure TiO_2 Nanoparticles

Amorphous Titania, general purpose reagent (GPR) was taken in a clean china dish and was placed in a muffle furnace at 400^0 C for 6 hours for calcination. The calcined material was then cooled down slowly by keeping in muffle furnace being switched off.

3.2.2 Synthesis of Ag-TiO_2 Nanoparticles

Silver ion doped titania nanoparticles were prepared by Liquid Impregnation (LI) method (Sahoo *et al.*, 2005). The steps involved mixing, settling, drying and calcination. For 1% doping of silver (mole ratio) on titanium oxide, 0.0639 g of silver nitrate was dissolved in 100 ml deionized water in 500 ml Pyrex beaker. 3 g titania GPR was added into that solution and stirred vigorously using a magnetic stirrer until a slurry was obtained. The slurry was allowed to settle down for 24 hours. After settling, the material was air dried in an oven at 105^0 C for 12 hours. The grinding of dried material was done using pestle and mortar to attain the fine powder and transferred into a clean china dish. Calcination was completed in a muffle furnace for 6 hours at 400^o C and the material was allowed to cool down slowly to obtain nanocrystalline structure.

Table 3.1: Amount of $AgNO_3$ and $Fe_2(NO_3)_3 . 9H_2O$ used for doping of 3 g TiO_2

Sr. No.	Dopant concentration (Mole ratio)	Precursor quantity (g)
1	1% Ag	0.0639
2	2% Ag	0.1237
3	3% Ag	0.1917
4	4% Ag	0.2556
5	5% Ag	0.3195
6	1% Fe	0.151

3.3 CHARACTERIZATION

3.3.1 Structure Determination

3.3.1.2 X-ray diffraction

The crystal structure evaluation is one of the basic information to characterize the materials. XRD is the most basic and powerful technique to identify the crystalline phases and their structural properties present in the material (Brundle *et al.*, 1992; Hosokawa *et al.*, 2007). Electron beam diffraction (ED) using Transmission Electron Microscopy (TEM), characterize the crystal structure more appropriately of each nanoparticle but XRD has some advantages for which it is preferred, i.e.,

i. It allows measurements in air and related atmosphere.
ii. The crystal structure is evaluated, quantitatively on an average.
iii. Sample preparation for XRD is easier (Hosokawa *et al.*, 2007) .
iv. It is noncontact and nondestructive technique and hence can be used in most environments especially for *In situ* studies (Brundle *et al.*, 1992).

X-rays (electromagnetic radiations) used, is of specific photon energy i.e., 100eV – 100 keV. Very short wavelength x-rays are used for diffraction analysis usually upto 0.1 angstrom with high energy, which can penetrate deep into the material and puts out the information of the bulk structures (Cullity, 1956).

The most widely used diffractometer is powder XRD, which can fulfill the needs of commercial laboratory. The X-rays source used is Cu$K\alpha$ with wavelength of 0.15418nm and recommended only for powder. CuK_β rays are also radiated from the x-ray tube used with a Cu target but a curved graphite monochromator or

Ni filter is used to eradicate the peaks produced CuK_{β}. Cu$K\alpha$ is a combination of Cu$K\alpha_1$ (0.15405nm) and Cu$K\alpha_2$ (0.15443 nm) in 2:1 ratio and it is usually suggested to use the Cu$K\alpha_1$ values to find interplanner distance. In modern systems, for rapid measurements and analysis a position-sensitive detector (PSD) is used.

The crystal size is determined usually by XRD analysis using Scherer equation

$$L = \frac{k\lambda}{\beta \cos\theta}$$

Where,

K = 0.9, a shape factor for spherical particles

λ = 0.15405 nm, Cu$K\alpha_1$ wavelength

β = Full width of a diffraction line at one half of maximum intensity (FWHM) radian

θ = The diffraction angle of crystal phase

3.3.2 Imaging of Material

3.3.2.1 Scanning electron microscopy (SEM)

SEM is one of the supplement of optical microscope, and, can magnify an object 10X (magnification of a powerful hand lense) to X300000 with the resolution of few nanometers (Brundle *et al.*, 1992). Not only the necessary information regarding topography and chemical composition near surface regions is provided, but also, crystalline structure and electrical behavior can be determined of the top 1µm or so of the specimen (Brundle *et al.*, 1992; Vernon-Parry, 2000). It is a non-destructive technique and specimen preparation is very easy for characterization (Vernon-Parry, 2000).

Scanning of the sample is done by high energy beam of electrons and the signals, in the form of secondary electrons, emitted by the object/sample are detected by detectors and are seen on CRT. The beam of electrons used is between 2-40 KeV and can be generated by three different sources i.e., Tungsten (W) hairpin filament, Lanthanum hexaboride (LaB_6) filament or Field Emission Gun (FEG). The most common of these, is Tungsten hairpin filament because others are much expensive. The THF is heated up to 2500^0 C by passing the electric current and electrons are emitted from the tip thermally (Vernon-Parry, 2000).

First, the electron beam is demagnified by 2 or 3 electromagnetic condenser lenses into a fine probe, and then scan coils scan it across a selected area of specimen surface in a raster. The penetration of electrons in the specimen is in the form of determinable tetrapod-shaped volume. Three factors determine the dimensions i.e., energy of the electron beam, atomic mass of element in the specimen and the angle at which the electron beam hits the specimen.

After the penetration of the electrons to the surface, a number of interactions occur which result in the emission of electrons or photons. Appropriate detectors collect the reasonable amount of emitted electrons from the specimen chamber and are fed on the Cathode Ray Tube (CRT). Wherever beam strikes on the sample surface, it is directly mapped on a screen onto a corresponding point. The signals produced include secondary electrons, backscattered electrons, auger electrons, X-ray and light, depending upon the interaction of electron beam and atoms at or near the surface of the sample. The magnification is determined by the ratio between the side length of the CRT display and the side length of the raster on the sample.

3.3.3 Elemental Identification

3.3.3.1 Energy-dispersive spectroscopy (EDS)

EDS is a standard technique to identify the elements present in the material and gives its chemical composition. Usually EDS systems are used with SEM (mounted with scanning electron microscopy), thus the source of electron used for EDS is the primary electron beam of the scanning electron microscopy, to produce the characteristic x-rays of the elements. Every element has its own x-ray characteristics, so the chemical composition is determined by analyzing the energy of characteristics x-rays (Hollerith *et al.*, 2004).

X-rays emission is influenced by the bombardment of high energy charged particles onto the atom. The collision of the charged incident particles with electrons of the atom excite it, and, eject an electron from the inner shell of the atom producing an electron hole thus ionizing the atom. To return to the ground state, an electron from the high energy outer shell fills the electron hole by

releasing the excessive energy which is unique for every atomic transition. The energy released in the form of x-ray photon or is absorbed by the atom itself and emitted as an auger electron.

An energy dispersive spectrometer is used to measure the frequency and energy of the x-rays emitted from the sample. Atomic structure and energy difference of the two shells is specific for every element and their determination gives the elemental constitution of the sample.

3.4 EXPERIMENTATION

3.4.1 Preparation of Bacterial Culture

To prepare 24 hrs old gram culture of pure *E. coli* (dh5a) culture, nutrient broth solution was prepared as per manufacturer instructions. The flask containing NB solution was autoclaved at 121^{o} C temperature and 15lb pressure for 15 minutes to eradicate any contamination. After autoclaving the flask was transferred into sterile laminar flow cabinet and allowed cool down. By using a sterile wire loop, a colony was selected at *E. coli* (dh5a) plate and inoculated into the autoclaved NB solution following which the flask was placed in the incubator for 24hrs at 37^{o} C.

3.4.2 Material Preparation

20g of N-agar (Merck) was dissolved into luke warm distilled water and dispensed into screw capped tubes i.e., approximatly15ml each. Four sets of saline blanks, including 7 tubes in each set, were prepared by dispensing 9ml of 0.85% Sodium chloride solution in each tube. Autoclaved both sets of tubes at 121^{o} C temperature and 15lb pressure for 15 minutes. The autoclaved saline blanks were

transferred to sterile environment of laminar flow cabinet and the agar tubes were placed into a water bath by maintaining their temperature at 45^{o} C to ensure their molten state.

3.4.3 Nanoparticles Used in Suspension

Biocidal effect through photo catalytic oxidation was studied in order to optimize the concentration of nanoparticles, percentage dopant and time. Nanoparticles in agglomerate form were applied on an overnight grown pure *E. coli* (dh5a) and *Staphyllococcus aureus* culture.

The UV-cell containing 24 hours old culture was adjusted on magnetic stirrer, Figure 3.1-3.2. The required concentration of nanoparticles was weighed and applied to the bacterial culture in UV-cell and stirred at 250rpm under the exposure of simple fluorescent light (built-in tube-light of laminar flow chamber). Standard Plate Count (SPC) was performed followed by serial dilution against zero min (after applying nanoparticles) 30 min, 60 min, 90 min and 120 min. For serial dilution, 1ml from the UV-cell was collected by using a micropipette (volac uni fully autoclaveable R 780/E 200-1000µl) and sterile blue tip (1000 µl) and dispensed in saline tube as shown in figure 3.3.

The petri plates were prepared from the 6th dilution tube and 7th dilution tube by dispensing 1 ml from both tubes in 2 separate plates, and pouring the molten agar into it. The plates were incubated at 37 ^{o}C for 24-48 hrs in an inverted position in incubator. Counted the colonies on colony counter against 0, 30, 60, 90 and 120 minutes from both the plates, and recorded.

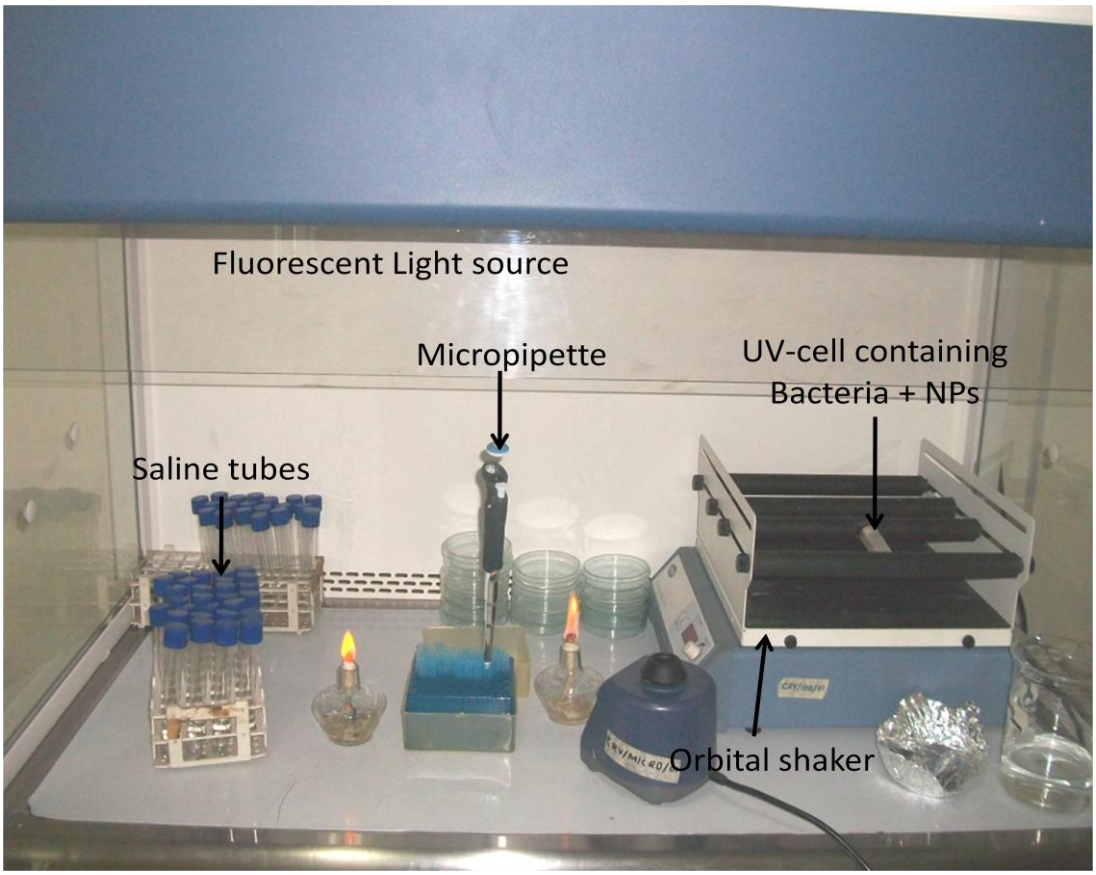

Figure 3. 1: Experimental setup

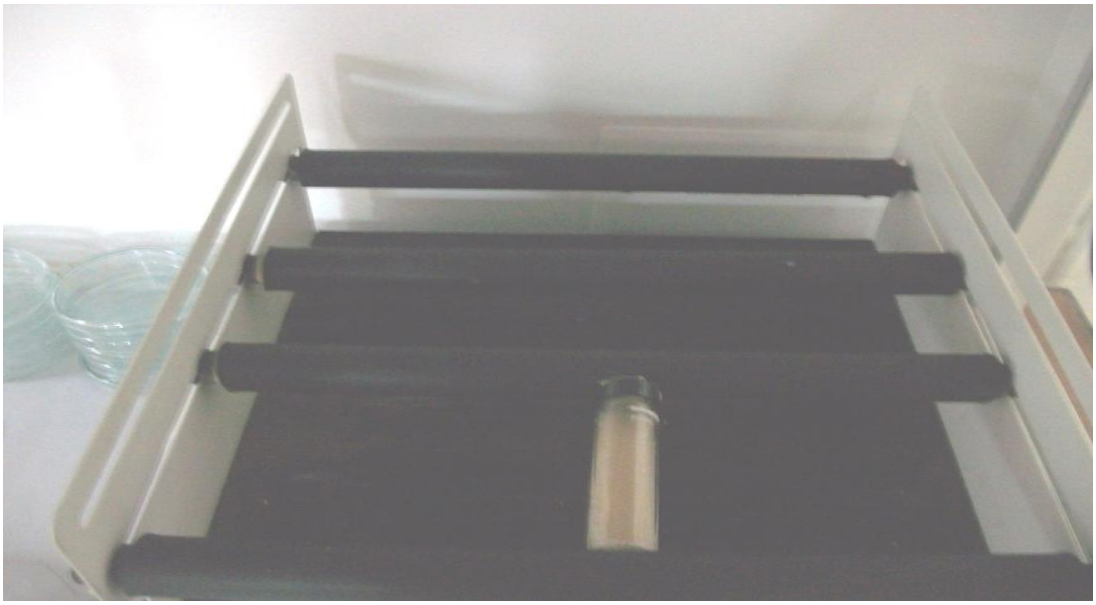

Figure 3. 2: UV-cell containing bacteria and NPs (exposed to Fluorescent light)

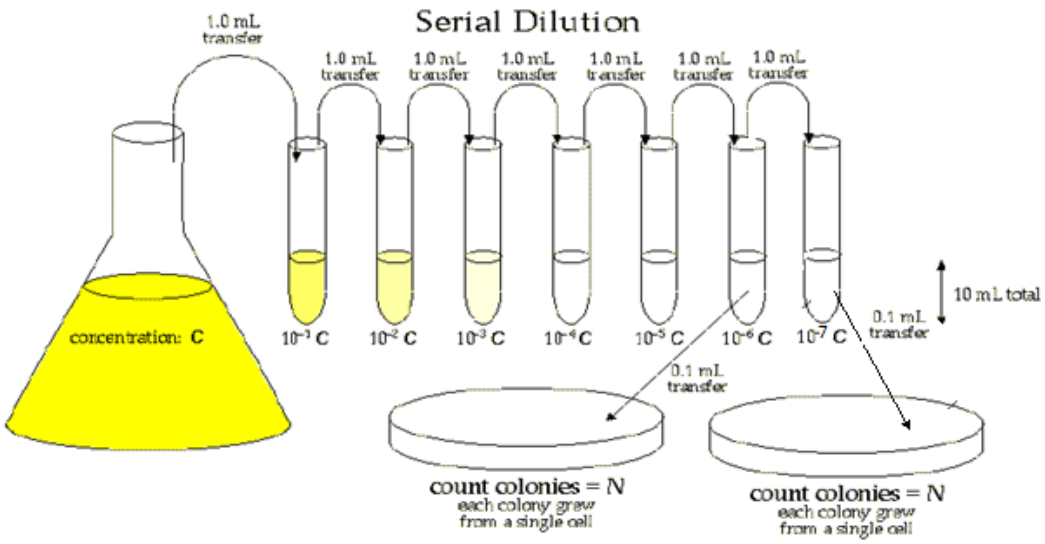

Figure 3. 3: Serial dilution of bacteria

3.4.3.1 Selection of dopant metal

In order to select the metal to be doped on TiO_2, to enhance the photocatalyic activity under low energy light (visible light), TiO_2 was doped with 1% Fe (mole ratio to Ti) and 1% Ag (mole ratio to Ti). The prepared metal doped titania NPs were applied to bacterial culture and SPC was performed followed by serial dilution. Based on initial results further work was done with Ag as a dopant.

3.4.3.2 Selection of Nanoparticles concentration

For optimization of concentration, 2% Ag-TiO_2 nanoparticles were used with increasing concentration in the suspension. 0.1 g/100ml, 2% Ag-TiO_2 was applied in the initial experiment. The loading of NPs with bacterial suspension was increased to 0.5 g/100ml, 1 g/100ml and 5 g/100ml until significant results were reported. At last 7.5 g/100ml was applied. All the experiments were performed

under the influence of fluorescent light (house hold tube light). Based upon the results obtained, 5 g/100ml concentration was selected and applied for the further experiments.

3.4.3.3 Selection of percentage dopant (Ag)

Proceeding with 5 g/100ml concentration, all prepared percentage dopants were applied to bacterial culture consecutively. Pure TiO_2, 1% Ag-TiO_2, 2% Ag-TiO_2, 3% Ag-TiO_2, 4% Ag-TiO_2 and 5% Ag-TiO_2 was prepared previously and applied. The control group of experiment do not contain any NPs rather the bacterial culture influenced by light. 1% Ag-TiO_2 was most promising, so, in further considerations 1% Ag-TiO_2 was applied to investigate further.

3.4.3.4 Antimicrobial effect in darkness

All the dopant percentages were applied with the selected concentrations to the cell culture to determine, whether or not, Ag solely plays a vital role in the disinfection process.

3.4.3.5 Comparison with conventional techniques

UV light, as used for disinfection, was selected to compare with TiO_2. UV-A spectrum was selected and bacterial culture was exposed to it exclusively and in combination with 1% Ag-TiO_2.

3.4.4 Nanoparticles Used After Immobilization

3.4.4.1 Immobilization of TiO_2 nanoparticles

The glass petri plates were selected as substrate for the immobilization of NPs. The lower parts of the petri plates were etched by immersing these for 24 hrs in 5% NaOH solution. The etched parts of the petri plates were thoroughly rinsed

with distilled water. 300 ml solution of NPs was prepared by dissolving 3 gm previously synthesized NPs in distilled water. The solution was vigorously stirred for some time. After stirring the lower etched part of the petri plates were kept into it for an hour. The petri plates were separated from the solution and oven dried at 150 ^{o}C for 2 hours. The oven dried plates were kept into muffle furnace at 600 ^{o}C for 2 hrs and cooled down by switching off the muffle furnace. The plates were rinsed with distilled water and air dried (Khataee, 2009).

3.4.4.2 Preparation of plates for disinfection experiment

The coated plates were closed with their lids and autoclaved at 121 ^{o}C with 15 lb pressure for 15 min. after autoclaving. The moisture in the plates was removed by oven drying at 105 ^{o}C.

3.4.4.3 Disinfection experiment

20 ml of overnight grown culture of bacteria was poured into each petri plate under sterile condition and covered with upper lid. The petri plate was stirred on rotatory shaker at 40 rpm for 360 mins. SPC was performed by following serial dilution against 0 min, 120 min, 240 min and 360 min.

3.4.5 Self Sterilization of Nanoparticles Coated Surface

A glass surface (petri plate) was coated with the same procedure described above for immobilization of NPs. A spray bottle was sterilized and overnight grown bacterial culture was poured into it. Two coated plates and two uncoated (control) plates were kept in sterile fume hood and bacterial culture was sprayed on the plates. Leave the fume hood for 15 minutes. The plates were transferred to laminar flow cabinet while covered. The plates were exposed to fluorescent light

(tube light in laminar flow cabinet) and with sterile cotton swab, the sample for bacterial count was taken from an uncoated plate. The sample was prepared by taking swab thoroughly from the whole plate. The tip of the cotton swab was broken into tube containing 9 ml sterile 0.85% NaCl solution and the tube was stirred vigorously on tube shaker. 1 ml sample from that tube was transferred to a sterile petri plate and 12-16 ml of molten sterile agar solution was poured into it. The sample and agar was mixed by gently revolving the plate anti clockwise twice and once clockwise. After 3 hrs a sample was taken from coated plate in the same manner and after 6 hrs samples were taken from coated and uncoated plates. Prepared the agar plates as mentioned above.

After solidification of agar, the plates were kept into incubator at 37 ^{o}C overnight. Performed bacterial count and recorded next day.

Chapter 4

RESULTS AND DISCUSSIONS

4.1 X-RAY DIFFRACTION

The crystal structure and the crystallite size of the prepared nanoparticles were analyzed by XRD, JEOL JDX-II, X-ray. The results are depicted in Figures 4.1- 4.8, show the characteristic peaks corresponding to anatase phase of TiO_2, so the NPs prepared were all of highest photocatalytic activity among the polymorphs. The relative information corresponding to the peaks are also reported.

All the samples were compared with card no. JCPDS 01-089-4921. The crystal structure was found to be tetragonal which was in agreement of that reported in literature. Peaks obtained at 25.356^o, 37.013, 37.847, 38.644, 48.145, 53.974, 55.186, 62.812, 68.879 and 75.203 were of (101), (103), (004), (112), (200), (105), (211), (204) and (215) planes respectively.

The crystallite size was determined in an indirect way, using Scherrer equation. It was found that all the particles prepared, whether pure titania, silver doped titania or iron doped titania were under 100 nm. Their size ranges between 11 nm to 42 nm. Hence, can strongly be recommended that all were nanoparticles,

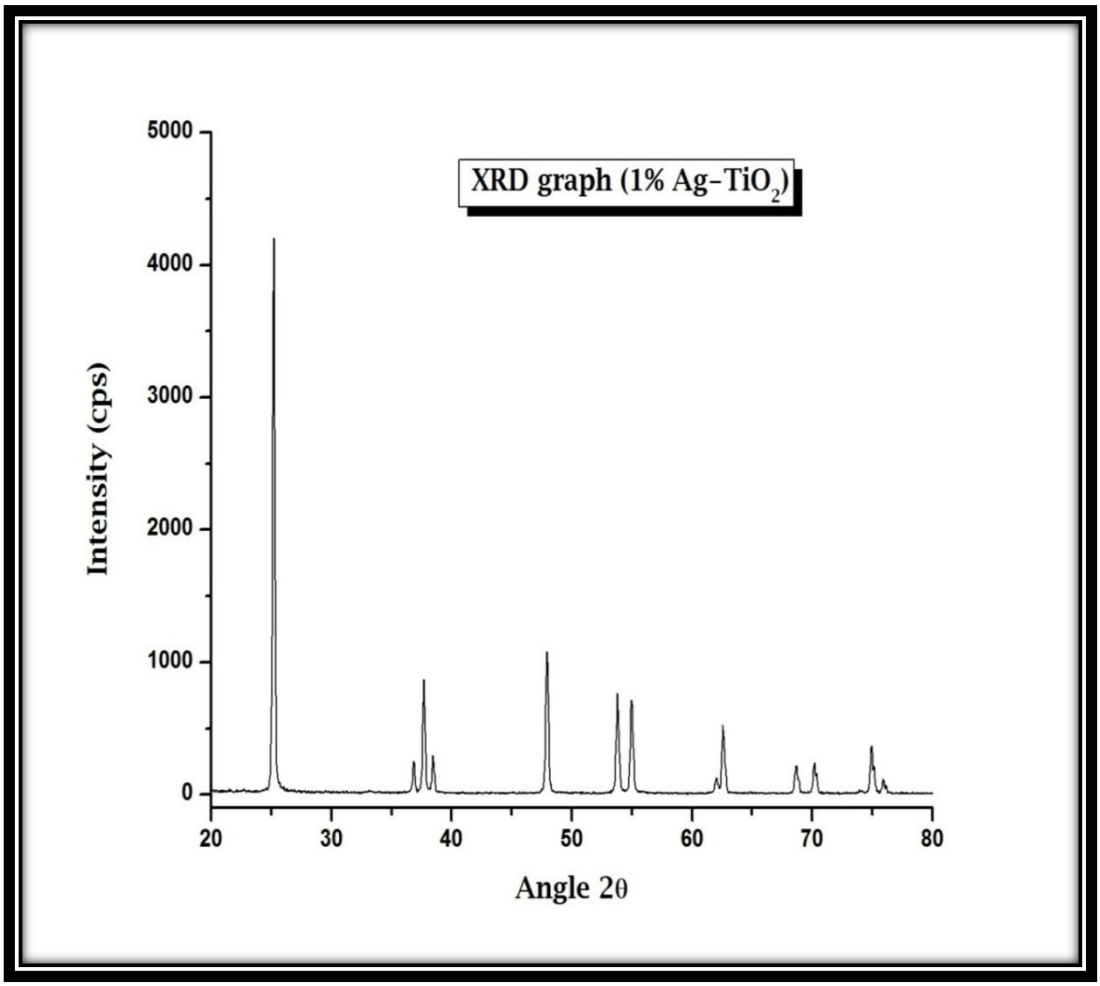

Figure 4. 1: XRD Pattern of 1 % Ag doped TiO_2

Table 4. 1: X-ray Diffractometer Results of 1 % Ag doped TiO_2

Sr. No.	Peak Angle	Spacing	CPS	FWHM
1	25.2	3.53	2478	0.2
2	37.7	2.38	851	0.3
3	47.95	1.89	1086	0.3
4	55	1.67	602	0.35

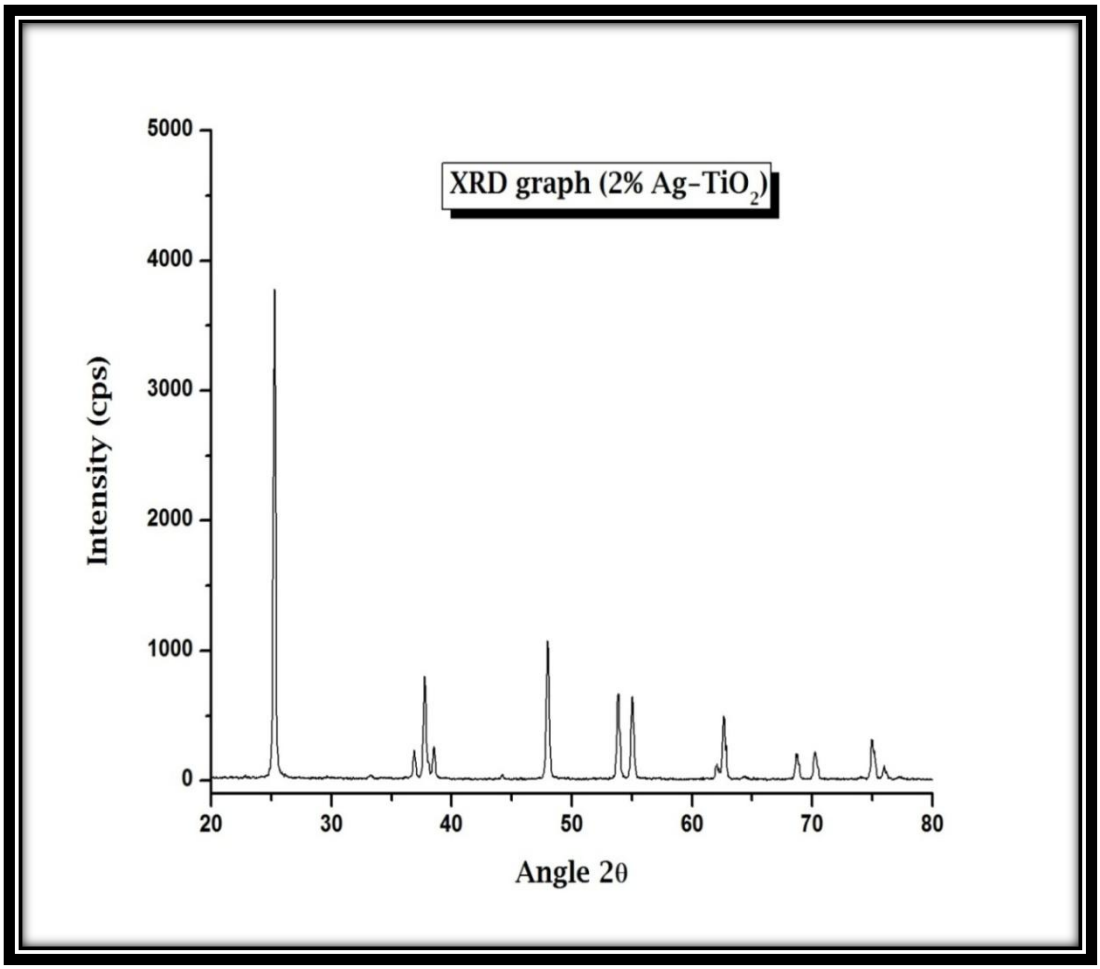

Figure 4. 2: XRD Pattern of 2 % Ag doped TiO_2

Table 4. 2: X-ray Diffractometer Results of 2 % Ag doped TiO_2

Sr. No.	Peak Angle	Spacing	CPS	FWHM
1	25.2	3.53	3867	0.2
2	37.7	2.38	838	0.3
3	47.95	1.89	1037	0.3
4	55	1.67	617	0.35

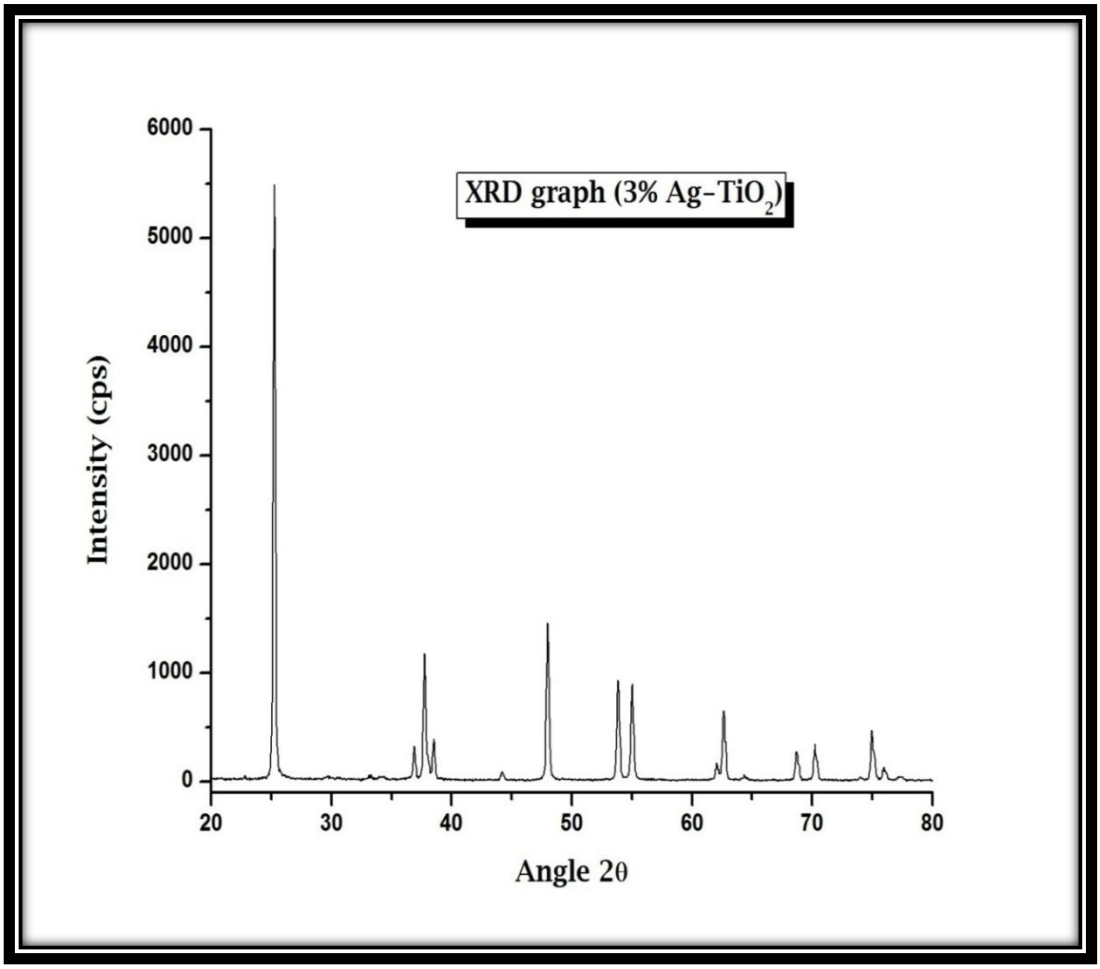

Figure 4. 3: XRD Pattern of 3 % Ag doped TiO_2

Table 4. 3: X-ray Diffractometer Results of 3 % Ag doped TiO_2

Sr. No.	Peak Angle	Spacing	CPS	FWHM
1	25.2	3.53	4345	0.2
2	37.7	2.38	954	0.3
3	47.95	1.89	1100	0.3
4	55	1.67	697	0.35

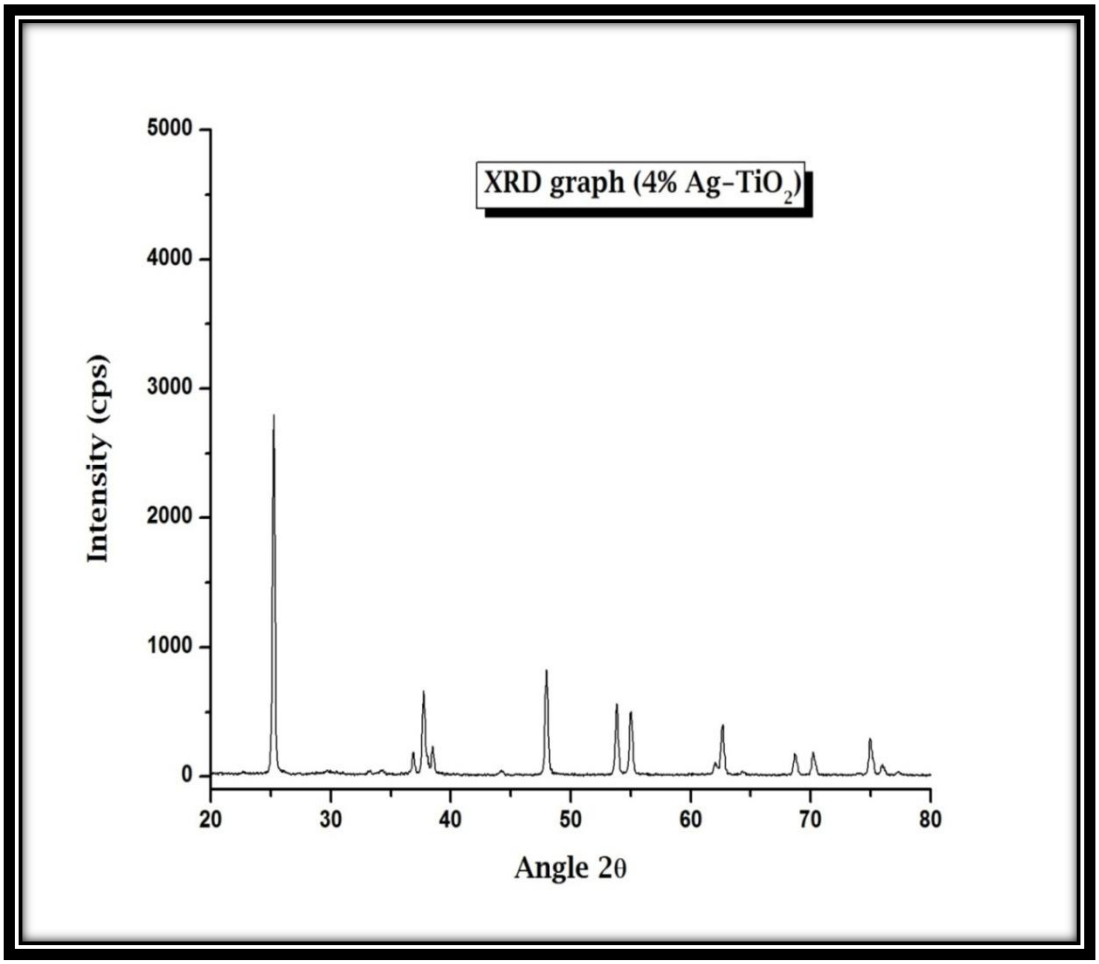

Figure 4. 4: XRD Pattern of 4 % Ag doped TiO_2

Table 4. 4: X-ray Diffractometer Results of 4 % Ag doped TiO_2

Sr. No.	Peak Angle	Spacing	CPS	FWHM
1	25.2	3.53	4418	0.2
2	37.7	2.38	935	0.3
3	47.95	1.89	1048	0.3
4	55	1.67	687	0.35

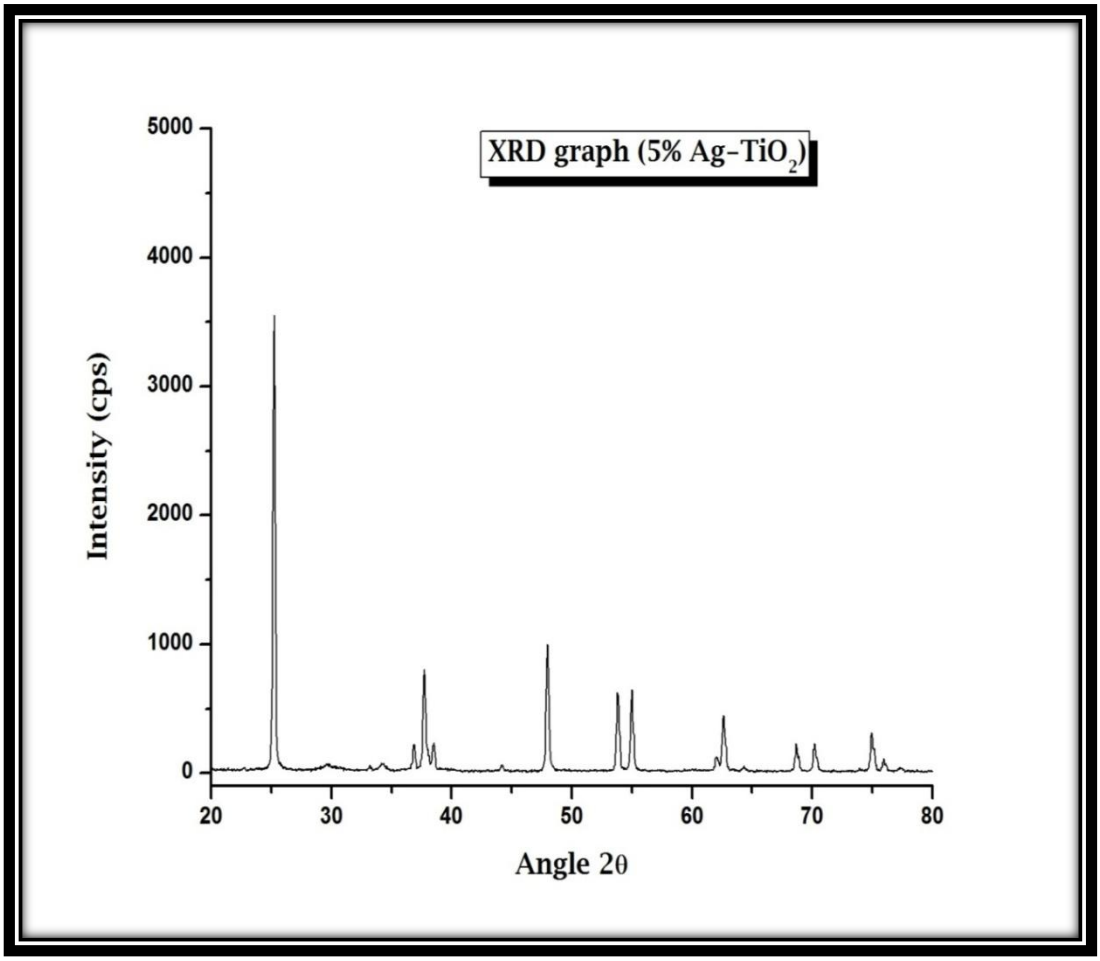

Figure 4. 5: XRD Pattern of 5 % Ag doped TiO_2

Table 4. 5: X-ray Diffractometer Results of 5 % Ag doped TiO_2

Sr. No.	Peak Angle	Spacing	CPS	FWHM
1	25.2	3.53	3867	0.2
2	37.7	2.38	838	0.3
3	47.95	1.89	1037	0.3
4	55	1.67	617	0.35

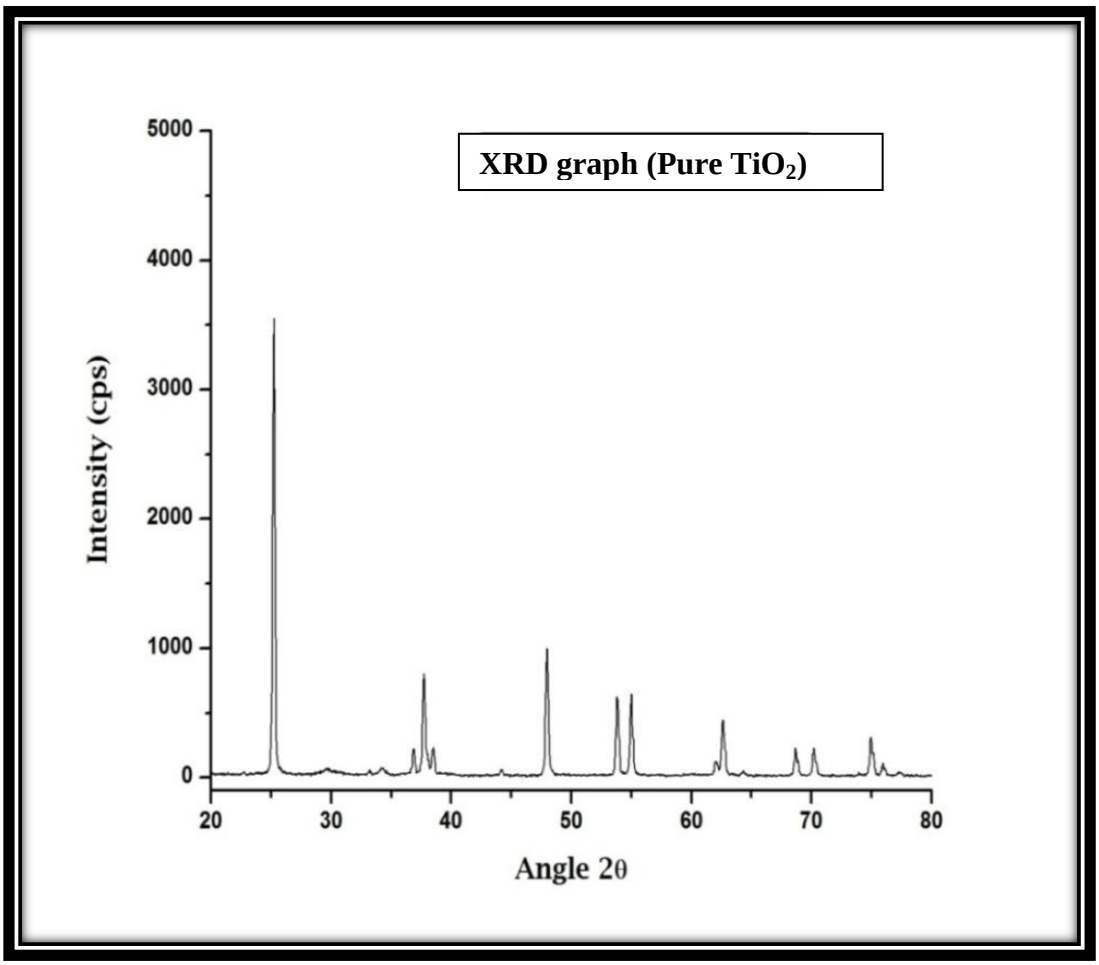

Figure 4. 6: XRD Pattern of 1% Fe doped TiO_2

Table 4. 6: X-ray Diffractometer Results of Pure TiO_2

Sr. No.	Peak Angle	Spacing	CPS	FWHM
1	25.2	3.53	3867	0.2
2	37.7	2.38	838	0.3
3	47.95	1.89	1037	0.3
4	55	1.67	617	0.35

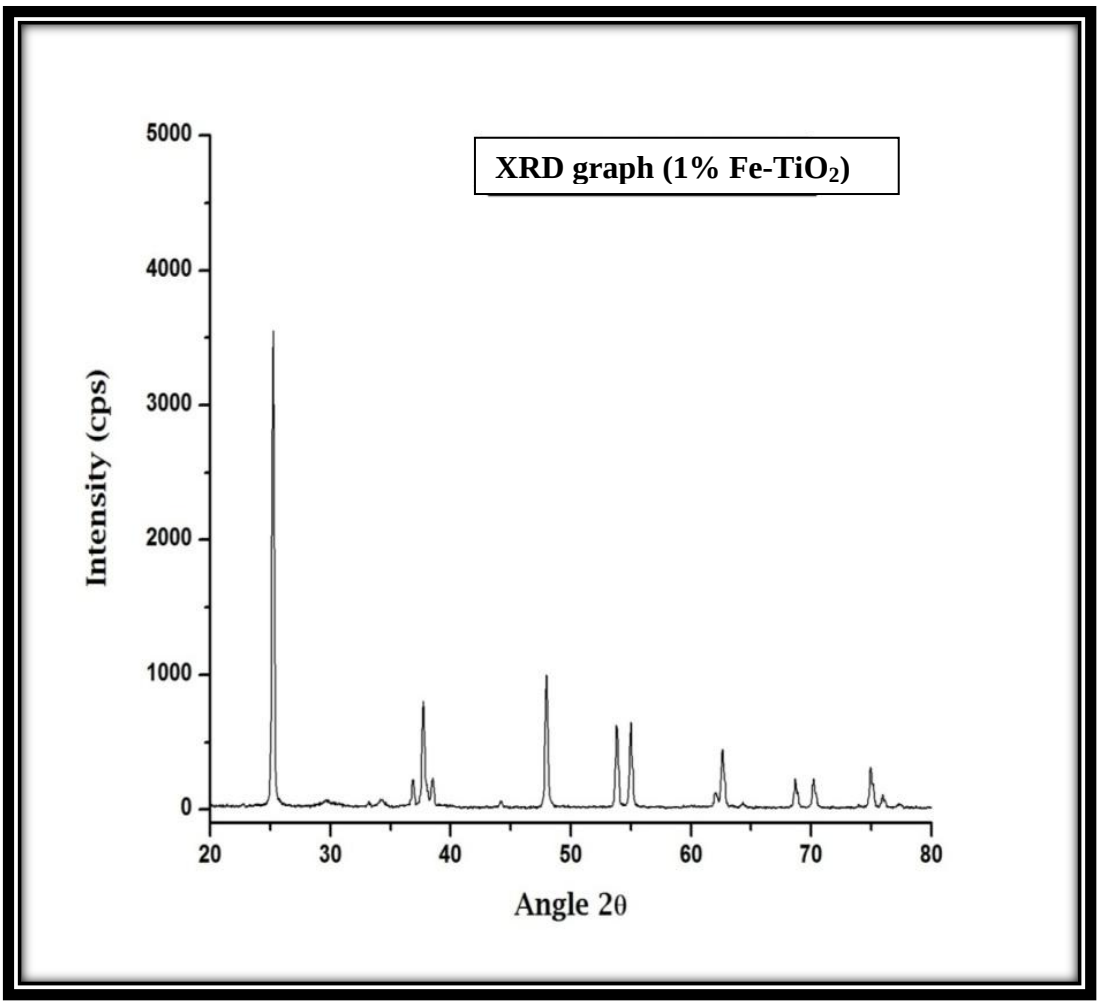

Figure 4. 7: XRD Pattern of 1% Fe doped TiO_2

Table 4. 7: X-ray Diffractometer Results of 1 % Fe doped TiO_2

Sr. No.	Peak Angle	Spacing	CPS	FWHM
1	25.2	3.53	3867	0.2
2	37.7	2.38	838	0.3
3	47.95	1.89	1037	0.3
4	55	1.67	617	0.35

4.2 SCANNING ELECTRON MICROSCOPIC IMAGES

Figures 4.9- 4.24 show the images of doped and undoped titania NPs by JEOL JSM-6460 at 500 and 10,000 magnification. Images of undoped TiO_2 (Figure 4.9, 4.10) confirms the presence of porous, sponge like structure of high roughness and complexity. Such structure indicates the high surface area which has been proven to be efficient for photo catalytic degradation purposes.

Metal deposition effects the surface characteristics of the resulting doped TiO_2 NPs. Images of doped titania NPs (Figure 4.11-4.24) show that the distribution of the dopant metal on surface of titania is not uniform and doped species contain irregular shaped particles which are the aggregations of the tiny crystals.

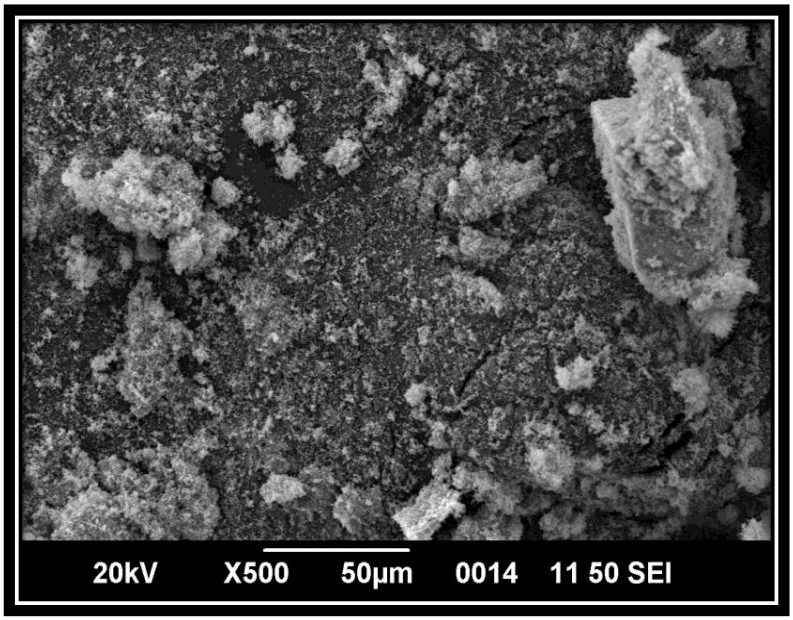

Figure 4. 8: SEM image of Pure TiO_2 taken at X500

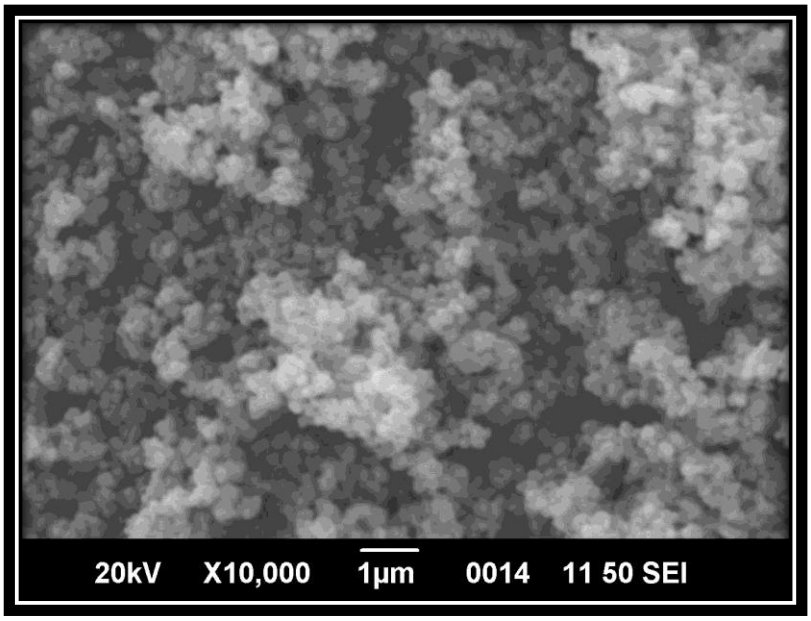

Figure 4. 9: SEM image of Pure TiO_2 taken at X10,000

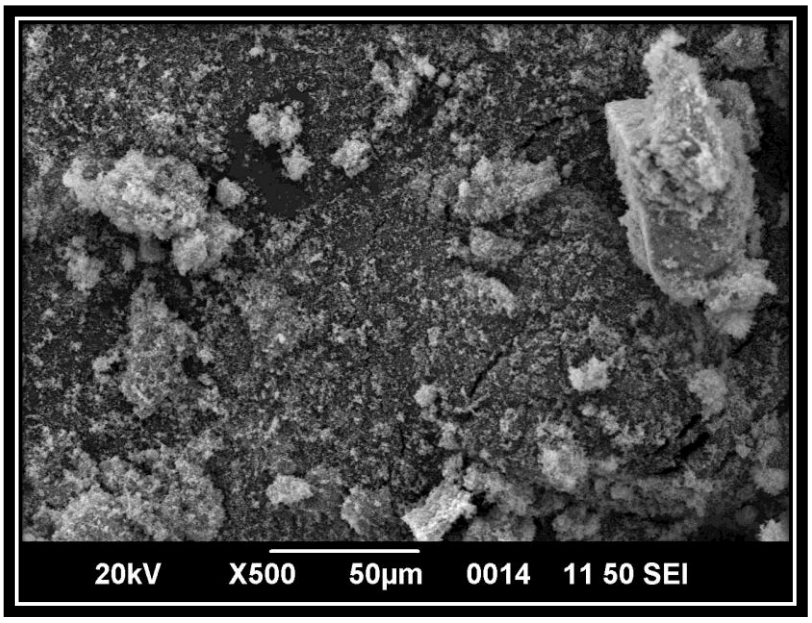

Figure 4. 10: SEM image of 1% Ag doped TiO_2 taken at X500

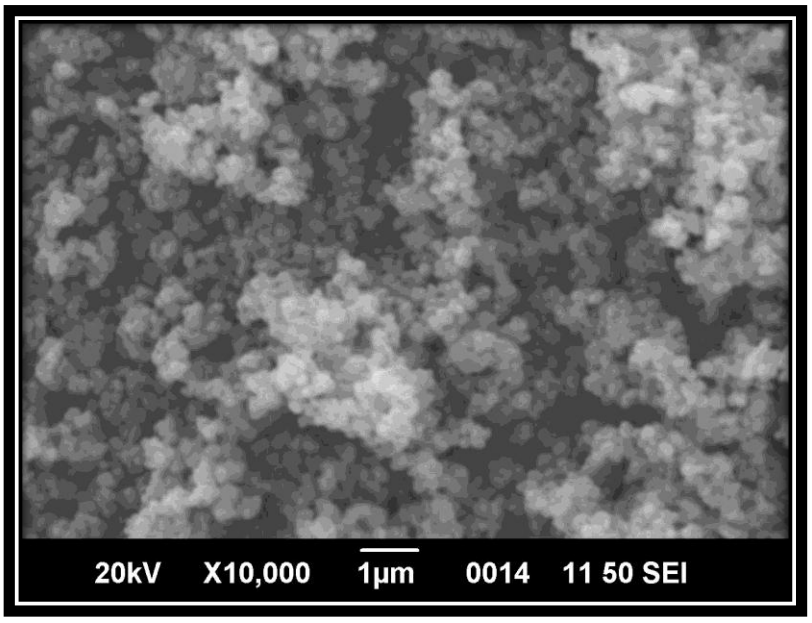

Figure 4. 11: SEM image of 1% Ag doped TiO_2 taken at X10,000

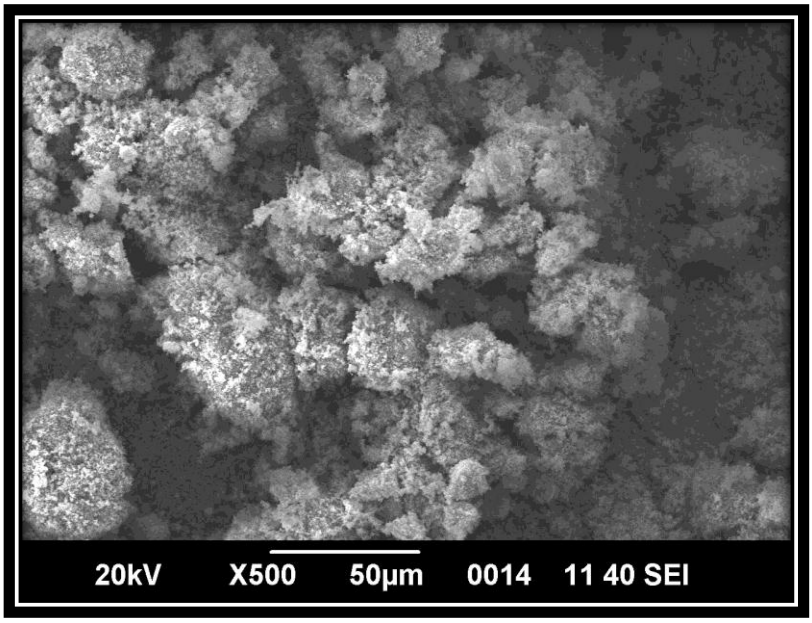

Figure 4. 12: SEM image of 2% Ag doped TiO_2 taken at X500

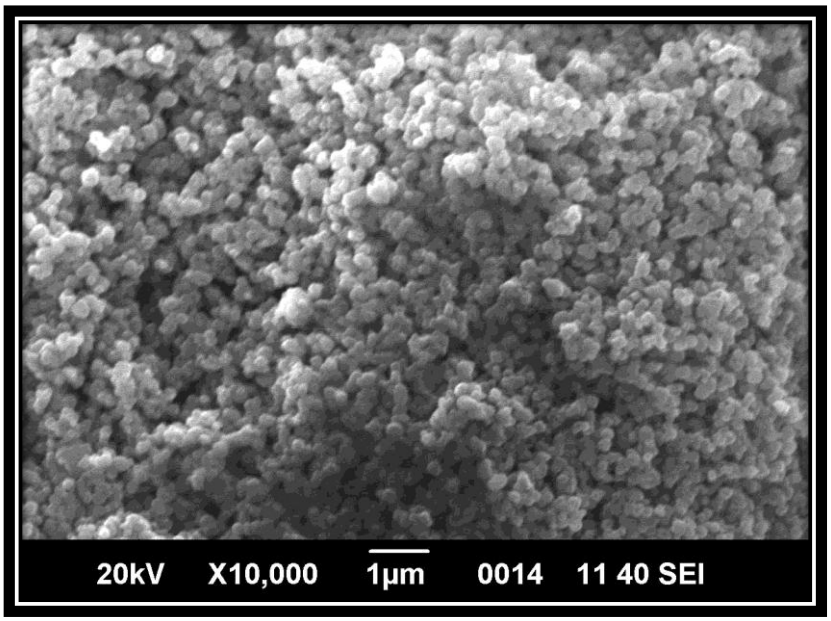

Figure 4. 13: SEM image of 2% Ag doped TiO_2 taken at X10,000

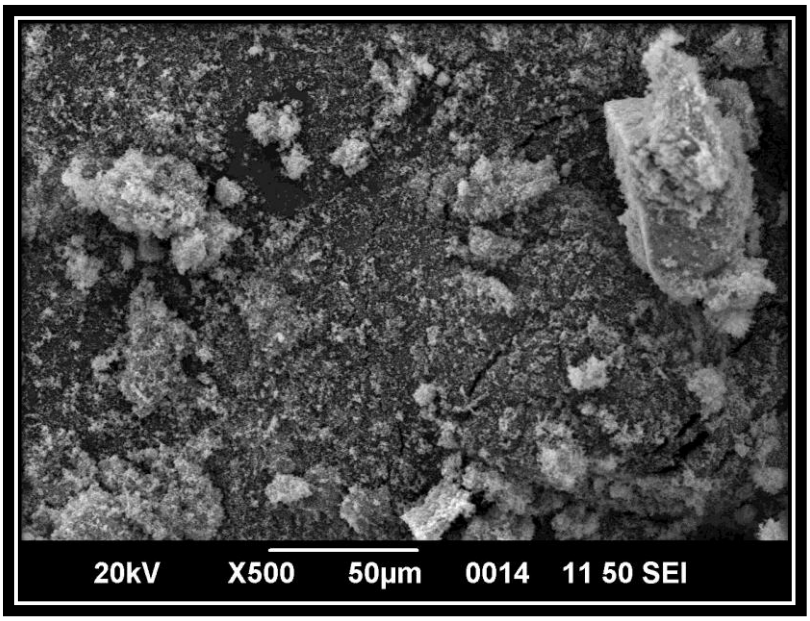

Figure 4. 15: SEM image of 3% Ag doped TiO_2 taken at X500

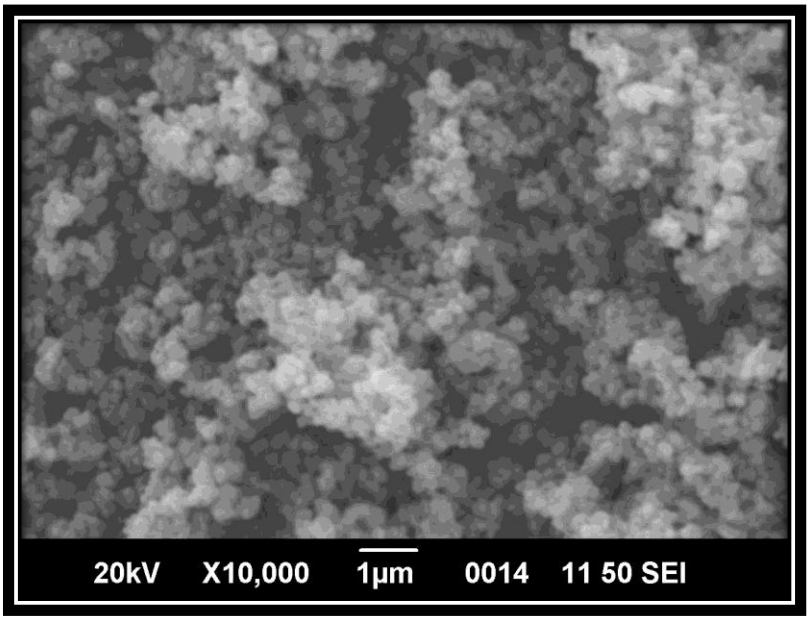

Figure 4. 14: SEM image of 3% Ag doped TiO_2 taken at X10,000

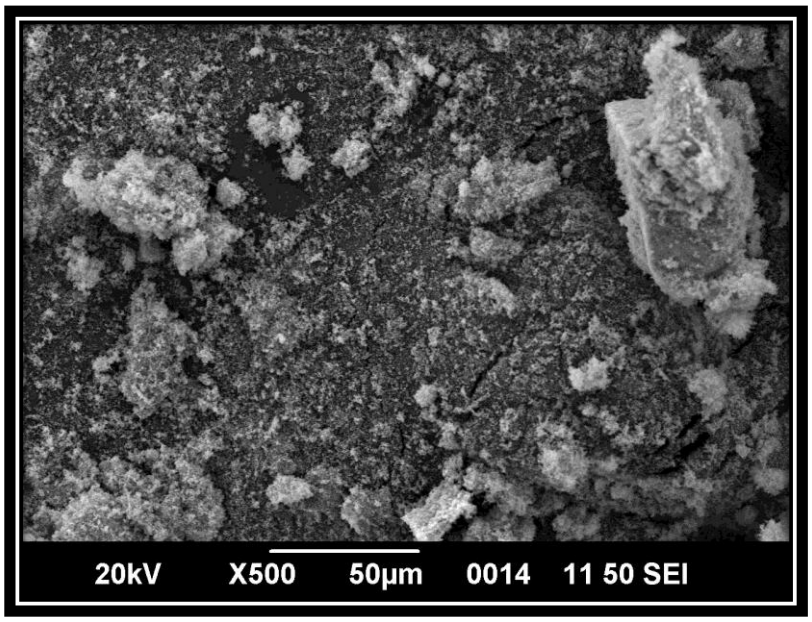

Figure 4. 17: SEM image of 4% Ag doped TiO_2 taken at X500

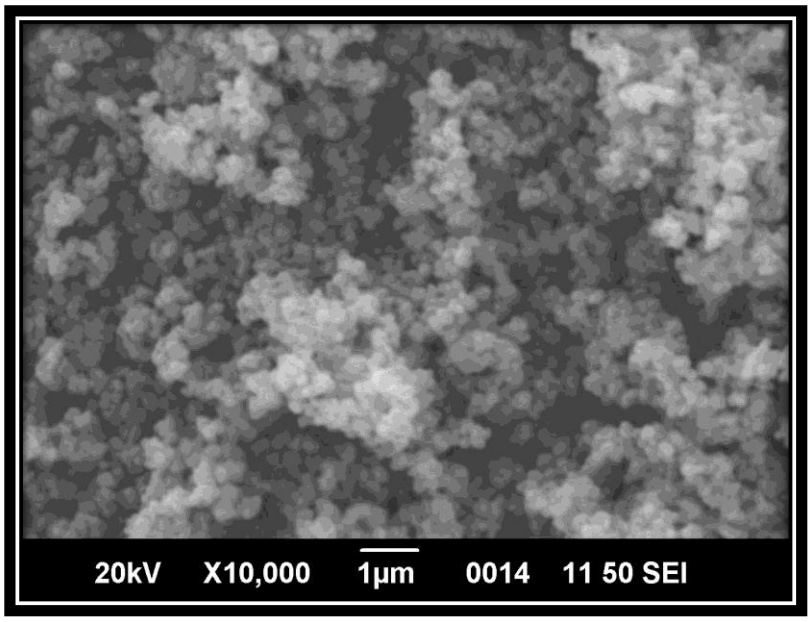

Figure 4. 16: SEM image of 4% Ag doped TiO_2 taken at X10,000

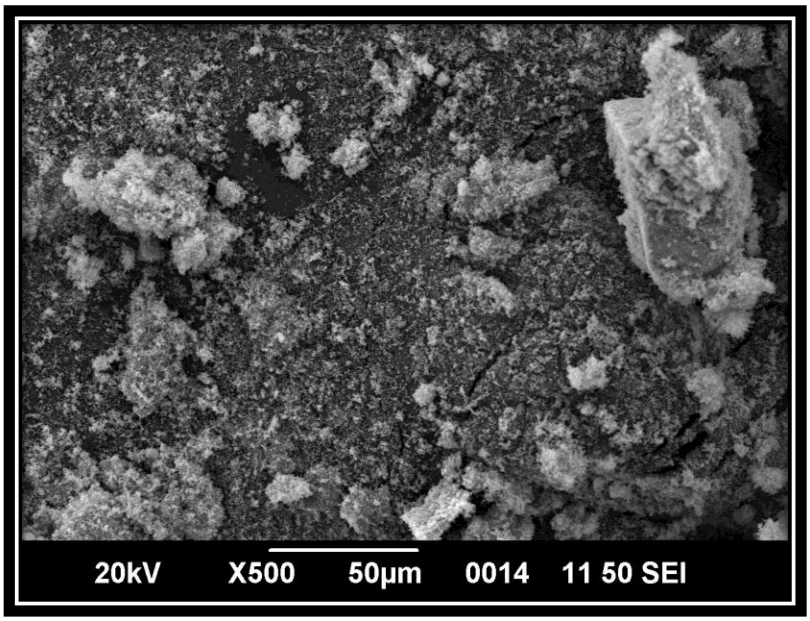

Figure 4. 19: SEM image of 5% Ag doped TiO_2 taken at X500

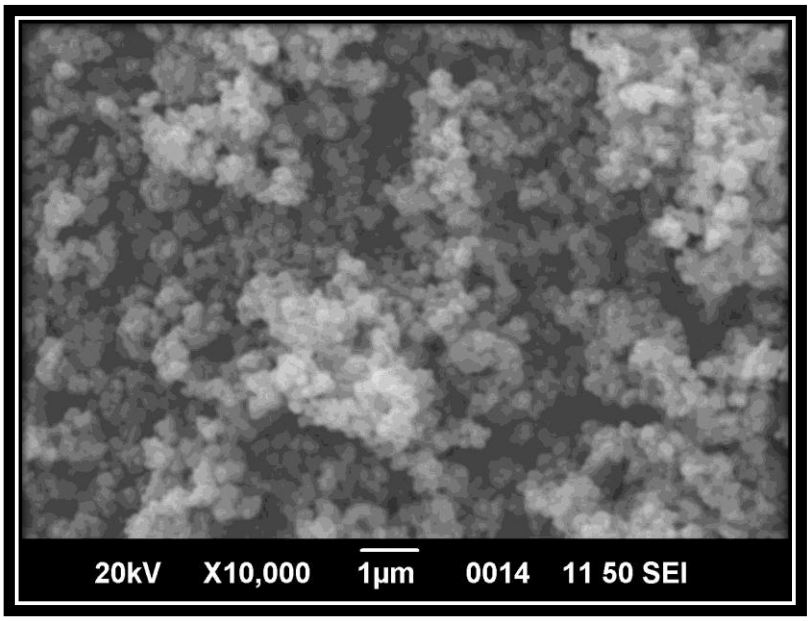

Figure 4. 18: SEM image of 5% Ag doped TiO_2 taken at X10,000

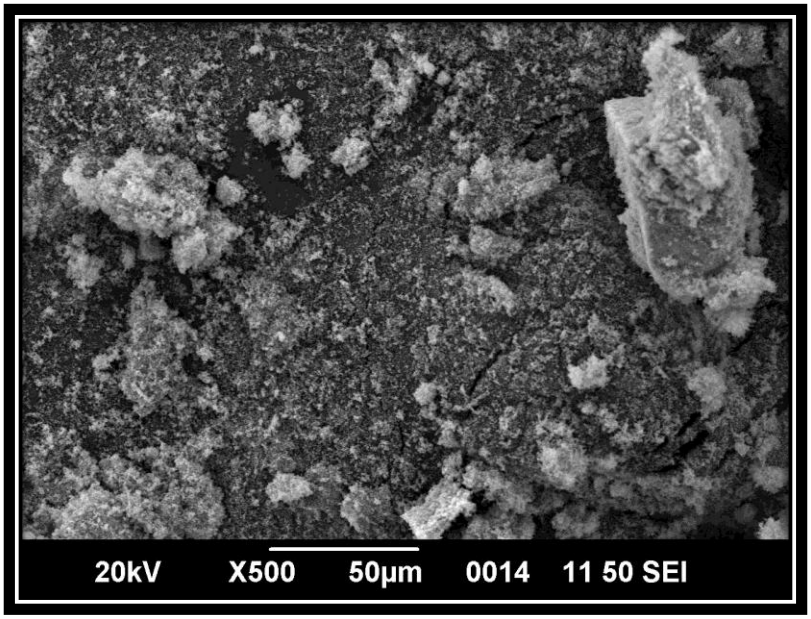

Figure 4. 21: SEM image of 1% Fe doped TiO_2 taken at X500

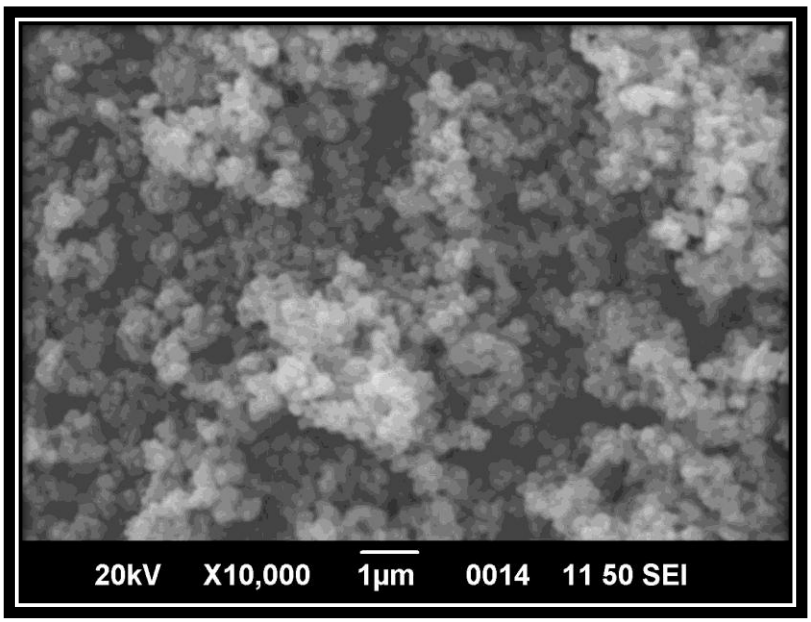

Figure 4. 20: SEM image of 1% Fe doped TiO_2 taken at X10,000

4.3 ENERGY DISPERSIVE SPECTROSCOPY

Energy dispersive spectroscopy analysis showed that the percent composition is not homogenous in the doped TiO_2 NPs. It varies from point to point showing diverse composition of the prepared NPs that confirms the SEM results.

The result obtained from EDS elemental analysis regarding the extent of metal doping were in accordance with the actual amount of the dopant employed in the lab for synthesis of doped titania NPs, the results obtained are shown in Table 4.9.

Table 4. 8: EDS analysis of doped and undoped TiO_2 NPs

Sr. No.	Sample	Average Relative Percent Elemental Atomic Ratios		
		Ti	Fe	Ag
1	Undoped TiO_2	100.00	--	--
2	1% Fe doped TiO_2	99.08	0.92	--
3	1% Ag doped TiO_2	99.02	--	0.98
4	2% Ag doped TiO_2	97.65	--	2.35
5	3% Ag doped TiO_2	96.48	--	3.52
6	4% Ag doped TiO_2	95.84	--	4.16
7	5% Ag doped TiO_2	94.40	--	5.60

4.4 BACTERICIDAL EFFECT STUDIES OF DIFFERENT NANOPARTICLES

4.4.1 Selection of Metal to be Doped

4.4.1.1 Fe-TiO_2

Table 4. 9: Percentage bacterial removal by 1% Fe-TiO_2

Sr. No.	Time of Plating (min)	%age bactericidal effect
1	0	0
2	30	47
3	60	60
4	90	70
5	120	76

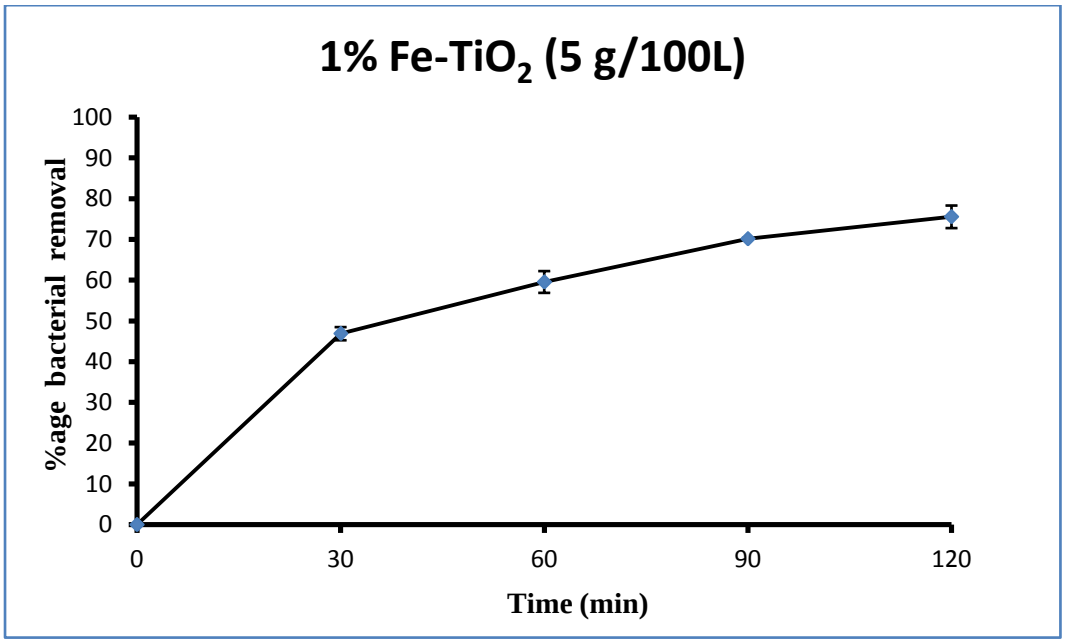

Figure 4. 22: Biocidal effect of Fe-TiO_2

4.4.1.2 Ag-TiO_2

5 g/100ml concentration of 1% Fe-TiO_2 was applied to *E. coli* culture and SPCs were recorded with 30 min time interval starting from the 0 min (time when NPs applied)

Table 4. 8: Percentage bacterial removal by 1% Ag-TiO_2

Sr. No.	Time of Plating (min)	%age bactericidal effect
1	0	0
2	30	87
3	60	99
4	90	100
5	120	100

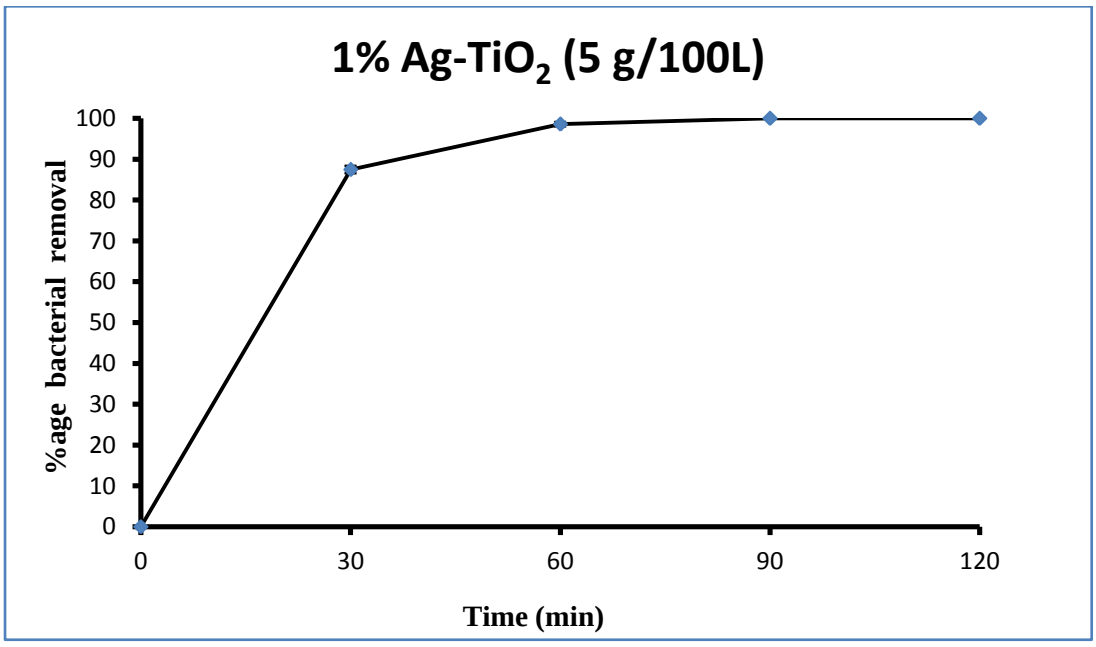

Figure 4. 23: Biocidal effect of 1% Ag-TiO_2

The results depict that 1% Fe-TiO_2 does not possess as high inactivation capability as 1% Ag-TiO_2. Ag-TiO_2 removed bacteria upto 99% in 60 min and Fe-TiO_2 was able to kill only 76% of the initial concentration of the bacteria. For further work, therefore, Ag-TiO_2 under different doping percentages was considered.

4.4.2 Optimization of Nanoparticles Concentration

For optimization of NPs concentration, 2% Ag-TiO_2 was used with different loadings. 0.1 g/100ml, 0.5 g/100ml, 1 g/100ml, 3 g/100ml, 5 g/100ml and 7.5 g/100ml of 2% Ag-TiO_2 was added to form suspension with bacterial culture. All experiments were performed under the influence of fluorescent light.

4.4.2.1 2% Ag-TiO_2 (0.1 g/100ml)

Table 4. 9: Percentage bacterial removal by 2% Ag-TiO_2 (0.1 g/100ml)

Sr. No.	Time of Plating (min)	%age bactericidal effect
1	0	0
2	30	7
3	60	12
4	90	17
5	120	23

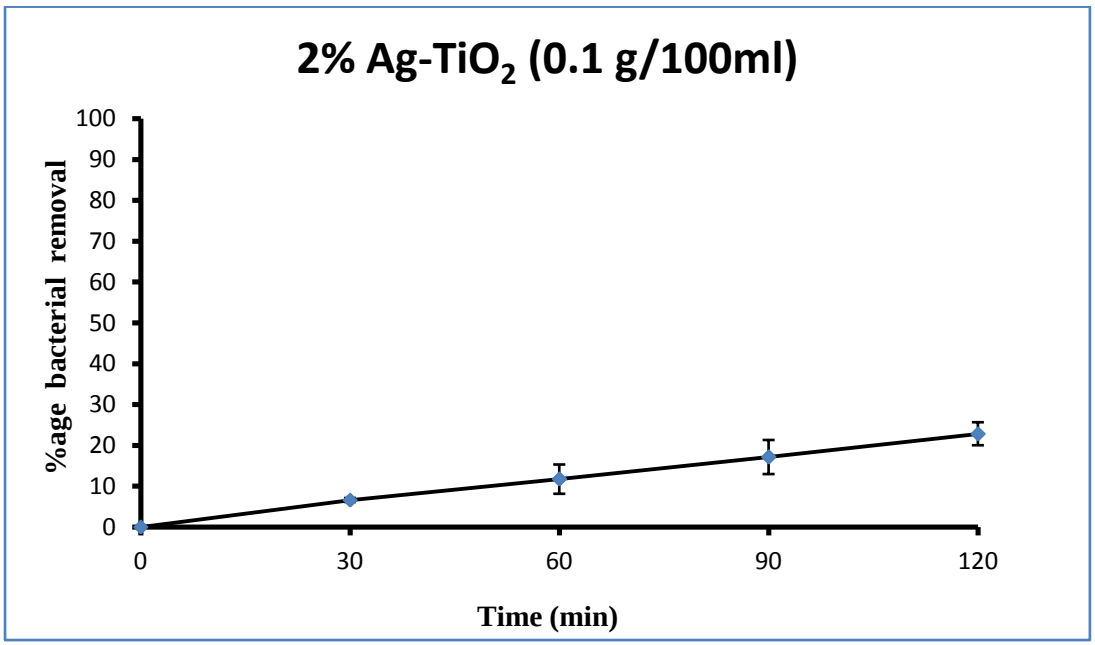

Figure 4. 24: Percentage bacterial removal by 0.1 g/100ml loading of 2% Ag-TiO_2

4.4.2.2 2% Ag-TiO_2 (0.5 g/100ml)

Table 4. 10: Percentage bacterial removal by 2% Ag-TiO_2 (0.5 g/100ml)

Sr. No.	Time of Plating (min)	%age bactericidal effect
1	0	0
2	30	28
3	60	42
4	90	49
5	120	54

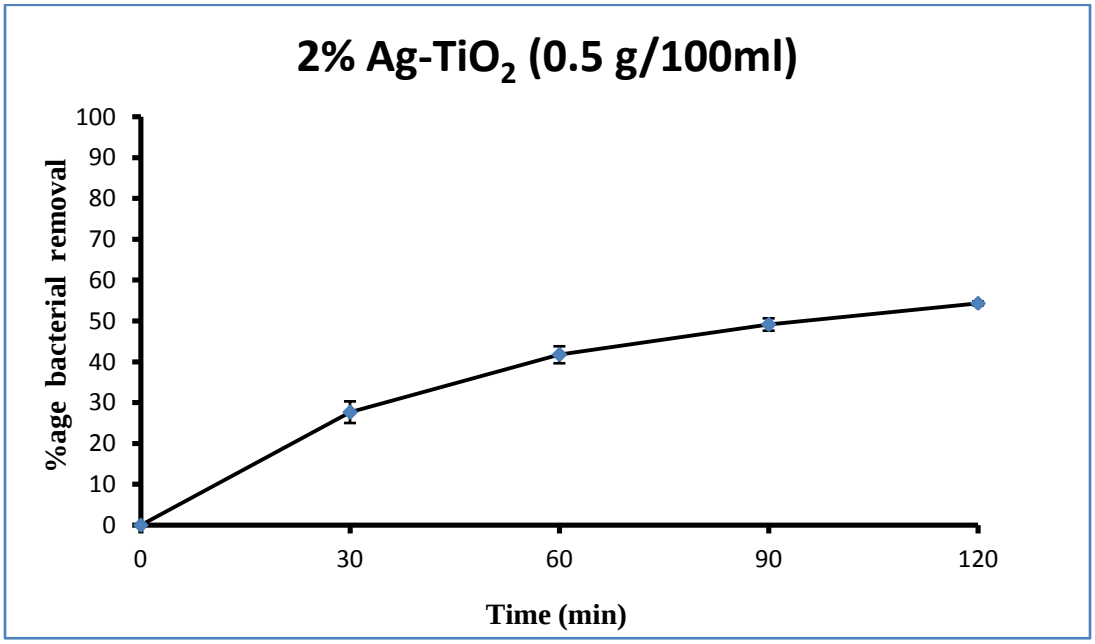

Figure 4. 25: Percentage bacterial removal by 0.5 g/100ml loading of 2% Ag-TiO_2

4.4.2.3 2% Ag-TiO_2 (1 g/100ml)

Table 4. 11: Percentage bacterial removal by 2% Ag-TiO_2 (1 g/100ml)

Sr. No.	Time of Plating (min)	%age bactericidal effect
1	0	0
2	30	37
3	60	47
4	90	59
5	120	70

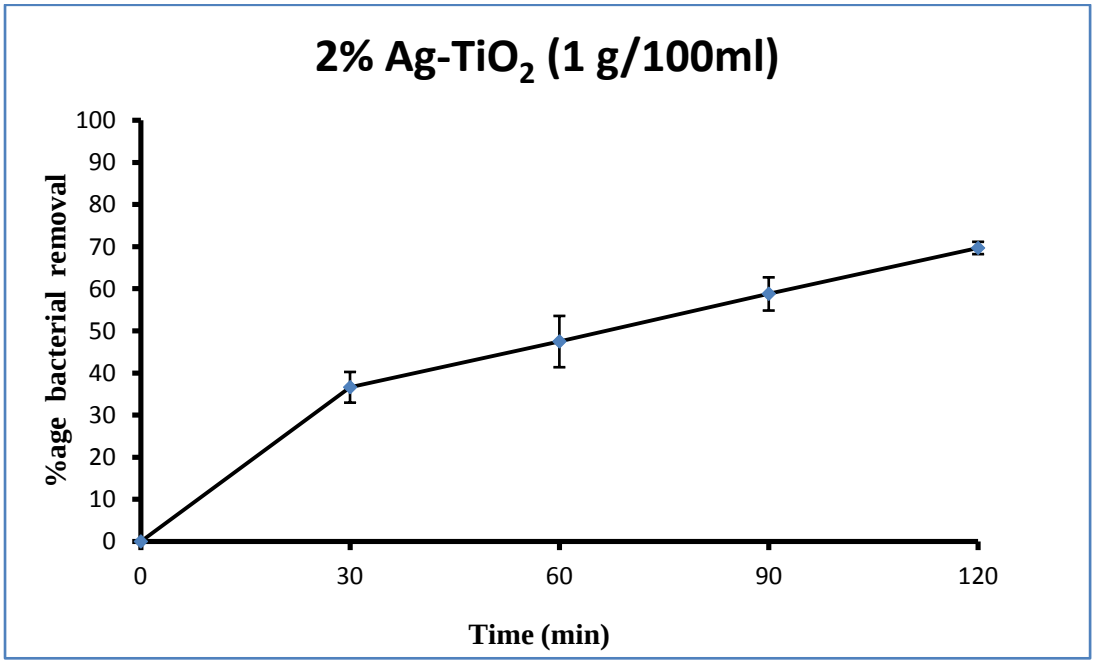

Figure 4. 26: Percentage bacterial removal by 1 g/100ml loading of 2% Ag-TiO_2

4.4.2.4 2% Ag-TiO_2 (5 g/100ml)

Table 4. 12: Percentage bacterial removal by 2% Ag-TiO_2 (5 g/100ml)

Sr. No.	Time of Plating (min)	%age bactericidal effect
1	0	0
2	30	81
3	60	97
4	90	100
5	120	100

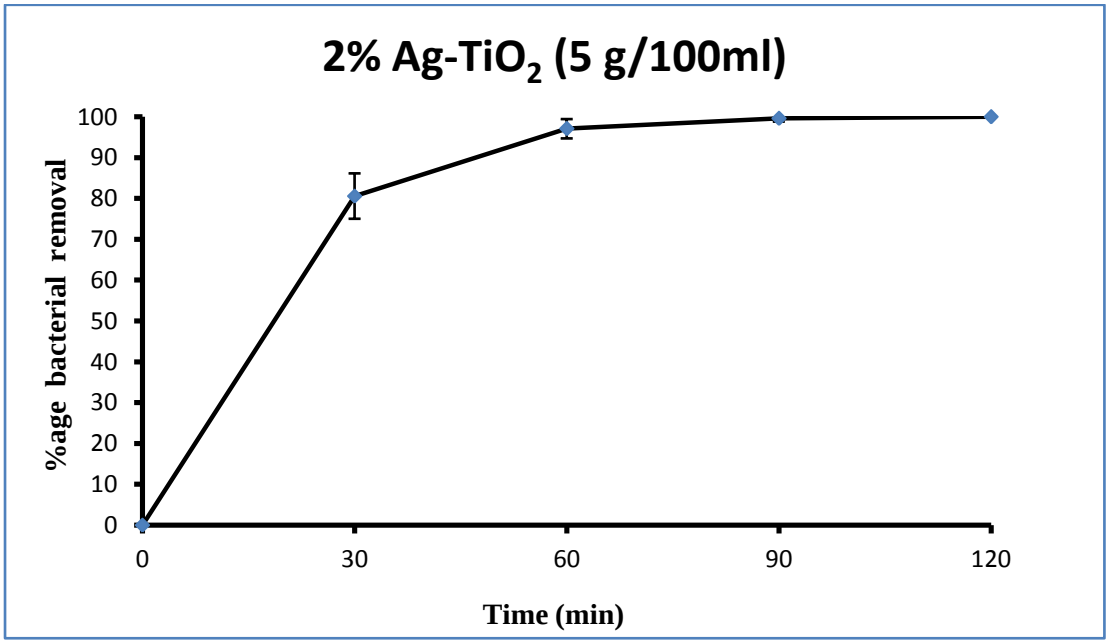

Figure 4. 27: Percentage bacterial removal by 5 g/100ml loading of 2% Ag-TiO_2

4.4.2.1 2% Ag-TiO_2 (7.5 g/100ml)

Table 4. 13: Percentage bacterial removal by 2% Ag-TiO_2 (7.5 g/100ml)

Sr. No.	Time of Plating (min)	%age bactericidal effect
1	0	0
2	30	84
3	60	96
4	90	100
5	120	100

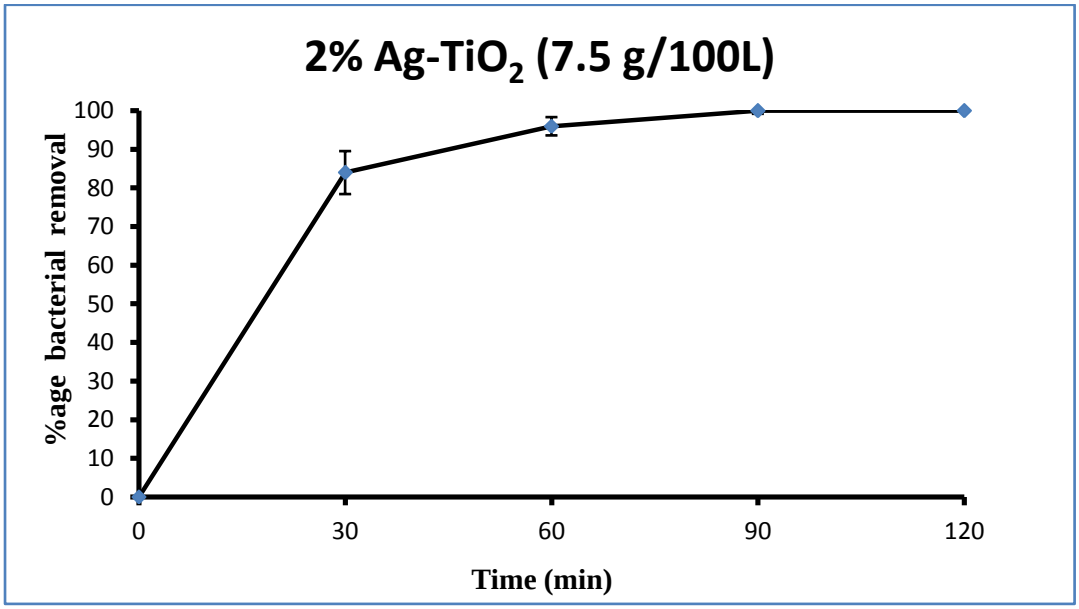

Figure 4. 28: Percentage bacterial removal by 7.5 g/100ml loading of 2% Ag-TiO_2

During the optimization study, it was observed that with the increase in the concentration of NPs the bacterial inactivation rate was also increased. The optimization was done under the influence of fluorescent light (household tube-light) built-in of laminar flow cabinet. The addition of 0.1 g/100ml, 0.5 g/100ml, 1 g/100ml and 5 g/100ml of 2% Ag-TiO_2 followed by constant agitation at 250 rpm was done. The bacterial plate counts were recorded at regular interval of time for 120 min. the data is illustrated in Fig. 12, 13, 14 and 15. As per the Figures, 23% of the initial concentration of the bacteria was inactivated after 120 min with the loading of 0.1 g/100ml of NPs. 54% of the bacteria were killed when the concentration of NPs was increased upto 0.5 g/100ml. The abatement of 70% of bacteria was observed when the NPs were 1 g/100ml and an interesting result of 100% disinfection was recorded with the 5 g/100ml loading of NPs, just after 90 min.

4.4.3 Optimization of Percentage Dopant

5 g/100ml concentration was selected from the previous results and same concentration was used for all %age dopants NPs and pure Titania NPs to optimize and to recommend % age dopant for futher experimentation. All experiments were performed under influence of fluorescent light.

4.4.3.1 0% Ag-TiO_2

Table 4. 14: Percentage bacterial removal by 0% Ag-TiO_2

Sr. No.	Time of Plating (min)	%age bactericidal effect
1	0	0
2	30	2
3	60	3
4	90	3
5	120	4

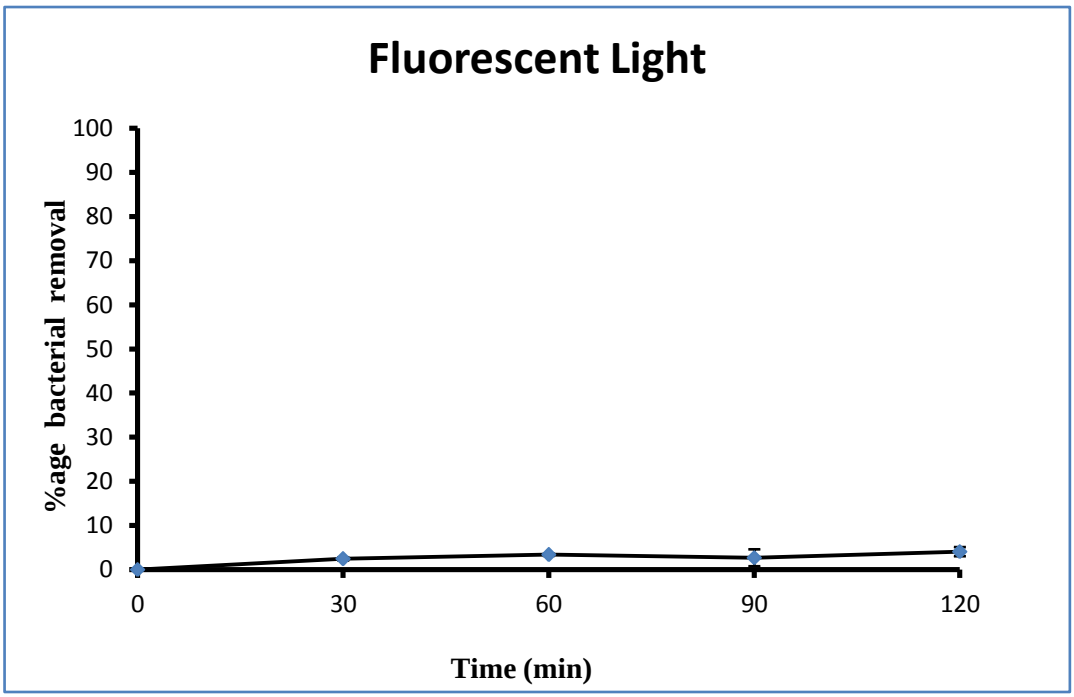

Figure 4. 29: Percentage bacterial removal in the absence of NPs (control exp.)

4.4.3.2 Pure TiO_2

Table 4. 15: Percentage bacterial removal by PureTiO_2 (5 g/100ml)

Sr. No.	Time of Plating (min)	%age bactericidal effect
1	0	0
2	30	4
3	60	4
4	90	3
5	120	3

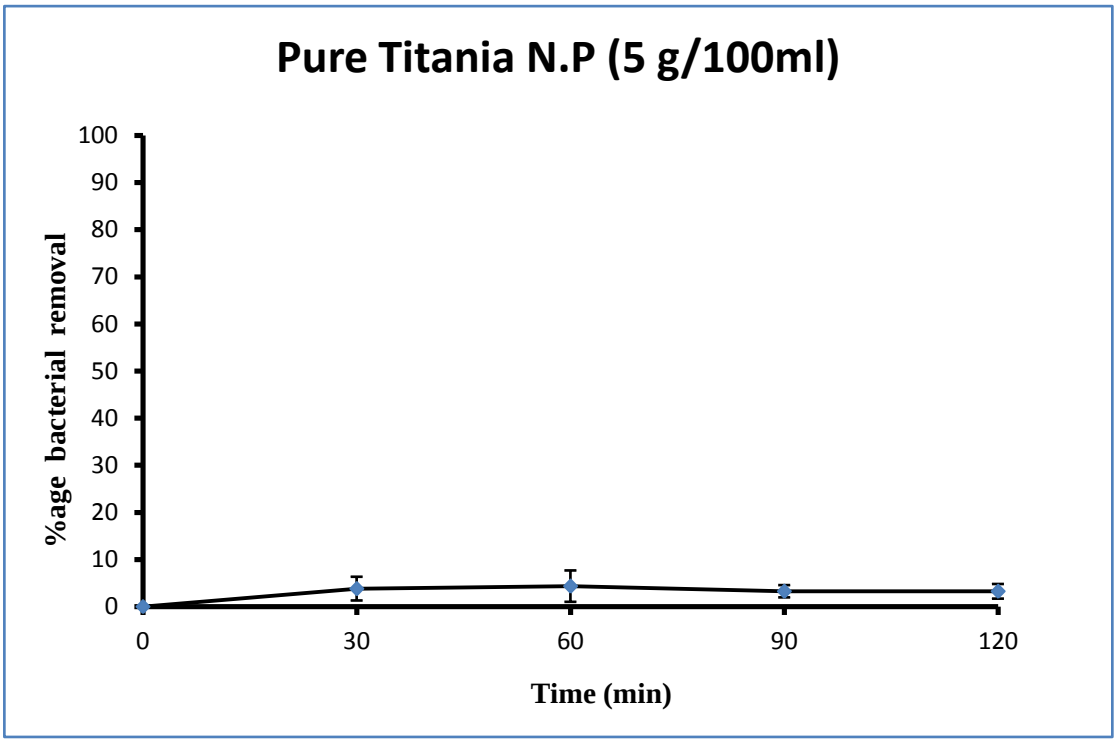

Figure 4. 30: Percentage bacterial removal by Pure TiO_2 NPs

4.4.3.3 1% Ag-TiO_2

Table 4. 16: Percentage bacterial removal by 2% Ag-TiO_2 (5 g/100ml)

Sr. No.	Time of Plating (min)	%age bactericidal effect
1	0	0
2	30	85
3	60	99
4	90	100
5	120	100

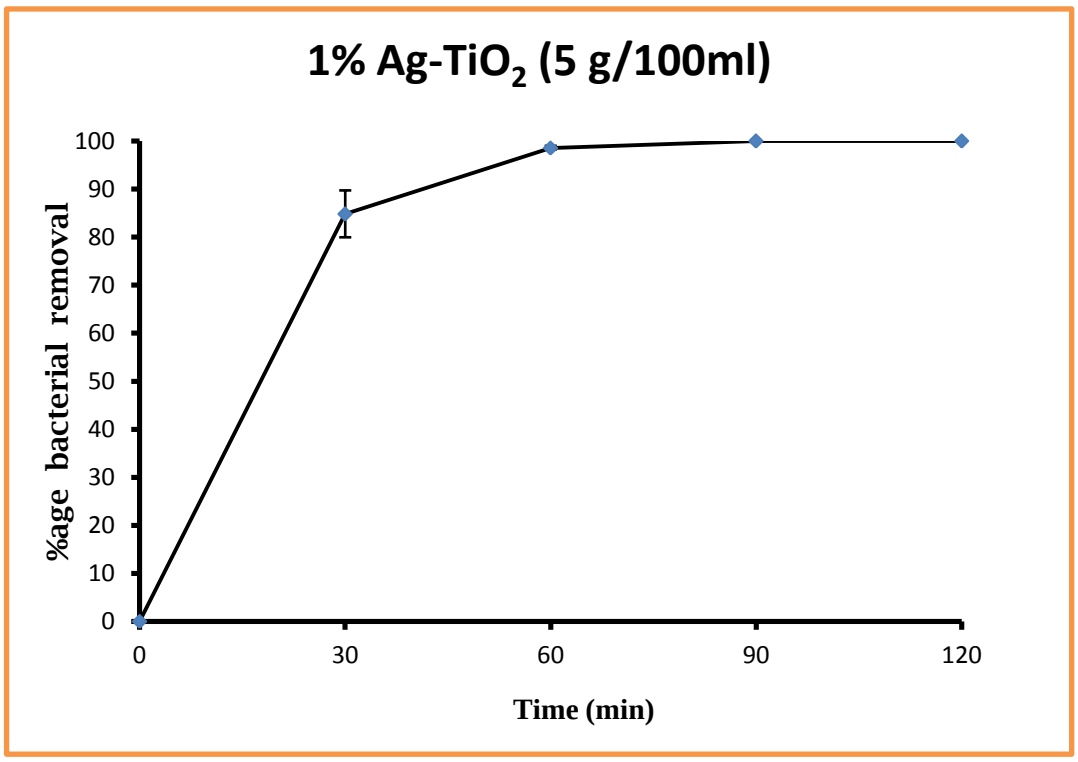

Figure 4. 31: Percentage bacterial removal by 1% Ag-TiO_2 NPs

4.4.3.4 2% Ag-TiO_2

Table 4. 17: Percentage bacterial removal by 2% Ag-TiO_2 (5 g/100ml)

Sr. No.	Time of Plating (min)	%age bactericidal effect
1	0	0
2	30	81
3	60	97
4	90	100
5	120	100

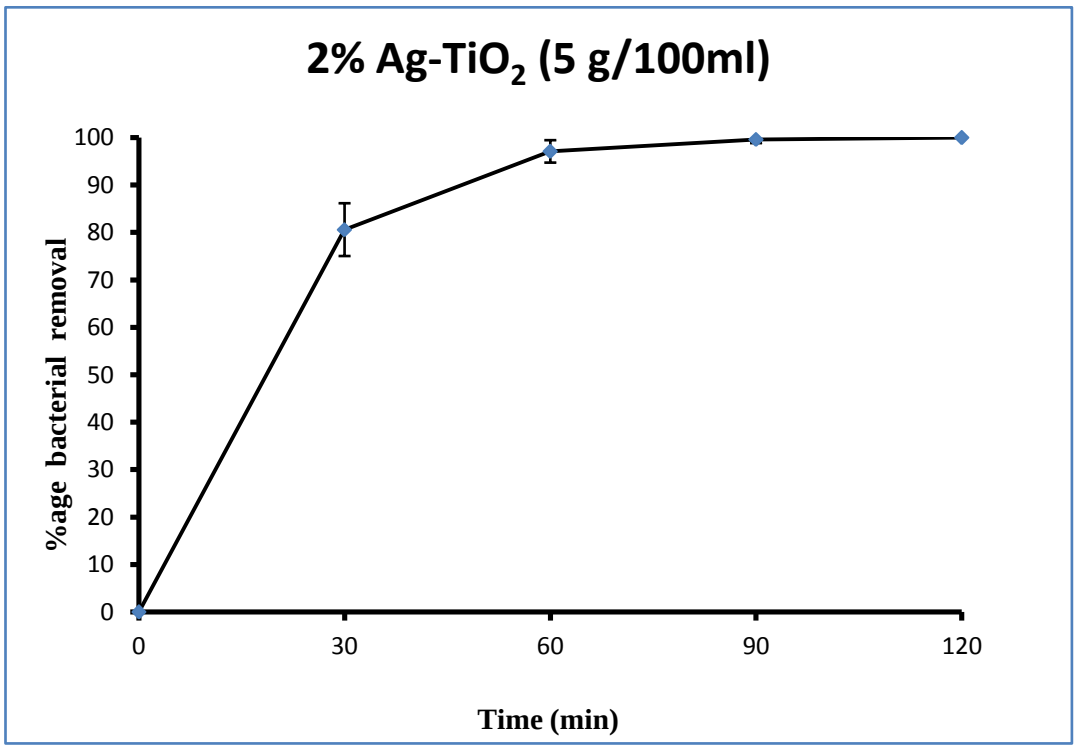

Figure 4. 32: Percentage bacterial removal by 2% Ag-TiO_2 NPs

4.4.3.5 3% Ag-TiO_2

Table 4. 18: Percentage bacterial removal by 3% Ag-TiO_2 (5 g/100ml)

Sr. No.	Time of Plating (min)	%age bactericidal effect
1	0	0
2	30	65
3	60	91
4	90	99
5	120	100

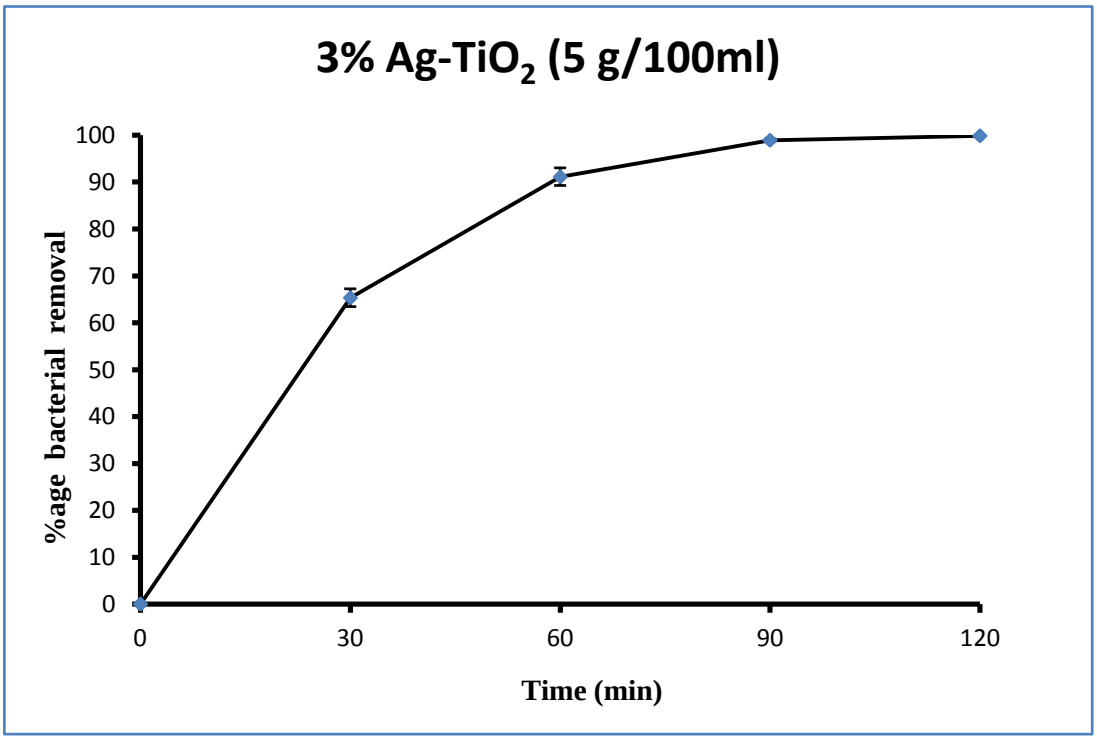

Figure 4. 33: Percentage bacterial removal by 3% Ag-TiO_2 NPs

4.4.3.6 4% Ag-TiO_2

Table 4. 19: Percentage bacterial removal by 4% Ag-TiO_2 (5 g/100ml)

Sr. No.	Time of Plating (min)	%age bactericidal effect
1	0	0
2	30	85
3	60	97
4	90	99
5	120	100

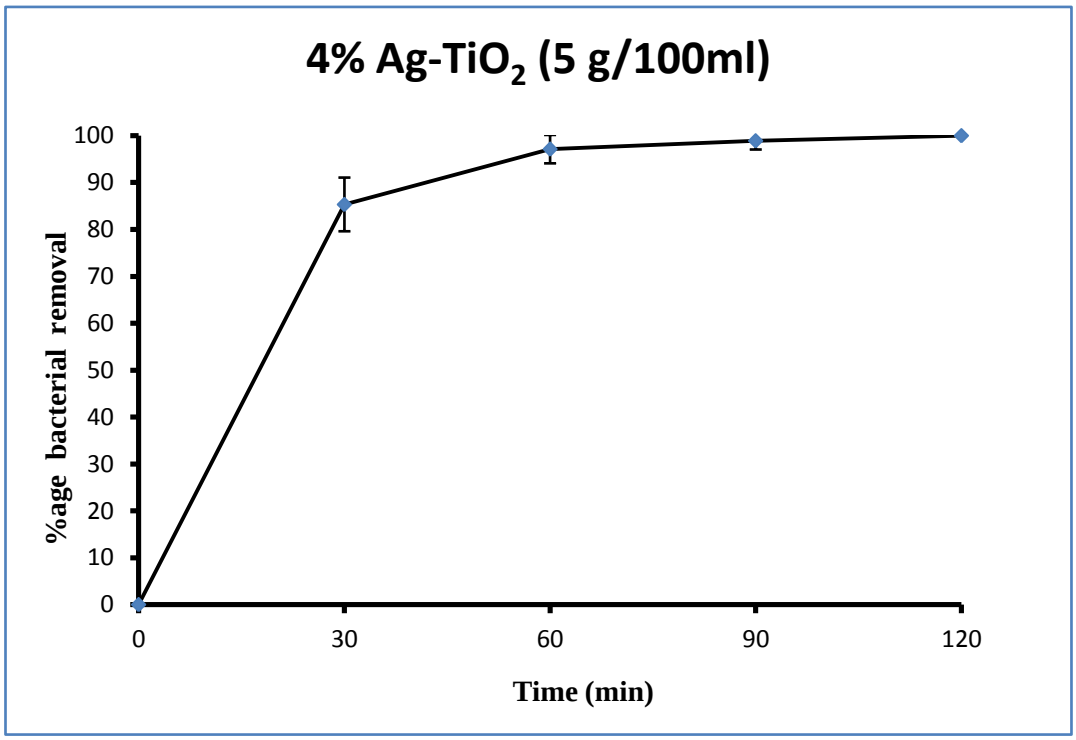

Figure 4. 34: Percentage bacterial removal by 4% Ag-TiO_2 NPs

4.4.3.7 5% Ag-TiO_2

Table 4. 20: Percentage bacterial removal by 5% Ag-TiO_2 (5 g/100ml)

Sr. No.	Time of Plating (min)	%age bactericidal effect
1	0	0
2	30	75
3	60	82
4	90	90
5	120	96

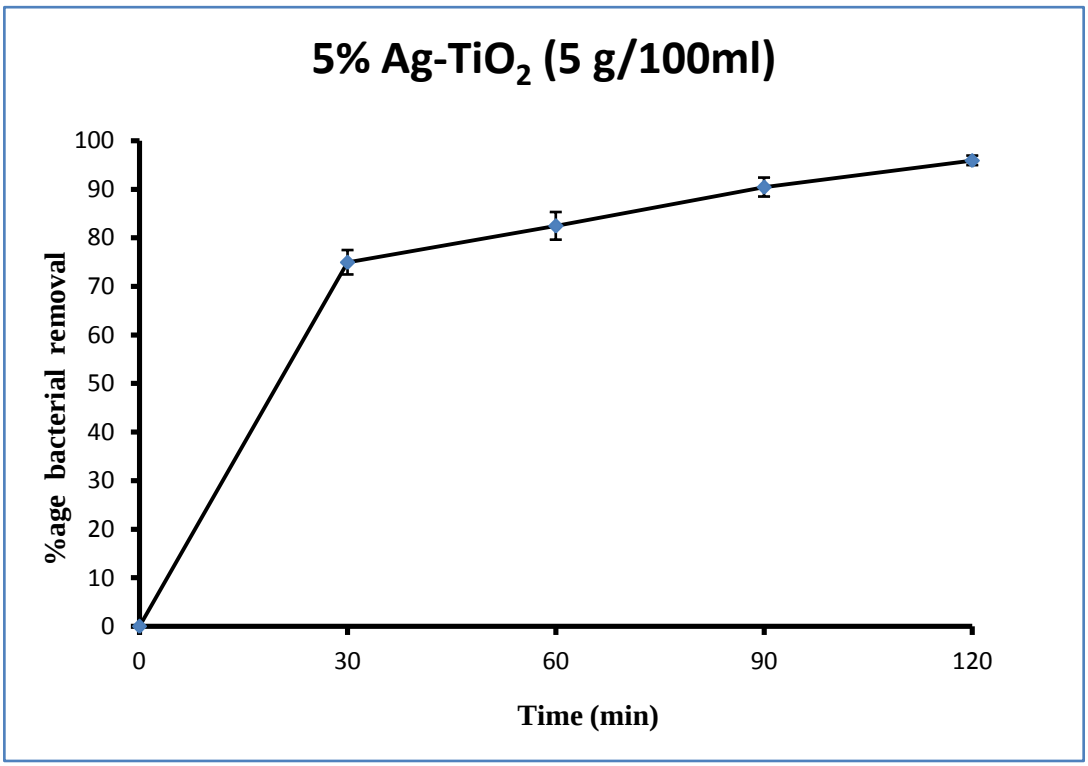

Figure 4. 35: Percentage bacterial removal by 5% Ag-TiO_2 NPs

From the previous experiments, 5 g/100ml concentration was selected and used for all the %age dopants. The bacterial inactivation was done under the influence of fluorescent light. A blank sample was run as control (without addition of NPs) and SPC was recorded after every 30 min till 120 min. Pure TiO_2 NPs, 1% Ag-TiO_2, 2% Ag-TiO_2, 3% Ag-TiO_2, 4% Ag-TiO_2 and 5% Ag-TiO_2 was applied in suspension with bacterial culture. Only 4% of bacteria were reduced after 120 min in control experiment. When applied pure TiO_2 NPs, the disinfection was upto 3%. The bacterial inactivation was evidenced 100% after 120 min when 1% Ag-TiO_2, 2% Ag-TiO_2 and 3% Ag-TiO_2 was applied. But only 98% and 96% bacteria were unable to grow after 120 min when 4% Ag-TiO_2 and 5% Ag-TiO_2 was applied respectively and the results depicted in Figures 16-22. An interesting fact was observed that after 60 min 1% Ag-TiO_2 removed 99% of bacteria from the culture while 2% Ag-TiO_2 and 3% Ag-TiO_2 were able to inactivate 97% and 91% of bacteria respectively.

4.4.4 Antimicrobial Effect of Darkness on Ag-TiO_2 Nanoparticles

4.4.4.1 0% Ag-TiO_2

Table 4. 21: Percentage bacterial removal by 0% Ag-TiO_2

Sr. No.	Time of Plating (min)	%age bactericidal effect
1	0	0
2	30	2
3	60	5
4	90	3
5	120	-1

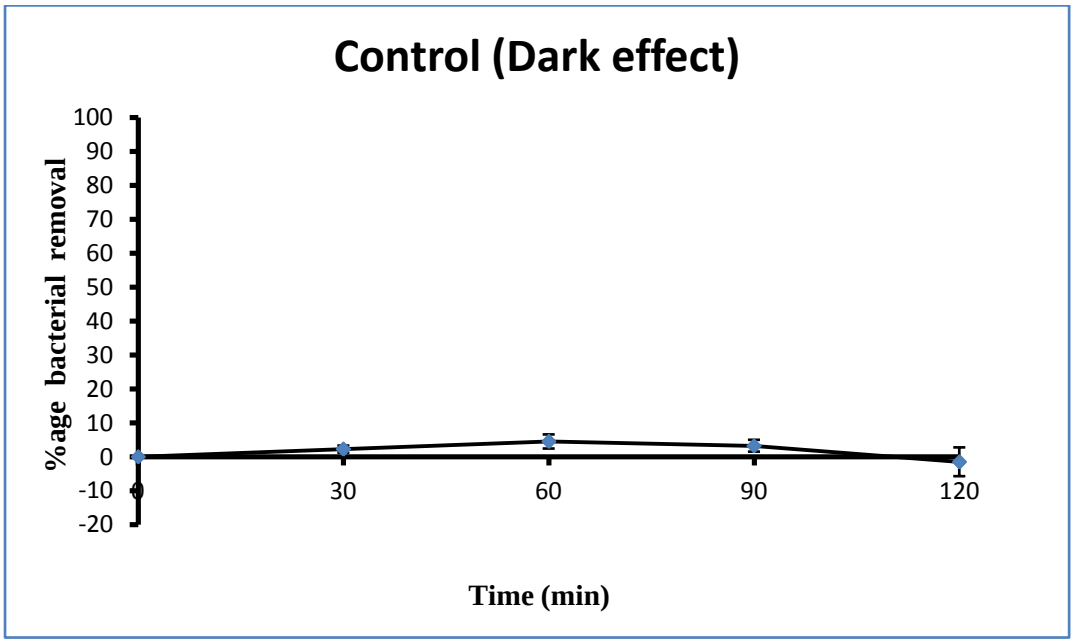

Figure 4. 36: Effect of darkness, control experiment without the addition of NPs

4.4.4.2 1% Ag-TiO_2 under dark

Table 4. 22: Percentage bacterial removal by 1% Ag-TiO_2 (5 g/100ml)

Sr. No.	Time of Plating (min)	%age bactericidal effect
1	0	0
2	30	6
3	60	6
4	90	6
5	120	7

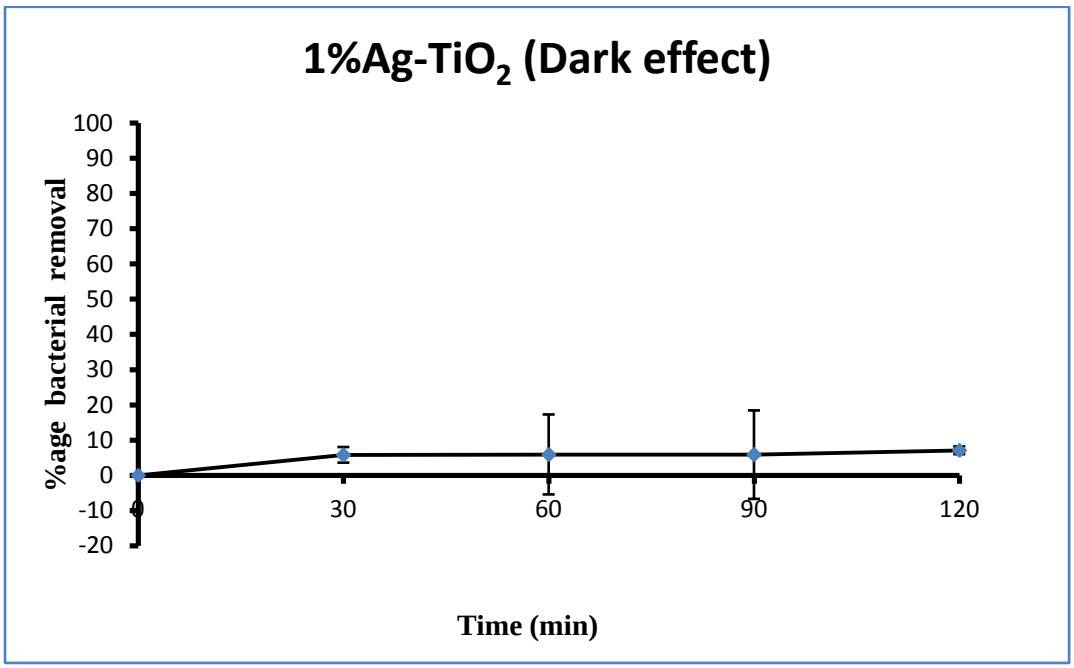

Figure 4. 37: Anti microbial activity of 1% Ag-TiO_2 under darkness

4.4.4.3 2% Ag-TiO_2 under dark

Table 4. 23: Percentage bacterial removal by 2% Ag-TiO_2 (5 g/100ml)

Sr. No.	Time of Plating (min)	%age bactericidal effect
1	0	0
2	30	1
3	60	1
4	90	4
5	120	3

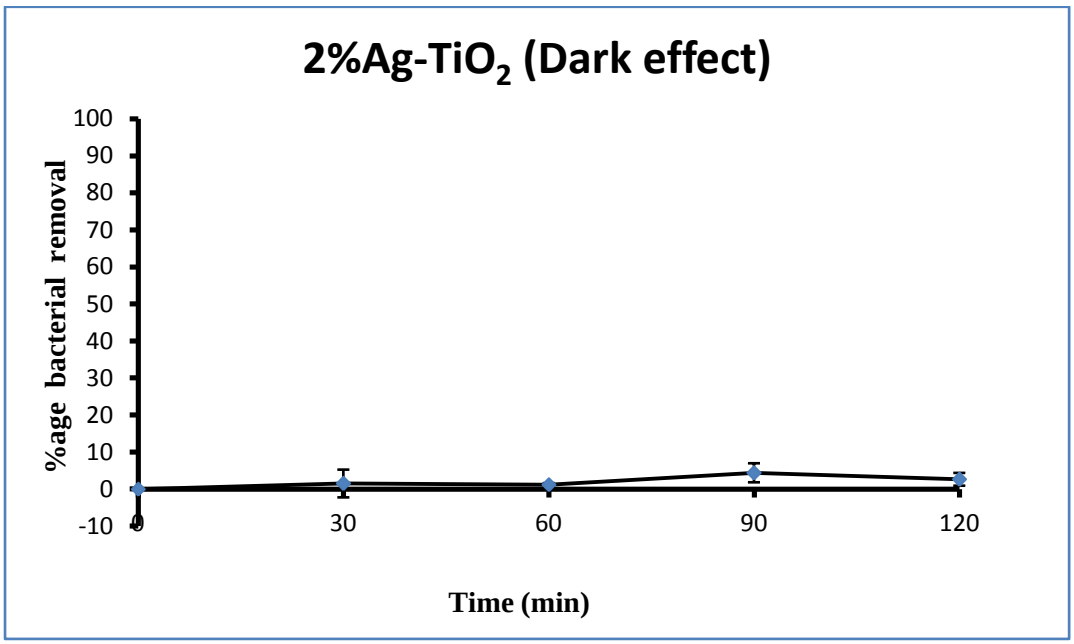

Figure 4. 38: Anti microbial activity of 2% Ag-TiO_2 under darkness

4.4.4.4 3% Ag-TiO_2 under dark

Table 4. 24: Percentage bacterial removal by 3% Ag-TiO_2 (5 g/100ml)

Sr. No.	Time of Plating (min)	%age bactericidal effect
1	0	0
2	30	5
3	60	7
4	90	2
5	120	1

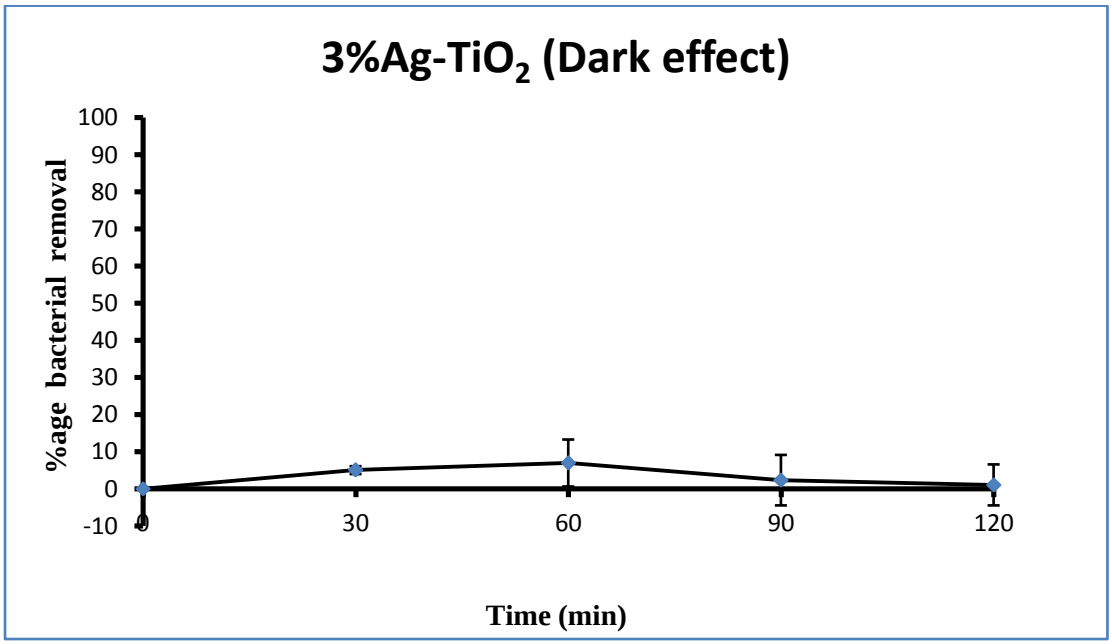

Figure 4. 39: Anti microbial activity of 3% Ag-TiO_2 under darkness

4.4.4.5 4% Ag-TiO_2 under dark

Table 4. 25: Percentage bacterial removal by 4% Ag-TiO_2 (5 g/100ml)

Sr. No.	Time of Plating (min)	%age bactericidal effect
1	0	0
2	30	6
3	60	4
4	90	7
5	120	1

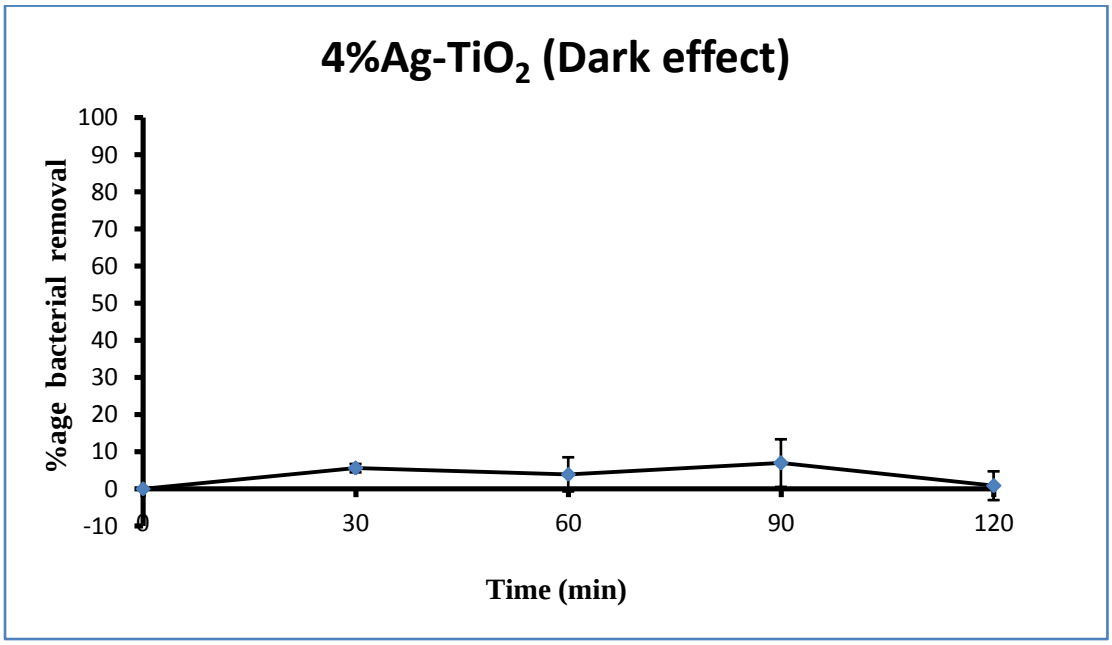

Figure 4. 40: Anti microbial activity of 4% Ag-TiO_2 under darkness

4.4.4.6 5% Ag-TiO_2 under dark

Table 4. 26: Percentage bacterial removal by 5% Ag-TiO_2 (5 g/100ml)

Sr. No.	Time of Plating (min)	%age bactericidal effect
1	0	0
2	30	2
3	60	1
4	90	3
5	120	4

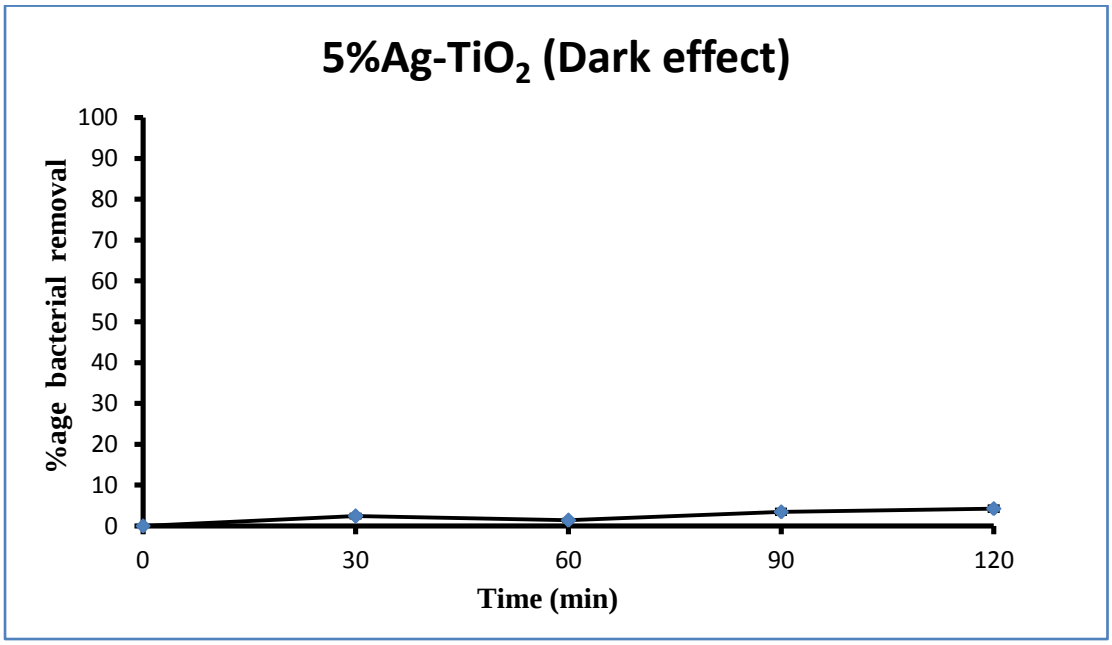

Figure 4. 41: Anti microbial activity of 5% Ag-TiO_2 under darkness

4.4.5 Effect of Ag-TiO_2 in Combination With UV-A

UV light, as used for disinfection, was selected to compare with TiO_2. UV-A spectrum was selected and bacterial culture was exposed to it exclusively and in combination with 1% Ag-TiO_2.

4.4.5.1 UV-A Light

Table 4. 27: Percentage bacterial removal by 0% Ag-TiO_2

Sr. No.	Time of Plating (min)	%age bactericidal effect
1	0	0
2	30	6
3	60	11
4	90	14
5	120	16

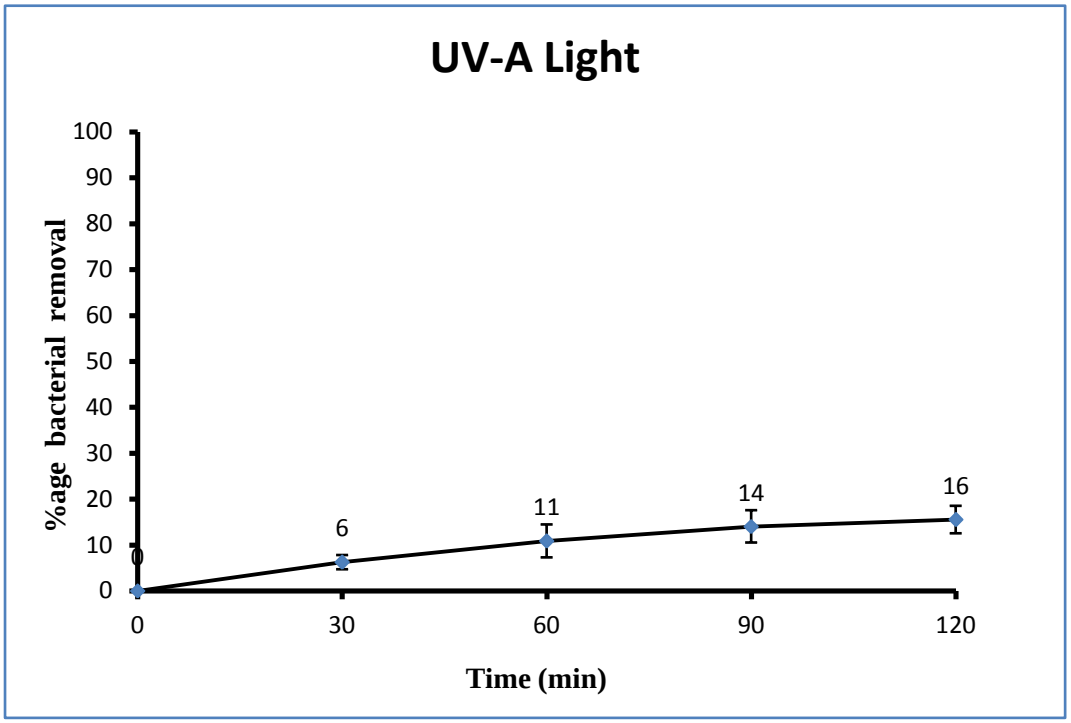

Figure 4. 42: Role of UV-A light in disinfection, control experiment

4.4.5.2 UV-A light + 1% Ag-TiO_2

Table 4. 28: Percentage bacterial removal by 1% Ag-TiO_2 (5 g/100ml)

Sr. No.	Time of Plating (min)	%age bactericidal effect
1	0	0
2	30	100
3	60	100
4	90	100
5	120	100

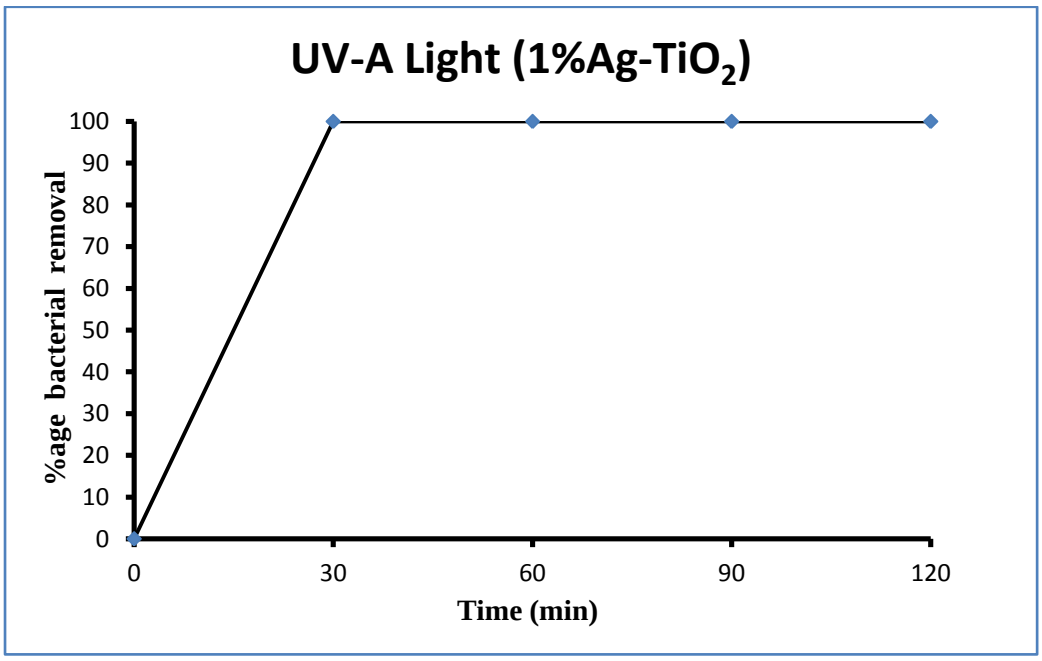

Figure 4. 43: Role of UV-A light with combination of 1% Ag-TiO_2 in disinfection

4.4.5.3 UV-A light + 1% Ag-TiO_2

It was found that 100 % bacterial removal was achieved under 30 min exposure of UV-A light in combination with 1% Ag-TiO_2, so experiment was performed by recording SPCs at 5 min interval to plot the sketch of bacterial removal.

Table 4. 29: Percentage bacterial removal by 1% Ag-TiO_2 (5 g/100ml)

Sr. No.	Time of Plating (min)	%age bactericidal effect
1	0	0
2	5	36
3	10	60
4	15	69
5	20	81
6	25	92
7	30	100

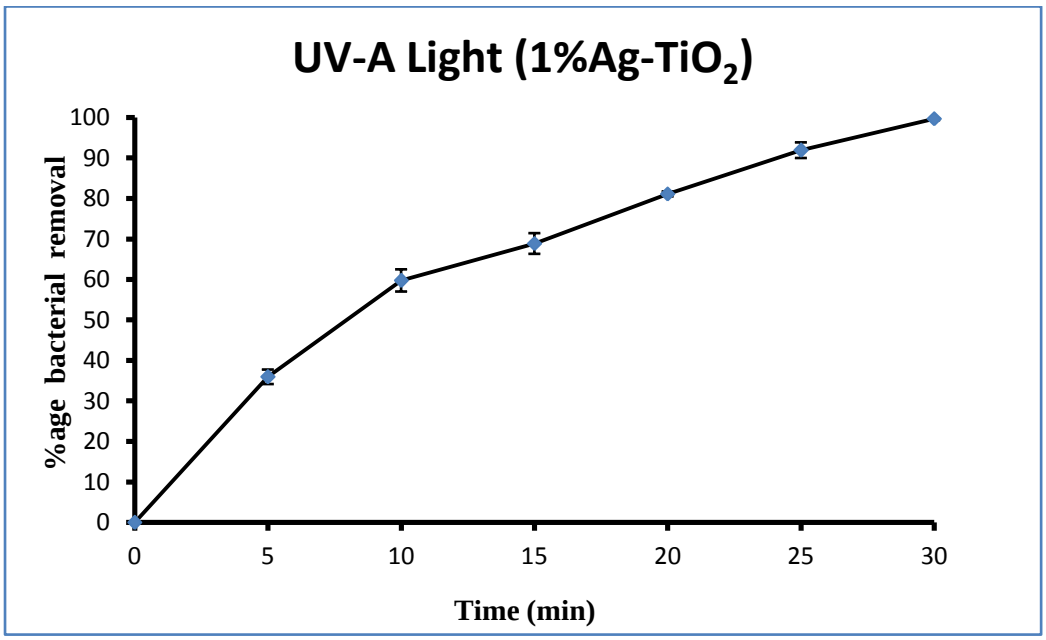

Figure 4. 44: Role of UV-A light with combination of 1% Ag-TiO_2 in disinfection

UV light, a renowned conventional disinfectant, kills the bacteria in UV-C range. UV-A light also has biocidal impact and it was compared with the biocidal impact of NPs and in combination of NPs and UV-A. After 120 min exposure of bacteria to UV-A, only 16% disinfection was recorded, illustrated in fig. 29. The synergistic effect of UV-A light and the addition of 1% Ag-TiO_2 was studied by adding 5 g/100ml in bacterial suspension. Remarkable results were obtained proving complete bacterial removal only in 30 min also verified in Figure 30. For further verification the experiment was repeated for 30 min and plate counts were recorded at 5 min interval. The same results in Figure 31, confirmed the complete disinfection within 30 min under combine effect of UV-A and 1% Ag-TiO_2.

4.4.6 Biocidal Effect of 1%Ag-TiO_2 coated Plates

4.4.6.1 Uncoated Plates

Table 4. 30: Percentage bacterial removal by Uncoated plates

Sr. No.	Time of Plating (Hrs)	%age bactericidal effect
1	0	0
2	2	4
3	4	6
4	6	8

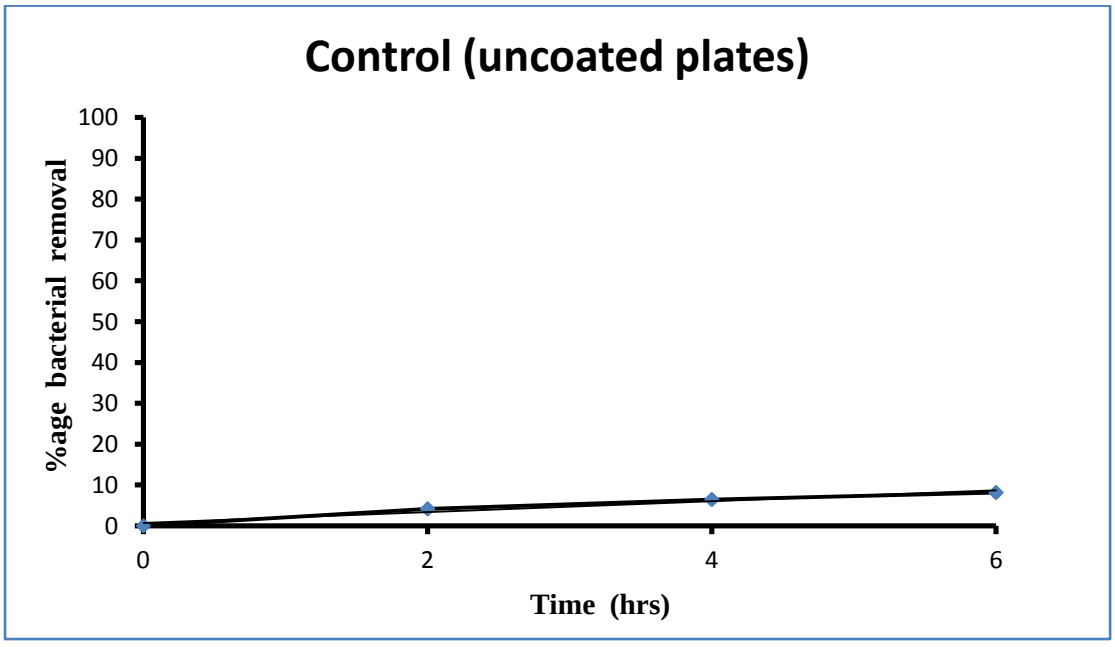

Figure 4. 45: Control experiment with uncoated plates

4.4.6.2 Experiment with coated plates

Table 4. 31: Percentage bacterial removal by 1% Ag-TiO_2 coated plates

Sr. No.	Time of Plating (Hrs)	%age bactericidal effect
1	0	0
2	2	84
3	4	92
4	6	97

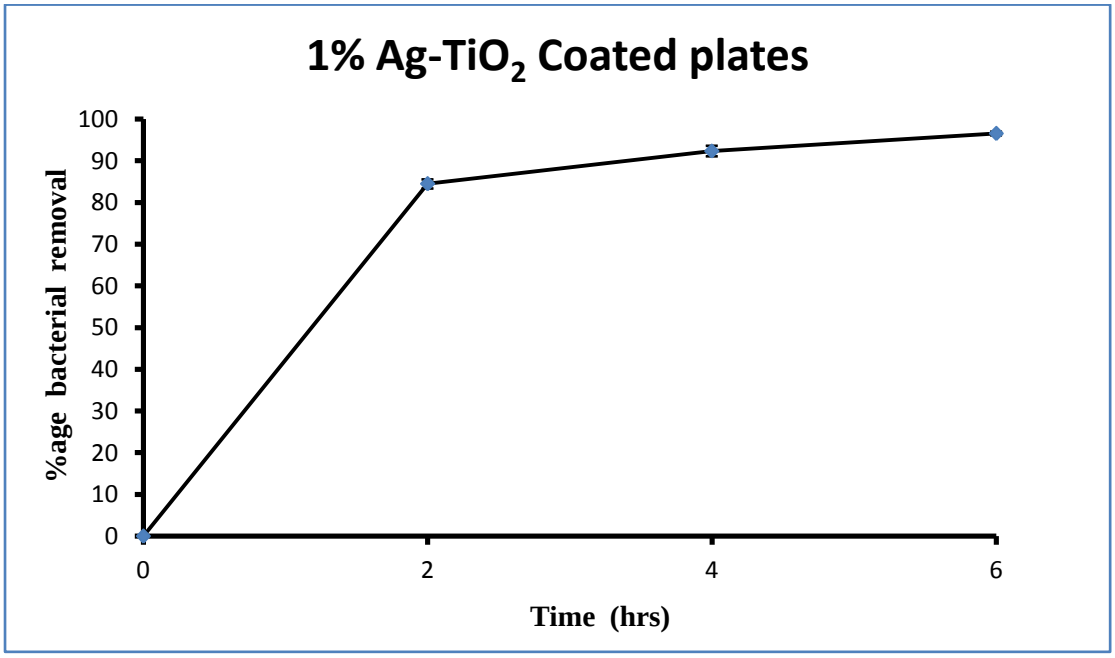

Figure 4. 46: Bactericidal effect of coated glass plates with 1% Ag-TiO_2

The antimicrobial effect of 1% Ag-TiO_2 was studied after immobilization of NPs on glass plates and influenced by fluorescent light for 6 hrs. SPCs were recorded after every 2 hrs. A control group of experiments was also prepared

which contain bacteria in uncoated plates. In control group, upto 8% of bacteria were inactivated with fluctuating rate. The bacteria were inactivated upto 97% with immobilized nano sized particles after 6 hrs. While 84% of inactivation was achieved after 2 hrs.

4.4.7 Experiment for Self Sterilized Surface

The experiment was performed to examine the antimicrobial effect of the surface in order to ensure the self sterilization of Ag-TiO_2 coated surface.

Table 4. 32: Data recorded for self sterilized surface

Sample Time (hrs)	Bacterial counts on 1% Ag-TiO_2 coated Glass Surface			Bacterial counts on un-coated Glass Surface	
	A	**B**	**C**	**A**	**B**
0	>2500	>1500	>1500	TNTC	TNTC
3	966	40	116	TNTC	TNTC
6	347	9	14	TNTC	TNTC

TNTC*= Too numerous to count

The results in Table 4.34 show that there was a remarkable decrease in bacterial count. This illustrates that if 1 % Ag-TiO_2 would be coated on a surface, that surface can be considered as self sterilizing surface. In control group of experiments, the number of bacterial count was above the countable range at the start of the experiment as well after 6 hrs. But a significant abatement in the number of bacteria was recorded as initially the bacterial count was more than 2500 reducing to 347 after 6 hrs.

Chapter 5

CONCLUSIONS AND RECOMMENDATIONS

5.1 CONCLUSIONS

The following conclusions can be drawn from the work done in this study

- TiO_2 performs better for inactivation of bacteria in doping with Ag than Fe.
- Ag, itself does not play any role in inactivation of bacteria in such small quantity.
- 1% Ag-TiO_2 is the most appropriate for inactivation among all percentage dopant concentrations.
- Synergistic effect of 1% Ag-TiO_2 NPs and UV-A demonstrates high inactivation rate than solitary.
- Fluorescent light results are also very encouraging.

5.2 RECOMMENDATIONS

Based on the results of the study, development of self sterile surface is suggested for further work, which would be applied as:

- House hold use (kitchen tops)
- Cafeterias
- Food processing units
- Hospitals
- Meeting rooms
- Wherever hygienic conditions are required.

Chapter 6

REFERENCES

Abdi, G., Salehi, H., & Khosh-Khui, M. (2008). Nano silver: a novel nanomaterial for removal of bacterial contaminants in valerian (Valeriana officinalis L.) tissue culture. *Acta Physiologiae Plantarum, 30*(5), 709-714.

Al-Rasheed, R. A. (2005). Water treatment by heterogeneous photocatalysis an overview. *4th SWCC Acquired Experience Symposium*.

Alrousan, D. M. A., Dunlop, P. S. M., McMurray, T. A., & Byrne, J. A. (2009). Photocatalytic inactivation of *E. coli* in surface water using immobilised nanoparticle TiO_2 films. *Water Research, 43*, 47-54.

Araña, J., Doña-Rodr´ıguez, J. M., González-D´ıaz, O., Rendóna, E. T., Melián, J. A. H., Colón, G., Nav´ıo, J. A., & Peña, J. P. (2004). Gas-phase ethanol photocatalytic degradation study with TiO_2 doped with Fe, Pd and Cu. *Journal of Molecular Catalysis A: Chemical, 215*, 153-160.

Azizullah, A., Khattak, M. N. K., Richter, P., & Häder, D.-P. (2011). Water pollution in Pakistan and its impact on public health — A review. *Environmental International, 37*, 479-497.

Benabbou, A. K., Derriche, Z., Felix, C., Lejeune, P., & Guillard, C. (2007). Photocatalytic inactivation of *Escherischia coli* Effect of concentration of TiO2 and microorganism, nature, and intensity of UV irradiation. *Applied Catalysis B: Environmental, 76*, 257-263.

Bettinelli, M., Dallacasa, V., Falcomer, D., Fornasiero, P., Gombac, V., Montini, T., Romanò, L., & Speghini, A. (2007). Photocatalytic activity of TiO_2

doped with boron and vanadium. *Journal of Hazardous Materials, 146*(3), 529-534.

Beydoun, D., Amal, R., Low, G., & McEvoy, S. (1999). Role of nanoparticles in photocatalysis. *Journal of Nanoparticle Research, 1*, 439-458.

Bhatkhande, D. S., Pangarkar, V. G., & Beenackers, A. A. (2002). Photocatalytic degradation for environmental applications – a review. *J Chem Technol Biotechnol, 77*, 102-116.

Braslavsky, S. E. (2007). Glossary of terms used in photochemistry, 3rd edition (IUPAC Recommendations 2006). *Pure and Applied Chemistry, 79*(3), 293-465.

Brundle, C. R., Evans, C. A., & Wilson, S. (1992). Encyclopedia of Materials Characterization.

Carp, O., Huisman, C. L., & Reller, A. (2004). Photoinduced reactivity of titanium dioxide. *Progress in Solid State Chemistry, 32*(1-2), 33-177.

Coleman, H., Chiang, K., & Amal, R. (2005). Effects of Ag and Pt on photocatalytic degradation of endocrine disrupting chemicals in water. *Chemical Engineering Journal, 113*(1), 65-72.

Gaya, U. I., & Abdullah, A. H. (2008). Heterogeneous photocatalytic degradation of organic contaminants over titanium dioxide: A review of fundamentals, progress and problems. *Journal of Photochemistry and Photobiology C: Photochemistry Reviews, 9*(1), 1-12.

Giolli, C., Borgioli, F., Credi, A., Fabio, A., Fossati, A., Miranda, M., Parmeggiani, S., Rizzi, G., Scrivani, A., & Troglio, S. (2007). Characterization of TiO_2 coatings prepared by a modified electric arc-

physical vapour deposition system☆. *Surface and Coatings Technology*, *202*(1), 13-22.

Hamal, D. B., & Klabunde, K. J. (2007). Synthesis, characterization, and visible light activity of new nanoparticle photocatalysts based on silver, carbon, and sulfur-doped TiO2. *Journal of Colloid and Interface Science*, *311*(2), 514-522.

Herrmann, J. M. (2005). Heterogeneous photocatalysis: state of the art and present applications In honor of Pr. R.L. Burwell Jr. (1912–2003), Former Head of Ipatieff Laboratories, Northwestern University, Evanston (Ill). *Topics in Catalysis*, *34*(1-4), 49-65.

Hollerith, C., Wernicke, D., Buhler, M., Feilitzsch, F., Huber, M., Hohne, J., Hertrich, T., Jochum, J., Phelan, K., & Stark, M. (2004). Energy dispersive X-ray spectroscopy with microcalorimeters. *Nuclear Instruments and Methods in Physics Research Section A: Accelerators, Spectrometers, Detectors and Associated Equipment*, *520*(1-3), 606-609.

Hosokawa, M., Nogi, K., Naito, M., & Yokoyama, T. (2007). Nanoparticle Technology Handbook.

Huang, Z., Maness, P.-C., Blake, D. M., Wolfrum, E. J., & Smolinski, S. L. (1999a). Bactericidal mode of titanium dioxide photocatalysis. *J. Photochem. Photobiol. A. Chem., In press*, 1-29.

Huang, Z., Maness, P.-C., Blake, D. M., Wolfrum, E. J., & Smolinski, S. L. (1999b). Bactericidal mode of titanium dioxide photocatalysis. *Journal of Photochemistry and Photobiology A-Chemistry*, *In Press*.

Ibáñez, J. A., Litter, M. I., & Pizarro, R. A. (2003). Photocatalytic bactericidal effect of TiO_2 on *Enterobacter cloacae* Comparative study with other Gram (-ve) bacteria. *Journal of Photochemistry and Photobiology A: Chemistry, 157*, 81-85.

ICPS. (2004). Disinfectants and disinfectant by-products. Geneva. *World Health Organization, International Programme on Chemical Safety (Environmental Health Criteria 216)*.

Ireland, J. C., Klostermann, P., Rice, E. W., & Clark, R. M. (1993). Inactivation of Escherichia coli by Titanium Dioxide Photocatalytic Oxidation. *Applied and Environmental Microbiology, 59*(5), 1668-1670.

Khataee, A. R. (2009). Photocatalytic removal of C.I. Basic Red 46 on immobilized TiO_2 nanoparticles: Artificial neural network modelling. *Environmental Technology, 30*(11), 1155-1168.

Kumar, R. V., & Raza, G. (2009). Photocatalytic disinfection of water with Ag–TiO2 nanocrystalline composite. *Ionics, 15*, 579-587.

Linsebigler, A. L., Lu, G., & Yates, J. T. (1995). Photocatalysis on TiOn Surfaces: Principles, Mechanisms, and Selected Results. *Chem. Rev., 95*, 735-758.

Maneerat, C., & Hayata, Y. (2006). Antifungal activity of TiO_2 photocatalysis against Penicillium expansum in vitro and in fruit tests. *International Journal of Food Microbiology, 107*(2), 99-103.

Marugán, J., van Grieken, R., Sordo, C., & Cruz, C. (2008). Kinetics of the photocatalytic disinfection of Escherichia coli suspensions. *Applied Catalysis B: Environmental, 82*(1-2), 27-36.

Masschelein, W. J. (2002). Ultraviolet Light in Water and Wastewater Sanitation. In CRC (Eds.)

Matsunaga, T., Tomoda, R., Nakajima, T., Nakamura, N., & Komine, T. (1988). Continuous-Sterilization System That Uses Photosemiconductor. *Applied and environmental microbiology, 54*(6), 1330-1333.

Migheli, Q., Balmas, V., Harak, H., Sanna, S., Scherm, B., Aoki, T., & O'Donnell, K. (2010). Molecular Phylogenetic Diversity of Dermatologic and Other Human Pathogenic Fusarial Isolates from Hospitals in Northern and Central Italy. *Journal of Clinical Microbiology, 48*(4), 1076-1084.

Neppolian, B., Choi, H. C., Sakthivel, S., Arabindoo, B., & Murugesan, V. (2002). Solar/UV-induced photocatalytic degradation of three commercial textile dyes. *Journal of Hazardous Materials*, 303-317.

Rincón, A. G., & Pulgarin, C. (2003). Photocatalytical inactivation of *E. coli*: effect of (continuous–intermittent) light intensity and of (suspended–fixed) TiO_2 concentration. *Applied Catalysis B: Environmental, 44*(3), 263-284.

Sahoo, C., Gupta, A., & Pal, A. (2005). Photocatalytic degradation of Crystal Violet (C.I. Basic Violet 3) on silver ion doped TiO_2 *Dyes and Pigments, 66*(3), 189-196.

Sakkas, V. A., Arabatzis, I. M., Konstantinou, I. K., Dimoua, A. D., Albanis, T. A., & Falaras, P. (2004). Metolachlor photocatalytic degradation using TiO_2 photocatalysts. *Applied Catalysis B: Environmental, 49*, 195-205.

Sheel, D. W., Brook, L. A., Ditta, I. B., Evans, P., Foster, H. A., Steele, A., & Yates, H. M. (2008). Biocidal Silver and Silver/Titania Composite Films

Grown by Chemical Vapour Deposition. *International Journal of Photoenergy, 2008*, 1-11.

Shun-wen, W., Bing, P., Li-yuan, C., Yun-chao, L., & Zhu-ying, L. (2008). Preparation of doping titania antibacterial powder by ultrasonic spray pyrolysis. *Trans. nonferous met. soc., 18*, 1145-1150.

Sun, H., Wang, C., Pang, S., Li, X., Tao, Y., Tang, H., & Liu, M. (2008). Photocatalytic TiO_2 films prepared by chemical vapor deposition at atmosphere pressure. *Journal of Non-Crystalline Solids, 354*, 1440-1443.

Sunada, K., Watanabe, T., & Hashimoto, K. (2003). Studies on photokilling of bacteria on TiO_2 thin film. *Journal of Photochemistry and Photobiology A: Chemistry, 156*(1-3), 227-233.

Thiel, J., Pakstis, L., Buzby, S., Raffi, M., Ni, C., Pochan, D. J., & Shah, S. I. (2007). Antibacterial Properties of Silver-Doped Titania. *Small, 3*(5), 799-803.

Vernon-Parry, K. D. (2000). Scanning Electron Microscopy: an introduction. *13*(4), 40-44.

WHO. (2006). *Guidelines for Drinking-water Quality First addendum to third edition*.

WHO. (2007). Economic and health effects of Increasing coverage of low cost household drinking-water supply and sanitation interventions to countries off-track to meet MDG target 10.

Wu, C., Chao, C., & Kuo, F. (2004). Enhancement of the photo catalytic performance of TiO catalysts via transition metal modification. *Catalysis Today, 97*(2-3), 103-112.

Zallen, R., & Moret, M. (2005). The optical absorption edge of brookite TiO_2. *Solid State Communications*.

APPENDICES

APPENDIX-A:

Data recorded in comparison of different metals as dopant

Time	1% Fe-TiO_2 (5 g/100L)					
	A		B		St. deviation of %age degradation	Avg
	No. of Colonies	%age disinfection	No. of Colonies	%age disinfection		
0	**700**	**0**	1346	0	0	0
30	**380**	**46**	700	48	2	47
60	**270**	**61**	570	58	3	60
90	**210**	**70**	400	70	0	70
120	**185**	**74**	303	77	3	76

Dilution Factor = 10^6
No. of Colonies = CFU/ml

Time	1% Ag-TiO_2 (5 g/100L)					
	A		B		St. deviation of %age degradation	Avg
	No. of Colonies	%age disinfection	No. of Colonies	%age disinfection		
0	190	0	168	0	0	0
30	25	87	20	88	1	87
60	2	99	3	98	1	99
90	0	100	0	100	0	100
120	0	100	0	100	0	100

Dilution Factor = 10^6
No. of Colonies = CFU/ml

APPENDIX-B:

Data recorded for optimization of concentration

Time	2% Ag-TiO_2 (0.1 g/100L)					
	A		B		St. deviation of %age degradation	Avg
	No. of Colonies	%age disinfection	No. of Colonies	%age disinfection		
0	240	0	274	0	0	0
30	225	6	255	7	0.5	7
60	218	9	235	14	3.6	12
90	206	14	219	20	4.2	17
120	190	21	206	25	2.8	23

Dilution Factor = 10^6
No. of Colonies = CFU/ml

Time	2% Ag-TiO_2 (0.5 g/100L)							
	A		B		C		St. deviation of %age degradation	Avg
	No. of Colonies	%age disinfection	No. of Colonies	%age disinfection	No. of Colonies	%age disinfection		
0	240	0	308	0	126	0	0	0
30	170	29	218	29	95	25	3	28
60	140	42	173	44	76	40	2	42
90	122	49	152	51	66	48	2	49
120	110	54	139	55	58	54	0	54

Dilution Factor = 10^6
No. of Colonies = CFU/ml

Time	2% Ag-TiO_2 (1 g/100L)							
	A		B		C		St. deviation of %age degradation	Avg
	No. of Colonies	%age disinfection	No. of Colonies	%age disinfection	No. of Colonies	%age disinfection		
0	337	0	328	0	280	0	0	0
30	200	41	218	34	180	36	4	37
60	162	52	195	41	140	50	6	47
90	130	61	150	54	110	61	4	59
120	97	71	104	68	85	70	1	70

Dilution Factor = 10^6
No. of Colonies = CFU/ml

Time	2% Ag-TiO_2 (5g/L)									
	A		B		C		D		St. deviation of %age disinfection	Avg
	No. of Colonies	%age disinfection	No. of Colonies	%age disinfection	No. of Colonies	%age disinfection	No. of Colonies	%age disinfection		
0	95	0	100	0	76	0	65	0	0	0
30	15	84	17	83	13	83	18	72	5.6	81
60	3	97	1	99	1	99	4	94	2.4	97
90	0	100	0	100	0	100	1	98	0.8	100
120	0	100	0	100	0	100	0	100	0	100

Dilution Factor = 10^6
No. of Colonies = CFU/ml

Time	2% Ag-TiO_2 (7.5 g/100L)					
	A		B		St. deviation of %age degradation	Avg
	No. of Colonies	%age disinfection	No. of Colonies	%age disinfection		
0	240	0	274	0	0	0
30	225	6	255	7	0.5	7
60	218	9	235	14	3.6	12
90	206	14	219	20	4.2	17
120	190	21	206	25	2.8	23

Dilution Factor = 10^6

No. of Colonies = CFU/ml

APPENDIX-C:

Data recorded for Optimization study for %age dopant

1% Ag-TiO_2 (5g/L)										
Time	A		B		C		D		St. deviation of %age disinfection	Avg
	No. of Colonies	%age disinfection	No. of Colonies	%age disinfection	No. of Colonies	%age disinfection	No. of Colonies	%age disinfection		
0	132	0	132	0	112	0	108	0	0	0
30	14	89	16	88	24	79	18	83	4.9	85
60	2	98	2	98	1	99	2	98	0.4	99
90	0	100	0	100	0	100	0	100	0	100
120	0	100	0	100	0	100	0	100	0	100

Dilution Factor = 10^6
No. of Colonies = CFU/ml

Time	2% Ag-TiO_2 (5g/L)									
	A		B		C		D		St. deviation of %age disinfection	Avg
	No. of Colonies	%age disinfection	No. of Colonies	%age disinfection	No. of Colonies	%age disinfection	No. of Colonies	%age disinfection		
0	95	0	100	0	76	0	65	0	0	0
30	15	84	17	83	13	83	18	72	5.6	81
60	3	97	1	99	1	99	4	94	2.4	97
90	0	100	0	100	0	100	1	98	0.8	100
120	0	100	0	100	0	100	0	100	0	100

Dilution Factor = 10^6
No. of Colonies = CFU/ml

Time	3% Ag-TiO_2 (5g/L)									
	A		B		C		D		St. deviation of %age disinfection	Avg
	No. of Colonies	%age disinfection	No. of Colonies	%age disinfection	No. of Colonies	%age disinfection	No. of Colonies	%age disinfection		
0	2351	0	2218	0	2296	0	2176	0	0	0
30	828	65	800	64	813	65	693	68	1.89	65
60	206	91	229	90	230	90	135	94	1.87	91
90	29	99	27	99	26	99	14	99	0.28	99
120	1	100	3	100	2	100	2	100	0.04	100

Dilution Factor = 10^6
No. of Colonies = CFU/ml

Time	4% Ag-TiO_2 (5g/L)									
	A		B		C		D		St. deviation of %age disinfection	Avg
	No. of Colonies	%age disinfection	No. of Colonies	%age disinfection	No. of Colonies	%age disinfection	No. of Colonies	%age disinfection		
0	447	0	570	0	112	0	108	0	0	0
30	36	92	71	88	24	79	18	83	5.7	85
60	6	99	42	93	1	99	2	98	3.0	97
90	2	100	22	96	0	100	0	100	1.9	99
120	0	100	0	100	0	100	0	100	0	100

Dilution Factor = 10^6
No. of Colonies = CFU/ml

Time	5% Ag-TiO_2 (5g/L)									
	A		B		C		D		St. deviation of %age disinfection disinfection	Avg
	No. of Colonies	%age disinfection	No. of Colonies	%age disinfection	No. of Colonies	%age disinfection	No. of Colonies	%age disinfection		
0	220	0	101	0	101	0	108	0	0	0
30	54	75	24	76	29	71	25	77	2.5	75
60	35	84	16	84	22	78	18	83	2.8	82
90	16	93	9	91	12	88	11	90	2.0	90
120	6	97	5	95	4	96	5	95	1.0	96

Dilution Factor = 10^6
No. of Colonies = CFU/ml

Time	Pure Titania N.P (5g/L)									
	A		B		C		D		St. deviation of %age disinfection	Avg
	No. of Colonies	%age disinfection	No. of Colonies	%age disinfection	No. of Colonies	%age disinfection	No. of Colonies	%age disinfection		
0	441	0	415	0	430	0	402	0	0	0
30	410	7	398	4	417	3	398	1	2.5	4
60	400	9	405	2	419	3	390	3	3.3	4
90	426	3	401	3	410	5	396	1	1.3	3
120	430	2	392	6	420	2	392	2	1.6	3

Dilution Factor = 10^6
No. of Colonies = CFU/ml

Time	Flourescent Light									
	A		B		C		D		St. deviation of %age disinfection	Avg
	No. of Colonies	%age disinfection	No. of Colonies	%age disinfection	No. of Colonies	%age disinfection	No. of Colonies	%age disinfection		
0	254	0	234	0	245	0	250	0	0	0
30	248	2	228	3	238	3	245	2	0.4	2
60	246	3	226	3	236	4	242	3	0.2	3
90	250	2	221	6	240	2	246	2	1.9	3
120	244	4	224	4	232	5	243	3	1.0	4

Dilution Factor = 10^6
No. of Colonies = CFU/ml

APPENDIX-D:

Effect of Darkness

Time	Control (Dark effect)					
	A		B		St. deviation of %age degradation	Avg
	No. of Colonies	%age disinfection	No. of Colonies	%age disinfection		
0	198	0	134	0	0	0
30	195	2	130	3	1	2
60	192	3	126	6	2	5
90	194	2	128	4	2	3
120	195	2	140	-4	4	-1

Dilution Factor = 10^6
No. of Colonies = CFU/ml

Time	1%Ag-TiO_2 (Dark effect)					
	A		B			
	No. of Colonies	%age disinfection	No. of Colonies	%age disinfection	St. deviation of %age degradation	Avg
0	95	0	165	0	0	0
30	88	7	158	4	2	6
60	97	-2	142	14	11	6
90	81	15	170	-3	13	6
120	89	6	152	8	1	7

Dilution Factor = 10^6
No. of Colonies = CFU/ml

Time	2%Ag-TiO_2 (Dark effect)					
	A		B		St. deviation of %age degradation	Avg
	No. of Colonies	%age disinfection	No. of Colonies	%age disinfection		
0	430	0	339	0	0	0
30	435	-1	325	4	4	1
60	426	1	334	1	0	1
90	419	3	318	6	3	4
120	424	1	326	4	2	3

Dilution Factor = 10^6
No. of Colonies = CFU/ml

Time	3%Ag-TiO_2 (Dark effect)					
	A		B		St. deviation of %age degradation	Avg
	No. of Colonies	%age disinfection	No. of Colonies	%age disinfection		
0	70	0	121	0	0	0
30	67	4	114	6	1	5
60	62	11	118	2	6	7
90	65	7	124	-2	7	2
120	72	-3	115	5	6	1

Dilution Factor = 10^6
No. of Colonies = CFU/ml

Time	4%Ag-TiO_2 (Dark effect)					
	A		B		St. deviation of %age degradation	Avg
	No. of Colonies	%age disinfection	No. of Colonies	%age disinfection		
0	84	0	157	0	0	0
30	80	5	147	6	1	6
60	78	7	156	1	5	4
90	82	2	139	11	6	7
120	81	4	160	-2	4	1

Dilution Factor = 10^6
No. of Colonies = CFU/ml

Time	5%Ag-TiO_2 (Dark effect)					
	A		B		St. deviation of %age degradation	Avg
	No. of Colonies	%age disinfection	No. of Colonies	%age disinfection		
0	540	0	506	0	0	0
30	529	2	492	3	1	2
60	534	1	498	2	0	1
90	524	3	486	4	1	3
120	520	4	482	5	1	4

Dilution Factor = 10^6
No. of Colonies = CFU/ml

APPENDIX-E:

Data recorded for Impact of Ag-TiO_2 in combination with UV-A

Time	UV-A Light (Control)									
	A		B		C		D		St. deviation of %age degradation	Avg
	No. of Colonies	%age disinfection	No. of Colonies	%age disinfection	No. of Colonies	%age disinfection	No. of Colonies	%age disinfection		
0	157	0	147	0	168	0	850	0	0	0
30	150	4	135	8	157	7	800	6	2	6
60	145	8	127	14	144	14	780	8	3	11
90	142	10	122	17	140	17	750	12	4	14
120	139	11	121	18	138	18	734	14	3	15

Dilution Factor = 10^6
No. of Colonies = CFU/ml

Time	UV-A Light (1%Ag-TiO_2)									
	A		B		C		D		St. deviation of %age degradation	Avg
	No. of Colonies	%age disinfection	No. of Colonies	%age disinfection	No. of Colonies	%age disinfection	No. of Colonies	%age disinfection		
0	456	0	530	0	338	0	296	0	0	0
30	0	100	0	100	0	100	0	100	0	100
60	0	100	0	100	0	100	0	100	0	100
90	0	100	0	100	0	100	0	100	0	100
120	0	100	0	100	0	100	0	100	0	100

Dilution Factor = 10^6
No. of Colonies = CFU/ml

Time	UV-A Light (1%Ag-TiO_2)					
	A		B			
	No. of Colonies	%age disinfection	No. of Colonies	%age disinfection	St. deviation of %age degradation	Avg
0	478	0	389	0	0	0
5	300	37	254	35	2	36
10	183	62	164	58	3	60
15	140	71	128	67	3	69
20	88	82	75	81	1	81
25	45	91	26	93	2	92
30	0	100	2	99	0	100

Dilution Factor = 10^6

No. of Colonies = CFU/ml

APPENDIX-F:

Biocidal Effect of 1%Ag-TiO_2 coated Plates

Time (Hrs)	Control (uncoated plates)					
	A		B		St. deviation of %age degradation	Avg
	No. of Colonies	%age disinfection	No. of Colonies	%age disinfection		
0	1066	0	1663	0	0	0
2	992	7	1642	1	4	4
4	950	11	1632	2	6	6
6	936	12	1596	4	6	8

Dilution Factor = 10^2
No. of Colonies = CFU/ml

Time (Hrs)	1% Ag-TiO_2 Coated Plates							
	A		B		C		St. deviation of %age degradation	Avg
	No. of Colonies	%age disinfection	No. of Colonies	%age disinfection	No. of Colonies	%age disinfection		
0	1307	0	1298	0	1372	0	0	0
2	219	83	190	85	209	85	1	84
4	88	93	118	91	98	93	1	92
6	46	96	50	96	41	97	0	97

Dilution Factor = 10^2
No. of Colonies = CFU/ml

APPENDIX-G:

Self Sterilization capability of 1%Ag-TiO_2 coated Plates

Sample Time (hrs)	Bacterial counts on 1% Ag-TiO_2 coated Glass Surface			Bacterial counts on un-coated Glass Surface	
	A	B	C	A	B
0	<2500	<1500	<1500	TNTC	TNTC
3	966	40	116	TNTC	TNTC
6	347	9	14	TNTC	TNTC

TNTC = Too numerous to count
Dilution Factor = 10^2